# Candida albicans ribosome : structure, function, and inhibition

David Bruchlen

# UNIVERSITÉ DE STRASBOURG

*ÉCOLE DOCTORALE DES SCIENCES DE LA VIE ET DE LA SANTÉ*

**IGBMC – CNRS UMR 7104 – INSERM 964**

**IPPTS – EA 7292 Dynamique des interactions hôte-pathogènes**

# THÈSE présentée par :

**David BRUCHLEN**

soutenue le : **23 novembre 2016**

pour obtenir le grade de : **Docteur de l'université de Strasbourg**

Discipline/ Spécialité : Biophysique et biologie structurale

# Structure, fonction et inhibition du ribosome de *Candida albicans*

## *Candida albicans* ribosome: structure, function, and inhibition

**THÈSE dirigée par :**

| | |
|---|---|
| **M. YUSUPOV Marat** | Directeur de recherche, CNRS |
| **M. CANDOLFI Ermanno** | Professeur des universités - praticien hospitalier, Université de Strasbourg |

**RAPPORTEURS :**

| | |
|---|---|
| M. MECHULAM Yves | Professeur associé, Ecole polytechnique de Paris |
| Mme. FAIRHEAD Cécile | Professeur des universités, Université Paris Sud |

**AUTRES MEMBRES DU JURY :**

| | |
|---|---|
| **M. RENAUD Jean-Paul** | Directeur de recherche, CNRS |
| **M. DALLE Frédéric** | Professeur des universités – praticien hospitalier, Université de Dijon |

Table des matières

# ACKNOWLEDGMENTS

Si la rédaction est une épreuve particulière quant aux différents états psychologiques et physiologiques qu'elle entraine, les remerciements eux ressemblent alors plus à un casse tête, qui se révèle également être déroutants et d'une extrême difficulté quant à leur écriture puisque là, aussi, il y aurait réellement de quoi disserter.

En premier lieu, **aux membres du jury,** qui me font l'honneur d'être présent à ma soutenance et d'évaluer mon travail de thèse, **Cécile Fairhead, Yves Mechulam, Frédéric Dalle** et **Jean-Paul Renaud** soyez assurer tous les quatre de ma profonde gratitude, de mon admiration certaine pour vos recherches respectives, pour votre engouement et votre engagement pour la science.

**Ermanno**, j'aurai tant à écrire pour expliquer, raconter, revivre… Merci pour ton enthousiasme, ton entrain, ta sollicitude, ton amour de la recherche, ton support et tes conseils. « Tu as le feu », ta phrase est marquée au fer rouge, elle m'accompagne. Merci d'avoir accepté le stagiaire de master que j'étais dans ton équipe il y a maintenant quelques années et d'avoir guidé mes choix quand il le fallait. Voici le manuscrit résultant de cette thèse, cette aventure, ce bout de vie et tu y es pour beaucoup, encore une fois et infiniment merci l'ami.

**Marat**, **Gula**, I have so much to say, but I will begin by thanking you a lot, for supporting me as a PhD student. Thanks for accepting the microbiologist that I was when I arrived. For taking the time to teach me your science and for showing me the ribosome world. For letting me work on my own project. It was sometimes difficult but it was a fantastic adventure. Thanks for your rigor and your exigence, you helped me grow up and I am more than thankful for that.

**Marcela**, si la science et la recherche permettent de voyager, d'échanger, d'apprendre, de rencontrer des collègues et des confrères elle permet aussi parfois, de très belle façon, de

rencontrer plus que cela, ainsi si la science ne nous permettra plus forcément d'échanger, l'amitié elle s'en chargera. Merci d'avoir partagé aussi cette aventure avec moi.

**Justine, Mélanie**, j'ai une multitude de signes, de grimaces ou même de phonèmes qui n'ont bien sûr rien à faire ici mais qui pourrait faire partie de l'explication du soutient et de la patience dont vous avez fait preuve avec moi, merci pour nos conversations à tel point personnelles qu'aucun de nous trois n'était réellement en mesure de les comprendre, merci pour ces fous rires et cet amour de la science partagé. Je vous souhaite le meilleur pour la suite.

**Julie**, merci pour ta pédagogie, ta patience et d'être c'est important de le dire quelqu'un en mesure de dire que c'est bien, **Hélène** je crois que cela a été un échange de bons procédés, à toi aussi, ta marque est là, merci, souffle et soit championne.

Thanks to all the current and past members of the ribosome team; **Eduardo**, merci pour le partage de ton amour pour la science et d'avoir accompagner mes premiers pas en biologie structurale, **Sylvie**, merci de m'avoir aussi accompagner pendant ces premières manip'. **Iskander**, thanks for your constant good mood, **Alexey,** too, for sure ! Thanks also to **Irina, Simone** and **Yuzuru**. **Natasha** and **Sergey**, I was so impressed by your widsom when I met you both, I hope everything is going how it should wherever you are, même remarque pour toi **Nicolas**. **Marie**, poto, **Ilaria**, coin-coin, merci à vous aussi pour cette adoration de la nourriture et tous ces repas partagés. **Mumin, Danyia**, you will be the next, I wish you the best for your research.

Merci aux beamline scientists du synchrotron SOLEIL, **Serena, Pierre, Andrew, Léonard, Martin** et ceux du SLS, **Laura et Vincent**, pour leur conseil avisé, leur pédagogie, leur enthousiasme et leur disponibilité.

Merci à **Fabrice** et **Yacine**, pour le temps consacré à la modélisation des ARNr.

Merci aussi aux invisibles du trop tôt ou du trop tard dans la nuit, de l'institut de parasitologie, d'avoir partager des manip' à minuit comme à 2 ou 5h le matin, **Valentin** un monde particulier de décalés s'ouvre à toi !

Merci aussi à tous ceux de cette équipe qui travaillent pendant les heures plus conventionnelles d'avoir apporter de la bonne humeur, mais aussi un regard critique et extérieur à mon travail de recherche.

Enfin, **Mélanie, Marie, Simone**, je vous souhaite de vous éclater autant que moi sur ce sujet, il m'a apporté de très grand moments !

Je tiens ensuite forcément à remercier tous les membres du SPB, ces 4 ans à l'IGBMC n'auraient pas eu la même saveur sans vous tous. J'en viens forcément à remercier **Justine** et **Angélique**, les filles, je me souviens bien de ce sentiment de douce panique au tout début de notre bureau, encore comment et pourquoi on va faire cela… mais ça aussi, le partager avec vous ça a été génial, merci d'avoir été les meilleures secrétaire et trésorière !

Si je parle du SPB, je dois forcément parler de toi, **Perrine**, tu es un être particulier qui gagne sincèrement à être connu, d'une efficacité incroyable, j'admire ta droiture et tes engagements, mais j'apprécie aussi le lâcher prise que l'on peut partager maintenant que la période d'apprivoisement est passée, que la suite arrive j'ai hâte !

**Claire**, merci pour toute la non-science que l'on a échangé, cela fait aussi partie de cette thèse, je te souhaite le meilleur pour la poursuite de ta carrière qu'elle soit avec une fourchette ou du jambon, **Steph** est là, ça ira bien.

Si SPB il y a, alors merci à la nouvelle équipe qui en a repris les reines, je suis certain, **Arnaud, Stéphanie, Mélanie** que vous serez très bons.

Merci à tous les doctorants qui partagent si bien cette vie si étrange, merci à tous ceux rencontrés au PhDprogram, durant les événements du SPB mais aussi pendant les retraites. On essaye de boucler la fin ensemble comme on a commencé, **Raphael** à fini, là c'est moi, **Karima, Jérôme** vous êtes les prochains.

I would like also to thanks all the people that I met during congres, seminar, workshop, with a particular wink to **Francesca, Manu, Sid, Pol, Simon, Angelica, Rebecca, Kamel, Andrea, Nastia, Angela, Dominik**.

**Hans, Yann, Ludovico, Joe**, merci d'accompagner mes journée, de m'avoir épauler et fait sourire pendant cette rédaction.

**A toute l'équipe pédagogique** qui a accompagné mon parcours scolaire et a contribué à mon éveil, à vos premiers cours de sciences comme à ceux moins adorés, une partie d'entre vous est aujourd'hui des collègues, d'autres un peu plus, vous y êtes tous pour quelque chose.

Un ENORME merci à tous les relecteurs et correcteurs de mes écrits, **Kévin, Ermanno, Marcela, Julie, Simone.**

Il y a ensuite les personnes que l'on souhaite remercier de façon plus personnelle, qui souvent oublient voire ignorent totalement à quel point elles sont vitales à l'élaboration de tel projet

**Papi, Mamie**, jamais de mots ne seront assez forts pour exprimer l'amour inconditionnel que je vous porte. Vous avez été des guides, des mentors, des meneurs d'âmes qui m'ont enseigné plus que tout autre la gentillesse et l'humanité. La stabilité et le réconfort que vous m'avez prodigué tout au long de ce travail et de ma vie ont été sans failles, l'énergie que vous déployez me fascine, ma gratitude est sans limites, je vous aime.

**Maman, Florine, Tristan**, merci pour votre soutient et votre amour, rien n'est jamais parfait mais ceci est proche d'un idéal et surtout d'un extrême secours, vous êtes aussi et bien plus que vous ne le pensez à l'origine de ce travail. Vous m'avez apporté une stabilité agréable, ou non, qui me permet d'avancer, vous êtes un gouvernail, des guerriers, je vous aime.

**Florent**, je ne suis pas sûre qu'une définition exacte et universelle de l'amitié puisse un jour exister mais sans décrire ce qui nous relie, tu sais que toi aussi tu es là, dans ma vie comme entre ces lignes à m'accompagner, j'attends maintenant simplement de pouvoir à nouveau plus en profiter, je t'aime mon poulet, **Elodie, Jessica**, on partage je crois quelque chose d'unique tous ensemble et je vous suis très reconnaissant pour cela, on a créé un endroit particulier qui nous rend extrêmement chanceux, que cela soit encore long.

**Anne**, les mots qu'on apprécie tant manier et échanger, parfois trouvent leur limite, ici il y en a surement une, merci pour tout, j'ai hâte d'avoir à nouveau le temps de prendre le temps avec toi et **Arsène**.

Merci à tous ceux aussi qui partagent du temps avec moi sur les terrains, **Damien**, **Maryline**, **Alizah** mes partenaires et toute mon équipe de badminton, vous m'apportez un havre qui permet de ne pas penser, c'est ressourçant et indispensable.

Merci à tous ceux rencontrés depuis 2011 à l'AMSED, **Lavi, Emilie, Sanae, Tarek, Rachida**, un carrefour où des vies, des âmes si différentes se croisent.

Merci à ceux qui sont là depuis longtemps, **Adeline, Mélisa, Gaelle, Jen** et les plus récents **Charlène, Tom, Jean, Marianna,** qui ont aussi de près ou de loin accompagné le déroulement de cette thèse.

Un clin d'œil à la rue Apffel, une colocation incroyable ou presque 20 personnes ont été plus ou moins établies pendant 2 ans pour ma part, félicitations **Pau**, c'est fait, sincèrement merci **Tim**, c'est toujours un plaisir de te voir, bon vent à toi **Caro**, brille, merci pour toutes ces corrections de copies et repas partagés **Chloé**, vole très haut **Kévin**, *animo*, **Sarai** et **Laurence** merci pour votre bonne humeur communicative, merci pour toutes ces soirées improvisées **Clément**, **Esteban** à très vite.

**Sara**, les histoires peu communes, j'en avais pourtant assez l'habitudes, mais toi tu es une découverte de ma vie d'adulte, le temps ne se rattrape jamais, c'est vrai, mais rien ne nous empêche de tenter, je suis heureux du partage d'aujourd'hui et toi aussi, vous aussi, **Jan, Noah** et récemment **Luca** avez accompagné ce travail.

« L'époque heureuse quand toute notre bande était enthousiaste, naïve et solidaire quand tous les rêves étaient autorisés. » Amin Maalouf, *Les désorientés*

Merci à toi, qui m'accompagne, merci de ton inconscience, peut être même de ta naïveté quant à la difficulté de l'exercice, merci d'avoir fait ce choix, merci d'avoir repoussé les limites, l'inconnu a été un délice. Cette étape a commencé au Népal, pour quoi ne pas y repartir. Libre, je suis prêt pour la prochaine aventure.

Home, 11:53

# PREFACE

In the collective imagination, fungi are known mainly for their sporophores or macroscopic spore-bearing structures, however they represent an enormous and varied group of living organisms. Fossils attest to their presence on Earth beginning in the Silurian period, and via mycorrhizae they would have evidently aided the first plants to colonize the newly emerged soils of the planet. Fungi are found in a large number of ecological niches where they play an essential role in biogeochemical cycles. Existent in symbolism, heraldry, mythology, and even in popular expression, fungi have been long considered mystical or supernatural.

History has left few written traces pertaining to fungi and their uses, however certain vestiges from the beginning of our era have been found in Discoride's *De materia medica*. There, the therapeutic utility of twenty species was detailed, as well as certain designations that remain in use in modern times, *Amanita* and *Boletus*.

Different ways of naming fungi are related to their deadly reputation; Seneca named them *voluptarium venenum* ("voluptuous poison") and Pliny the Elder named them *anceps cibus* ("hazardous food"). Etymology has long tied these organisms to their harmful properties. Their current appellations, denoted by the suffix *-mycete* or the word *Fungi*, attest to this; *-mycete* comes from the Greek *mykes* ("mucus"), due to these organisms' proximity to mold and putrefaction, while *Fungi* comes from a popular contraction between the Latin words *funus*, for funerary, and *ago*, "to produce", which thus denotes the numerous deaths caused by fungi.

Fungi have been long considered as primitive or degenerated plants, even to the point where they were the lowest-classed organisms in the *Scala naturæ* in the Middle Ages due to their exclusive association to death and putrefaction. With a reputation for being the "excrement of the earth", fungi have been used in black magic rituals during the preparation of elixirs thanks to their hallucinogenic properties. They have been used in similar manners

by shamans, oracles, and other healers throughout history in many different civilizations on Earth.

The first studies that focused on these organisms supposedly date back to the sixteenth century, with descriptions of certain species being published by Junius, Reiner Solenander, and Fabi Columna, as well as some classification attempts carried out by Hermolaus, Charles de L'Ecluse, and Matthiole. At the end of this century, Giambattista della Porta, who was interested in dissecting the divine and the magic of natural mechanisms of life, was the first to affirm that fungi do not reproduce through seeds.

It wasn't until the seventeenth century when the invention of the microscope allowed for the observation of the invisibles parts of fungi: spores, thalli, and other mycelia were described without a knowledge of their function.

*"Plants with a secret marriage"*

*Carl Von Linné, Species Plantarum, 1753*

Carl Von Linné posed the systematic bases for their classification with his *Systema Naturae* in 1753 via the introduction of a binomial nomenclature and of a hierarchization of the classification, which divided living organisms into three kingdoms: bacterial, animal, and plant. At this time, fungi, molds, algae, and some ferns were considered as being members of the 24 classes of plants and were classed in the cryptogam category, which included plant organisms whose reproductive organs are not evident or hidden.

In 1975, the science which devoted itself to study fungi was baptized *mycology*, a term proposed by Jean-Jacques Paulet. This term replaced the other proposed word, *fungology*.

Due to fungal development, and their capricious and ephemeral culture which was not yet well understood, mycology was deprived of a great number of means that have permitted other branches of natural history to advance more rapidly. Moreover, *in vitro* observations do not give more than a vague idea of the global physiology of fungi because a great number of their characteristics disappear in a laboratory setting.

In 1827, fungi were still considered by most to be products of spontaneous generation. In 1832 Elias Magnus Fries established the bases of modern mycology by presenting the first

systematic classification of fungi in *Systema Mycologicum*. Between 1836 and 1840, Stephan Landislaus Endlicher proposed in *Genera plantarum secundum ordines naturales disposita* a separation of the kingdom *Plantae* into cormophytes, plants whose structure is composed of a stem and leaves, and thallophytes, inferior or non-vascularized plants that possess an undifferentiated body or thallus. This classification grouped fungi, molds, lichens, hepaticas, algae, and even cyanobacteria.

After the publication of Charles Darwin's *The Origin of Species* in 1859 and the popularization of the evolution theory, botanists ceased believing in the spontaneous generation of fungi and began to remove them from classifications of vascularized plants, but naturalists continued to classify these organisms in plant categories until the mid-twentieth century. In 1969, however, they were finally placed into their own individualized kingdom: *Fungi*. It was the botanist Robert Harding Whittaker who proposed a division of living beings into five kingdoms: *Procaryotae, Protozoan, Plantae, Animalia,* and *Fungi* (Whittaker, 1969).

Thanks to the work of Carl Woese and Georges E. Fox in 1977, this classification was shaken with the confirmed discovery of archaebacteria and the creation of not only their own domain, but also of their own kingdom.

The advent of technological improvements in genomic sequencing allowed the individualization of the fungal kingdom to flourish. Indeed, the comparison of gene sequences effectively permitted a retracement of the evolutionary history of living beings following the modification of their genome. These technological improvements not only called into doubt the *Fungi* kingdom, but also the division into six kingdoms, the clarity of the limit between eukaryotes and prokaryotes, and the certainty of the division between the animal and plant kingdoms, which meant that the unity of the fungal kingdom was no longer more than a pseudo-concept.

In 2005, a new classification was proposed and revised in 2012 by Adl *et al*. This classification is still the object of many discussions and debates. At the same time, the opisthokont group appeared as a proposition to bring closer organisms with varied appearances, such as fungi and metazoans. This approximation of the taxon was founded on the study of several genes analyzed individually, which lends credence to the theory. Based on this molecular evidence, other synapomorhies appeared and confirmed the holophyly of this group.

Fungi are currently considered an artificial and polyphyletic taxon, comprised of two different lines: eumycetes, or real fungi, close parents of animals; and pseudomycetes, which are closer to plants. This last group is the fruit of numerous evolutionary convergences and this leads to the idea that it will change very soon.

Overall, fungi have surely not finished making us rechecking, changing, and perfecting their classification.

# LIST OF FIGURES

# LIST OF TABLES

# ABBREVIATIONS

| | |
|---|---|
| AIDS | Acquired Immune Deficiency Syndrome |
| AmB | Amphotericin B |
| AM3 | Antibiotic Medium 3 |
| ANM | Anisomycin |
| A-site | Aminoacyl-tRNA site of the ribosome |
| aa-tRNA | Aminoacyl-tRNA |
| BLC | Blasticidin S |
| CGD | Candida Genome Database |
| CHX | Cycloheximide |
| CRY | Cryptopleurine |
| Cryo-EM | Cryo-Electron-Microscopy |
| Da | Dalton unit |
| DC | Decoding Center |
| DTT | Dithiothreitol |
| EFs | Elongation Factors |
| eIFs | eukaryotic Initiation Factors |
| eRFs | eukaryotic Release Factors |
| E-site | Exit tRNA site of the ribosome |
| GEN | Geneticin |
| LAC | Lactimidomycine |
| LSU | Large Sub-Unit |
| MIC | Minimum Inhibitory Concentration |
| mRNA | messenger RNA |
| OD | Optical Density |
| PDB | Protein Data Bank |

| | |
|---|---|
| PEG | PolyEthylene Glycol |
| PHY | Phyllantoside |
| PTC | Peptidyl Transferase Center |
| P-site | Peptidyl-tRNA site of the ribosome |
| RAT | Riz - Agar – Tween medium |
| RPMI | Roswell Park Memorial Institute medium |
| r-protein | Ribosomal-protein |
| rRNA | ribosomal RiboNucleic Acid |
| S | Sevdberg |
| SSU | Small Sub-Unit |
| SU | Sub-Unit |
| tRNA | transfert RiboNucleic Acid |
| YPD | Yeast extract Peptone Dextrose |
| Å | Angstrom unit (1 Å = $10^{-10}$ m) |
| 5-FC | 5-fluorocytosine |

- Amino acids are described according to the standard nomenclature using either one or three letters, nucleotides are described using a one letter code.

- All ribosomal proteins are named according to the current nomenclature (Ban *et al*., 2014)

# I. *CANDIDA ALBICANS*, AN OPPORTUNISTIC PATHOGENIC YEAST

## 1. GENERALITIES

*Candida albicans* is a cosmopolitan polymorphic yeast. It is the most frequently occurring pathogenic fungus in humans, and it is responsible for diverse and common infections, such as oral candidiasis or vaginitis. This yeast has complex adaptation mechanisms, which allow it to survive in diverse environmental conditions. These also cause a large amount of infections, which may be superficial (cutaneous or mucosal) or deep, such as systemic candidiasis (Segal, 2005).

*C. albicans* is a natural part of the vaginal and orogastrointestinal flora of humans and many other homeothermic species (Odds, 1988); it is found in at least 70% of the healthy population (Ruhnke & Maschmeyer, 2002). Under normal conditions, an equilibrium exists between the host and the microbes who maintain the commensal state of *C. albicans*, but in some cases it becomes a pathogen with the help of certain factors such as an immunodeficiency or a decrease of the bacterial population. *C. albicans* infections also represent the majority of fungal infections in AIDS patients. These patients predominantly develop thrush or oropharyngeal candidiasis, which can lead to malnutrition and interfere with the absorption of medication (Sardi, 2016). *C. albicans* is the most common fungal and eukaryotic nosocomial agent worldwide (Sydnor & Emily, 2011). It is the third etiological factor of septicemia in the United States, and estimations of annual incidence are of 24 in 100,000 patients, with a mortality rate of 40% (Perloth *et al.*, 2007). Furthermore, the incidence of candidemia has greatly increased during the past 2 decades (Perloth *et al.*, 2007).

Present-day treatments have an extremely high cost of 2 to 4 billion dollars per year in the United States only, and are mostly inefficient (Perloth *et al.*, 2007). This is due to the fact that the yeast tends to resist modern drugs, especially in at-risk-departments where fungistatic and not fungicidal doses are used to combat yeast. Most importantly, however, there are

severe secondary effects that arise from therapy due to the fact that the cellular targets in yeast are often shared with humans (Berman & Sudbery, 2002).

It is necessary to decipher the physiology and adaptation mechanisms of *C. albicans* in order to define new therapeutic targets and to create more efficient and less toxic treatments.

| Factors | Examples |
|---|---|
| **Immune deficiencies** | Physiological (newborns, elderly people) or acquired (HIV infections, malignancies) |
| **Endocrine factors** | Pregnancy, oral contraceptives, diabetes, hypothyroidism, Addison's disease |
| **Nutritional factors** | Carbohydrates, iron and vitamin deficiencies |
| **Endogenous hyposalivation** | Sjögren's syndrome |
| **Genetic factors** | Chronic familial candidiasis |
| **Antimicrobial agents** | Broad-spectrum antibiotics, antiseptics |
| **Immunosuppressive treatments** | Corticotherapy, antitumor therapy |
| **Exogenous hyposalivation** | Addictions, radiotherapies, psychotropic treatments |
| **Mechanical factors** | Traumatism, dental prostheses |
| **Medical implants** | Catheters, endothoracic tubes, artificial cardiac valves, articular prostheses |
| **Smoking** | |

*TABLE 1: MAJOR FACTORS THAT FAVOR CANDIDAL INFECTIONS (ODDS, 1998; PERLROTH ET AL., 2007; SINGH ET AL., 2015; MARTINS ET AL., 2015)*

# 1. DISCOVERY AND TAXONOMY

Hippocrates was the first person to report fungal infections in the 5th century B.C., when he described thrush (candidiasis) (Ainsworth, 1986). The first description of a yeast as an etiologic agent of an oral candidiasis was made in November 1839 in Germany by Bernhard von Langenbeck (Knocke & Bernhardt, 2006). This particular yeast did not escape the controversy of fungal classification, so during almost two centuries it did not have an established name accepted by the scientific community. This yeast had several names throughout the years: *Oidium albicans* (Robin, 1853), *Saccharomyces albicans* (Ress, 1877) and *Monila albicans* (Zopf, 1890). It was Christine Marie Berkhout who finally introduced the denomination *Candida albicans* in 1923, and for the first time, the differentiation between a medical yeast and a vegetal cell was made. The name comes from the Latin expression *toga candida* which was used to describe the white garments worn by the Roman Senate members (Calderone, 2002). Consequently, this classification became *nomen conservandum* and was adopted internationally in 1939 during the third International Congress of Microbiology of New York (Samson, 1990).

*C. albicans* was considered an asexual yeast and, as such, used to be classified in the phylum of *Deuteromycota* for *fungi imperfecti*, or imperfect fungi. The presence of sexual characteristics is necessary to be classified in the phylum of *Ascomycota*, which initially excluded *C. albicans*, but due to genomic sequence comparison and non-sexual phenotypic characteristics, this finally changed and scientists integrated *C. albicans* into the *Ascomycota* phylum (Taylor, 1995). Today, the *Deuteromycota* phylum is no longer recognized as a taxon and several laboratories have shown by experimental approaches that *C. albicans* does indeed have a sexual cycle, or mating (Hull *et al.*, 2000; Magee & Magee, 2000).

The present classification of *C. albicans* has not changed since 2005:

Domain: *Eukaryota* (Whittaker & Margulis, 1978)

Subdomain: *Unikonta* (Cavalier-Smith, 2002)

Super kingdom: *Opistonkonta* (Adl *et al.*, 2005)

Kingdom: *Fungi* (R.T. Moore, 1980)

Subkingdom: *Dikarya* (Hibbett, T. Y. James & Vilgalys, 2007)

Phylum: *Ascomycota* (Cavalier-Smith. 1998)

Subphylum: *Saccharomycotina* (O.E. Erikss. & Winka 1997)

Class: *Saccharomycetes* (O.E. Erikss. & Winka 1997)

Order: *Saccharomycetales* (Kudryatsev, 1960)

Family: *Saccharomycetaceae* (G. Winter, 1881)

Genus: *Candida* (Berkhout, 1923)

Species: *albicans* (supposition Robin, 1853)

## 2. PHYSIOLOGY AND GROWING CONDITIONS

*C. albicans* is known for its high adaptability, and can be found on different media: minimum, synthetic, poor, or rich, but it needs organic carbon, nitrogen and phosphate sources. It can grow in conditions ranging from 2 to 8 on the pH scale and between 20 to 40°C with an optimum temperature at 37°C (Sheperd, 1990). Finally, this yeast is a prototroph for biotin.

Similar to mammals, the $CO_2$ concentration inside this organism is almost 140 times (5%) higher than in atmospheric air (0,036%), and during its life cycle, *C. albicans* can be exposed to drastically different $CO_2$ concentrations (Bahn & Muhlschlegel, 2006). During cutaneous superficial infections, *C. albicans* needs to be adapted to a lower level of $CO_2$ than when it infects deep tissues, as the skin is in balance with the atmosphere (Frame *et al.*, 1972). This organism is a facultative anaerobe and it is at least 4 times more resistant to antifungal treatments when it is in anaerobic rather than aerobic conditions (Dumitru *et al.*, 2004).

## 3. GENOME

Even given its medical and scientific importance, the elucidation of the *Candida albicans* genome took comparatively longer than for other organisms. This fact is due to the difficulties faced during experimental genetic approaches. Since it is a diploid organism which has an incomplete sexual cycle, conventional genetic analyses were not efficient or applicable to *C. albicans*. In spite of these obstacles, alternative strategies were developed and are available today (Noble & Johnson, 2007; Kabir & Hussain, 2009).

In 2004, the complete sequence of *C. albicans* was published. It is composed of 8 chromosome peers where one can find ribosomal information, the biggest of which is named R, and the others are numbered from 1 to 7 according to their decreasing sizes (Jones *et al.*, 2004). Its haploid genome corresponds to 16Mb and codes 6400 genes, with less than 5% of introns, whose 774 genes are specific to the *Candida* genus with mostly unknown functionality (van her Hoog *et al.*, 2007; Kabir & Hussain, 2009). A lot of genes are conserved between *Saccharomyces cerevisiae* and *C. albicans*, and thanks to this similarity, several mechanisms of biological processes were discovered in *C. albicans* (Biswas *et al.*, 2007). However, the *C. albicans* genome is extremely dynamic with highly frequent translocations, deletions, and chromosomic duplications, and this makes gene function determination complicated. Due to this, there are no two lab strains that have the same karyotype, even if they share the same parental strain.

The *C. albicans* genetic code is not exactly the same as the universal genetic code. Indeed, the CUG codon, which normally specifies leucine, specifies serine in these species (Santos *et al.*, 1993), moreover it is found in almost 70% of all *C. albicans* genes (Odds *et al.*, 2004). This is an unusual example of a departure from the standard genetic code, and most

departures such as this one are in start codons (Arnaud *et al.*, 2009; Tourisol *et al.*, 2003) even present for ribosomal proteins (Abramczyk *et al.*, 2003). This alteration may help *C. albicans*, in some environments by inducing a permanent stress response, a more generalized form of the heat shock response (Santos, 1999). Recently, it has been shown that *C. albicans* tolerates ambiguity from multiple codons and not only from the CUG codon (Simoes *et al.*, 2016).

The most common hypothesis about the genomic instability and particularity of *C. albicans* is that these allow this opportunistic pathogen to acquire enough genetic diversity (Bezzera *et al.*, 2013) in order to survive in different ecological niches (Rustchenko, 2007; Kabir & Hussain, 2009) and to be more ready to colonize the host (Miranda *et al.*, 2013).

A centralized database for all scientists who are working on the *Candida* yeast genus exists. It is possible to find there an important amount of information about genes, metabolism, and physiology (Costanzo *et al.*, 2006). Different yeast genomes are available as well and there are several corrected and revised assemblies of the *C. albicans* genome. It is accessible on the Internet without a subscription at the following website: The *Candida* Genome Database (http://www.candidagenome.org).

## 4. *CANDIDA ALBICANS* CLINICAL ISOLATE SC5314

The clinical isolate SC5314 is the best characterized *C. albicans* strain (Fonzi & Irwin, 1993). The strain was isolated from a patient with a generalized infection and is highly susceptible to all clinical antifungal drugs (Odds *et al.*, 2004), and it is also extremely virulent in animal models (Odds *et al.*, 2000). It is the strain used most frequently for virulence, antifungal susceptibility studies, and molecular and biochemical analysis, and it was the first strain to be sequenced (Jones *et al.*, 2004). The last assembly of its genome is the 22$^{nd}$, improved and corrected this year (Berman & Forche, 2016).

# 2. *CANDIDA ALBICANS*: A MORPHOLOGIC, METABOLIC, AND VIRULENT ALL-TERRAIN PATHOGEN

## 1. MICROSCOPIC POLYMORPHISMS AND THEIR REGULATION

The biggest characteristic of this yeast is its capacity to grow in different morphological forms, of which six are currently identified: blastospores, hyphae, pseudohyphae, shmoos, chlamydospores, and hyperpolarized buds (Whiteway & Bachewich, 2007). This diversity is considered as a survival strategy to allow its dissemination in the host (Berman & Sudbery, 2002). Blastospores, hyphae, and pseudohyphae are the most frequently found forms on the infection site (Sudbury *et al.*, 2004). When exposed to an environmental stress signal, this yeast can quickly and reversibly switch from one of these three forms to another (Whiteway & Bachewich, 2007). In laboratories, an effort is made to obtain only one morphological form in the medium for biomass production, and this is usually blastospores, but in other contexts, like diagnostics, scientists utilize other morphological forms such as hyphae or chlamydospores to identify *C. albicans* in the studied sample.

Blastospores are ovoid cells around 3 to 5 µm who reproduce by asymmetric budding. Budding sites depend on the temperature. Parental cells generate a blastoconidium that is separated by a septum and produces a daughter cell. Separation of parental and daughter cells takes place right after cytokinesis and before the daughter cell reaches the size of the parental cell (Whiteway & Bachewich, 2007). Major constituents of the cell wall are glucans, mannans, and chitin, and the amount of these constituents changes depending on the morphological form (Chaffin *et al.*, 1998). The presence of glucose as a unique source of carbon, a pH below 6.5 - 7, a temperature below 35°C, and an inoculum superior to $10^6$ cell/mL are factors that favor *C. albicans* growing into blastospores *in vitro* (Odds, 1988).

Hyphae are microscopic tubes, long and thin, around 2 µm in diameter, that hold within several cellular entities divided by septa, whose parallel walls do not show visible constriction at the separation sites. These come from blastospores or other hyphae. Their formation is initiated by a germination process, where the nucleus is separated at the future septum site; after that, the first nucleus goes back to the parental cell and the second goes

forward into the germination tube. In comparison to blastospores, hyphae have polarized growing enhanced by the polarisome and the Spitzenkorper, both located at the germination tube extremity (Odds, 1988; Berman, 2006). The cell wall is composed of three times more chitin than that of the blastospores (Chaffin *et al.*, 1998). The aggregate composed by hyphae and their lateral buds is called mycelium (Odds, 1988). A nutrient deficiency, a $CO_2$:$O_2$ ratio superior to 2, a pH superior to 6.5 - 7, an incubation temperature superior to 35°C, an inoculum below $10^6$ cells/mL, and the presence of serum or N-acetylglucasomine as a nitrogen source are the principal factors of hyphae development (Odds, 1988). As mentioned before, the observation of filamentation in rabbit plasma incubated at 37°C was for a long time an identification technique used for *C. albicans*. However, since the discovery of *Candida dubliniensis* and *Candida africana* filamentation (Sullivan *et al.*, 1995) new techniques have been developed.

Pseudohyphae were seen for a long time as an intermediary form between the two previously described forms, before being considered as a distinct form (Sudbery *et al.*, 2004). The growth and the cell cycle are essentially the same as for blastospores, but the major differences are that the cells are longer by no more than 2.8 μm in diameter, there is unipolar budding, and no separation between parental and daughter cells (Berman, 2006; Whiteway & Bachewich, 2007). Pseudohyphae can grow from the two previous forms described, moreover they can be as long as hyphae and the only difference is the constrictions at septa sites. Since they are so similar, they are both called filamentous forms of *C. albicans* (Odds, 1988; Sudbery *et al.*, 2004). A pH at 6, an incubation temperature at 35°C, a nitrogen deficiency (Sudbery *et al.*, 2004), or a high phosphate concentration (Hornby *et al.*, 2004) are conditions that favor the pseudohyphae formation.

Chlamydospores are big spherical cells ranging in size from 8 to 12 μm with a thick cell wall. They are observable *in vitro* during long and unfavorable culture conditions but rather rarely *in vivo* (Chabasse *et al.*, 1988). Nutrient deficiency, incubation temperature lower than 30°C, a low oxygen concentration, small inoculum, an absence of light and a presence of detergent are favorable conditions under which to observe chlamydospores (Jansons & Nickerson, 1970). One of the *C. albicans* identification tests consists of highlighting the presence of chlamydospores in an RAT medium.

Shmoos are cell elongations in an opaque phase that are characteristic of mating-competent cells. They are observed in a cell mix containing opposite sexual types (Whiteway

& Bachewich, 2007) The regulation of phenotypic switching between opaque and white phases would restrict the apparition of shmoos only in suitable host niches (Morschhauser, 2010).

Hyperpolarized buds are close to hyphae in structure, except for a constriction between blastopores and the elongated bud. There is no DNA replication in the close bud and their biological role is not clear. They appear during specific cellular stress as exposition to DNA synthesis inhibitors (Whiteway & Bachewich, 2007), and inhibition of essential cell cycle genes (Bachewich *et al.*, 2003).

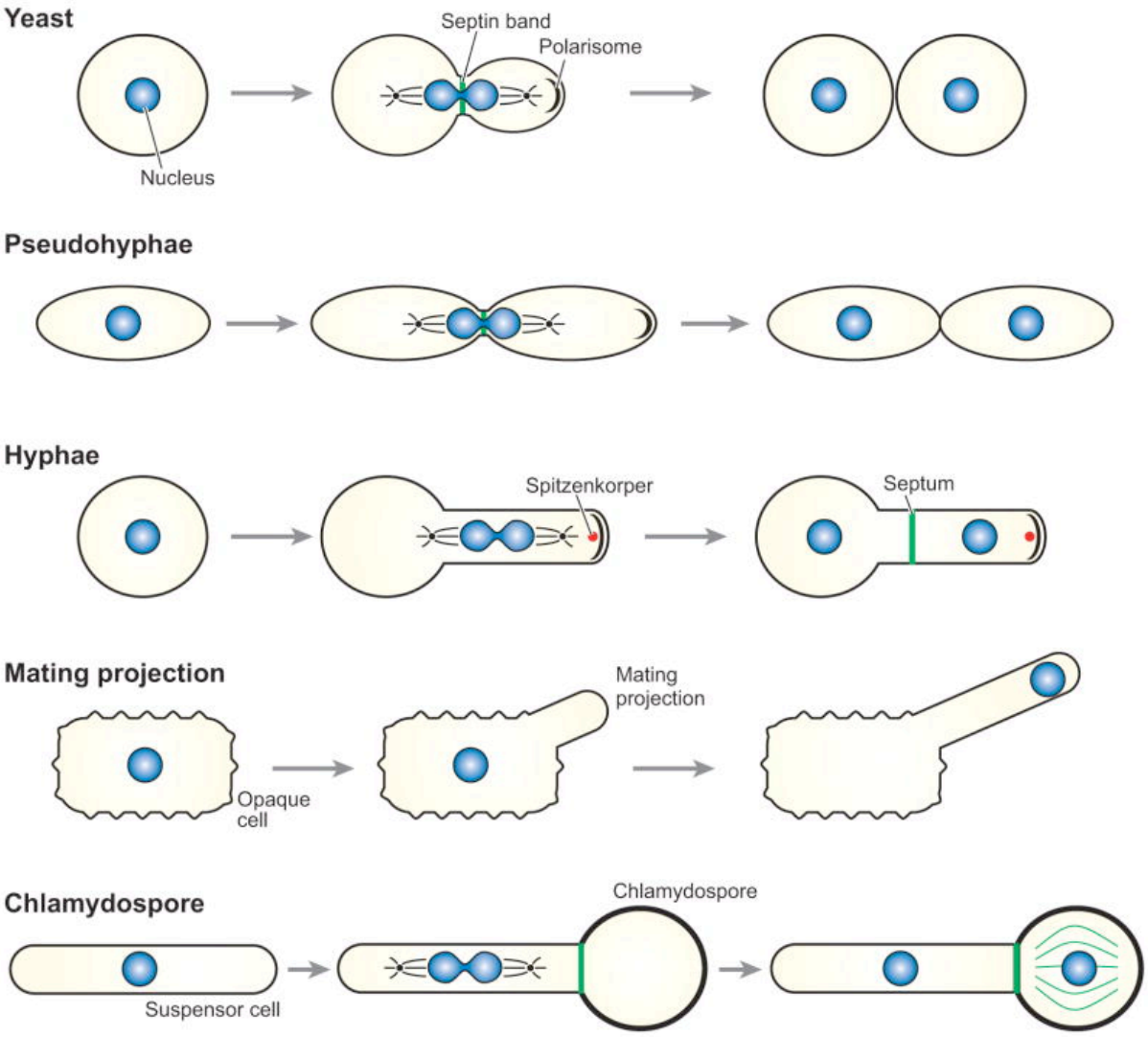


*FIGURE 1: MORPHOLOGICAL FORMS OF CANDIDA ALBICANS (WHITEWAY & BACHEWICH, 2007)*

## 2. REGULATION OF *CANDIDA ALBICANS* POLYMORPHISM

*C. albicans* has the capacity to switch from a filamentous form to blastopores and *vice versa*. This morphological transition is induced by several chemical and environmental signals such as pH, $O_2$ concentration, nutrient deficiencies, cell density, and even the support, but the most important signal for filamentous growing is an incubation temperature higher than 35°C (Hall *et al.*, 2009). All of these conditions influence the morphological behavior of *C. albicans* by means of complex pathways directed by transcriptional regulators (Biswas *et al.*, 2007). As was already explained during the *C. albicans* genome description, there is a high variability between two yeasts of the same strain, and this is also the case for the polymorphism phenotype (Merson-Davies & Odds, 1989).

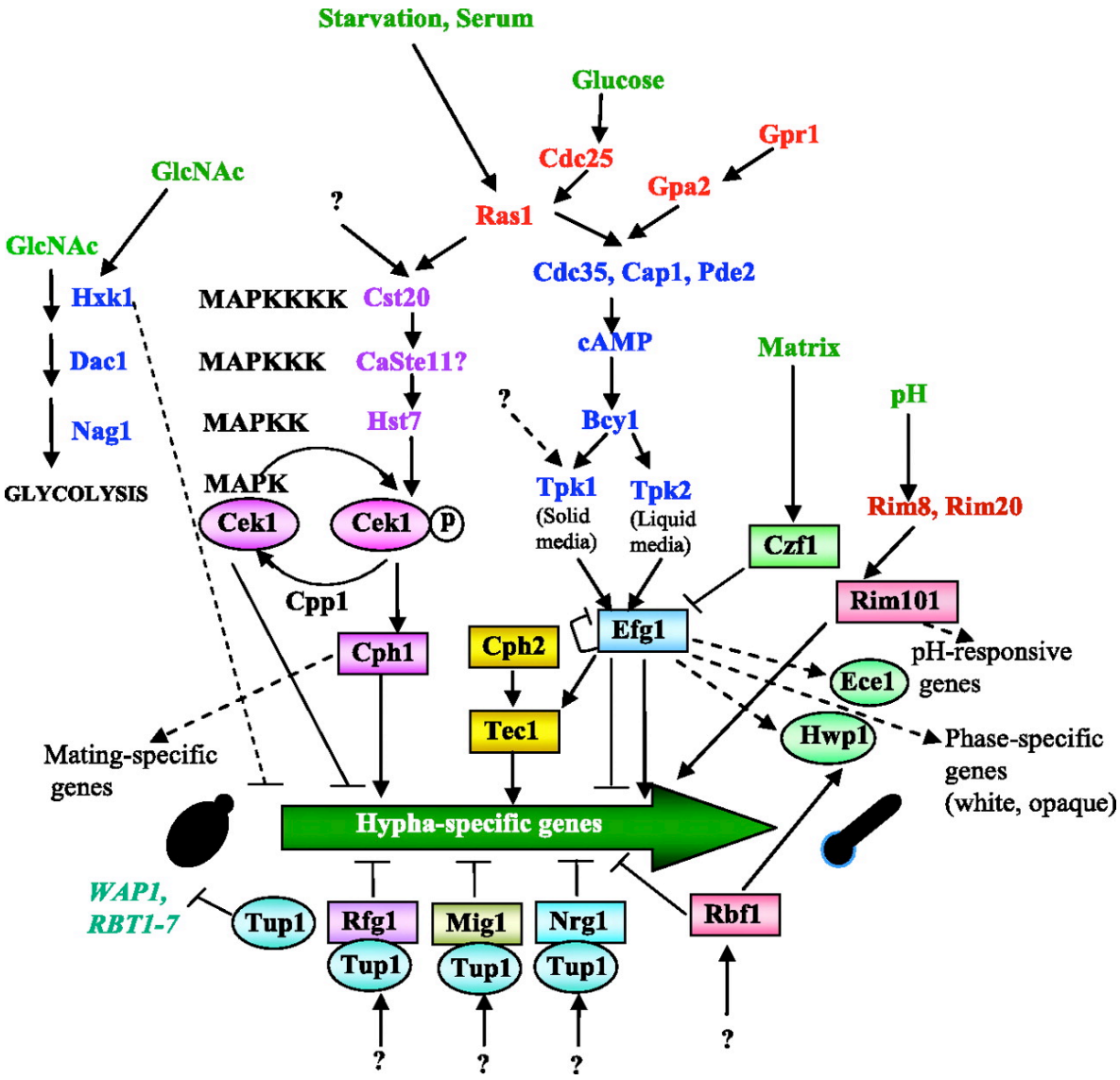


*FIGURE 2: REGULATION OF DIMORPHISM IN C. ALBICANS BY MULTIPLE SIGNALING PATHWAYS (BISWAS ET AL., 2007)*

*Multiple signaling pathways regulating the transition from yeast form to hypha form. Transcription factors are framed by rectangles.*

## 3. MACROSCOPIC MORPHOLOGY

The previous morphological forms described induce different possible colony aspects on a solid medium. Almost 400 colonial morphologies have already been described (Rustchenko-Bulgac *et al.*, 1990), though only 5 types are the most common (Radford *et al.*, 1994). These differences are induced by the ratio between blastospores, pseudohyphae, and hyphae inside the colonies. Smooth colonies are formed by blastospores, and when more filamentous forms are present, the colony will look hairier (Radford *et al.*, 1994); it has been shown that this variability is related to different levels of adaptation to the environment (Vargas *et al.*, 2004).

In addition to this, *C. albicans* is able to undergo reversible and hereditary phenotypic switching induced by different external stimuli. The best known switching mechanism is the white-opaque system. It is easily identified on a solid medium, where there are two colony phenotypes: white (standard, white, and smooth colony) formed by common blastospores, and opaque (larger, grey, and flattened colony) formed by elongated and blastospores that are at least three times bigger than white-phase blastospores. In the host, opaque-phase cells are more efficient ($10^6$ times more) than white-phase cells for mating. Despite this, they are weaker and more instable, which means that genomic recombinations are certainly limited to specific environmental niches (Soll, 2009).

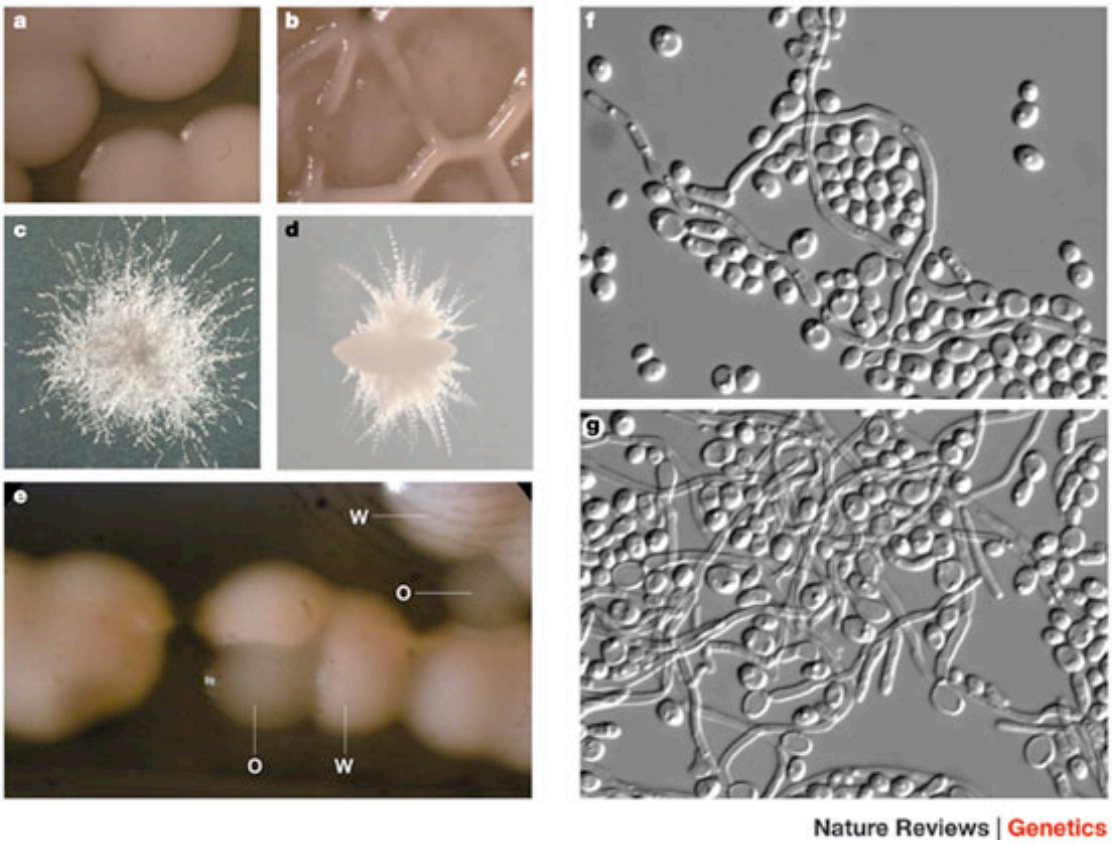


*FIGURE 3: COLONIAL MORPHOLOGIES OF C. ALBICANS (BERMAN & SUDBERY, 2002).*

*One strain may have several colonial morphologies on different media or following phenotypic switching. a - smooth colonies on medium SDC (Salt Dextrose Complete); b - pleated Colony on middle Spider; c - Colony hairy milk on medium-Tween; d - Colony embodied in a medium rich in sucrose matrix; e - phenotypic switching on white-opaque medium SDC, W - colonies white phase, O - Colony opaque phase; f, g - Colonies folded, hairy incorporated and are formed of a mixture of blastospores, pseudohyphae, and hyphae. The photos show cell populations derived from different portions of a wrinkled colony.*

# 4. BIOFILM

Biofilms are formed by unicellular microorganisms that stick to each other to form a community and that, most of the time, are irreversibly attached to a support by an exopolymeric matrix composed mostly of polysaccharides, which can be compared to the rate of growth of planktonic cell phenotypes (Donlan & Costerton, 2002). There are biofilms on extremely diverse supports including living tissue, medical devices, or other supports found in aquatic environments (Donlan, 2002) and it is the predominant form of microorganism growth (Costerston *et al.*, 1995). It first appeared around 325 billion years ago, and this type of organization allowed microorganisms to survive in hostile environments (Hall-Stoodeley *et al.*, 2004).

Biofilms in general cause many problems in industrial and agricultural fields, but *C. albicans* biofilms specifically are involved in many infections and human diseases, though they also have positive effects and essential implications like the biofilm found in the intestinal flora. *C. albicans* biofilms are found on most medical implants such as catheters, contact lenses, or pacemakers (Kojic & Darouiche, 2004), but also in cases of living tissue infections (Douglas, 2003).

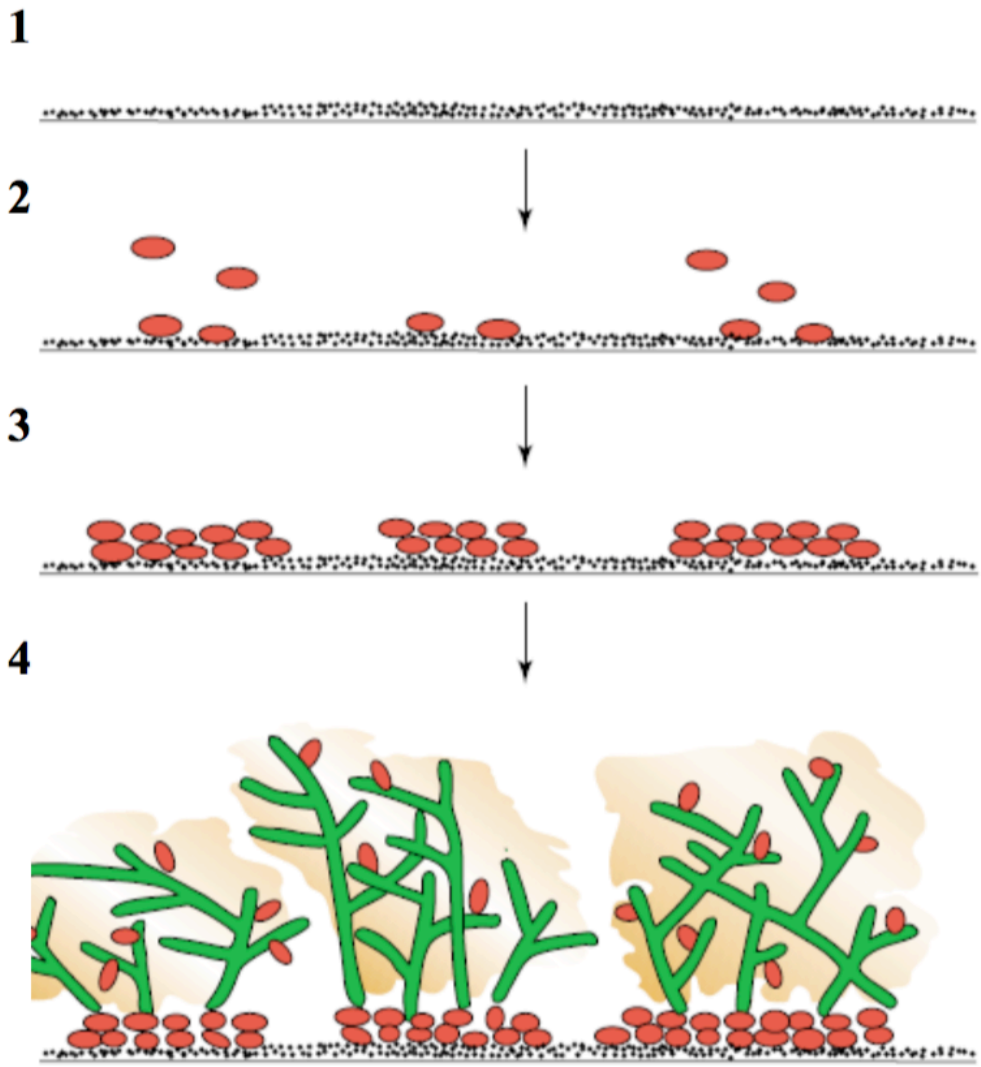


*FIGURE 4: THE STAGES OF DEVELOPMENT OF CANDIDA ALBICANS BIOFILM (DOUGLAS ET AL., 2003)*

*1 – The surface of a catheter covered in a film composed of proteins from the host (black dots); 2 – Initial attachment of blastospores (red) to the surface; 3 – Formation of the basal layers of microcolonies; 4 – Development of microcolonies by the addition of a top layer comprised mainly of filamentous forms (green) and by the production of an extracellular matrix (yellow) that surrounds the two layers of the microcolony (Douglas, 2003).*

The development of *C. albicans* biofilm (which lasts around 24 to 48 hours) follows the typical stages of biofilm development, with one particularity: the presence of a combination of morphological forms in the microcolonies. At the beginning of the process, the blastospores adhere to the surface and form a basal layer. This contact with the surface

triggers morphogenesis (after 3 to 6 hours following the attachment), which leads to the formation of a second layer, composed primarily of hyphae and pseudohyphae (Figure 4) (Chandra *et al*., 2001; Douglas, 2003). The mechanisms which lead to the development of *C. albicans* biofilms following the attachment to surfaces are currently unknown. (Seneviratne *et al*., 2008; Ramage *et al*., 2009; ten Cate *et al*., 2009).

## 5. VIRULENCE

Numerous virulence factors are associated with *C. albicans* pathogenesis. *C. albicans* has a lot of surface receptors, called adhesins, which allow it to interact with the host cells' surface by attachment to the external plasmic membrane protein. There are covalent (Hwp1p protein), reversible (lectin bond), and non-covalent bonds (agglutinin-like-sequence protein family) involved in this adhesion mechanism (Sheppard *et al.*, 2004). Moreover, *C. albicans* has a range of secreted hydrolytic enzymes expressed differently according to environmental factors and the yeast morphology. These include the secreted aspartyl proteinase family, phospholipases, and even lipases who are involved in protein degradation, cellular and tissue structure degradation, and immune system avoidance (Borg-von Zepelin, 1998). However, morphological and phenotypic switching have a big impact in pathogenic virulence. Nevertheless, all these factors do not seem to be able to unsettle the normal host defenses, but they do allow the pathogen to colonize the skin and the mucosa in order to be a part of the commensal flora. On the other hand, for a weakened or immunocompromised patient, this natural equilibrium is tilted in the yeast's favor (Odds, 1988). Indeed, the *C. albicans* polymorphism plays an important role in the infection process. Filamentous forms are phagocytized with greater difficulty due to their morphology and the fact that their consumption can cause the macrophage's death. More than that, there can be an intracellular multiplication of blastopores inside macrophages and a possible destruction of them by filamentation. These forms are involved in the epithelium and endothelium invasion (Karkowska-Kuleta *et al.*, 2009), and as such, blastospores contribute to systemic infection by blood dissemination (Saville *et al.*, 2003).

Morphologies are important and complementary to infection to such an extent that published studies demonstrate that only filamentous mutants (Bendel *et al.*, 2003) or

nonfilamentous mutants (Lo *et al.*, 1997) are completely nonvirulent. This is useful in order to highlight that there is a cross regulation between morphological genes involved in the morphological cell differentiation but also in biofilm development and other virulence factors such as hydrolases and adhesins (Kumamoto & Vinces, 2005). If morphological transition is involved in infection, then phenotypic transition is, as well. It has been shown that virulent strains switch more frequently than commensal strains (Jones *et al.*, 1994). This phenotypic switching reversibly affects pseudohyphae and hyphae formation, hydrolase secretion, epithelium adherence, antigenicity, antifungal drugs, and immune system susceptibility (Karkowska-Kuleta *et al.*, 2009). More than that, opaque-phase cells are more implicated in cutaneous infection than white-phase cells, who are much more aggressive in other kinds of infections such as systemic ones (Kvaal *et al.*, 1999).

## 6. INCIDENCE, EPIDEMIOLOGY, AND COST

Being a ubiquitous yeast as an endo-saprobiont of mammals, *C. albicans* is identified worldwide as a causal agent in more than 80% of human mucocutaneous mycoses. Cutaneous candidiasis is favored by local factors: humidity, maceration, microtrauma, small wounds, local irritation, hyperacidity, and contact with sugars, but also by general factors (Table 1). On average, it is the 4$^{th}$ most common agent in nosocomial septicemia in the world (Diekema *et al.*, 2012), but it is the 3$^{rd}$ most common in the United States (Perlroth *et al.*, 2007) and it has a high mortality rate (Weinberger, 2016). When referring to candidemia or deep fungal infection, between 40 to 60% of cases are due to *C. albicans,* depending on the geographical area (Figure 5). There are different risk factors and fungemia can be found in many different medical services (Figure 6).

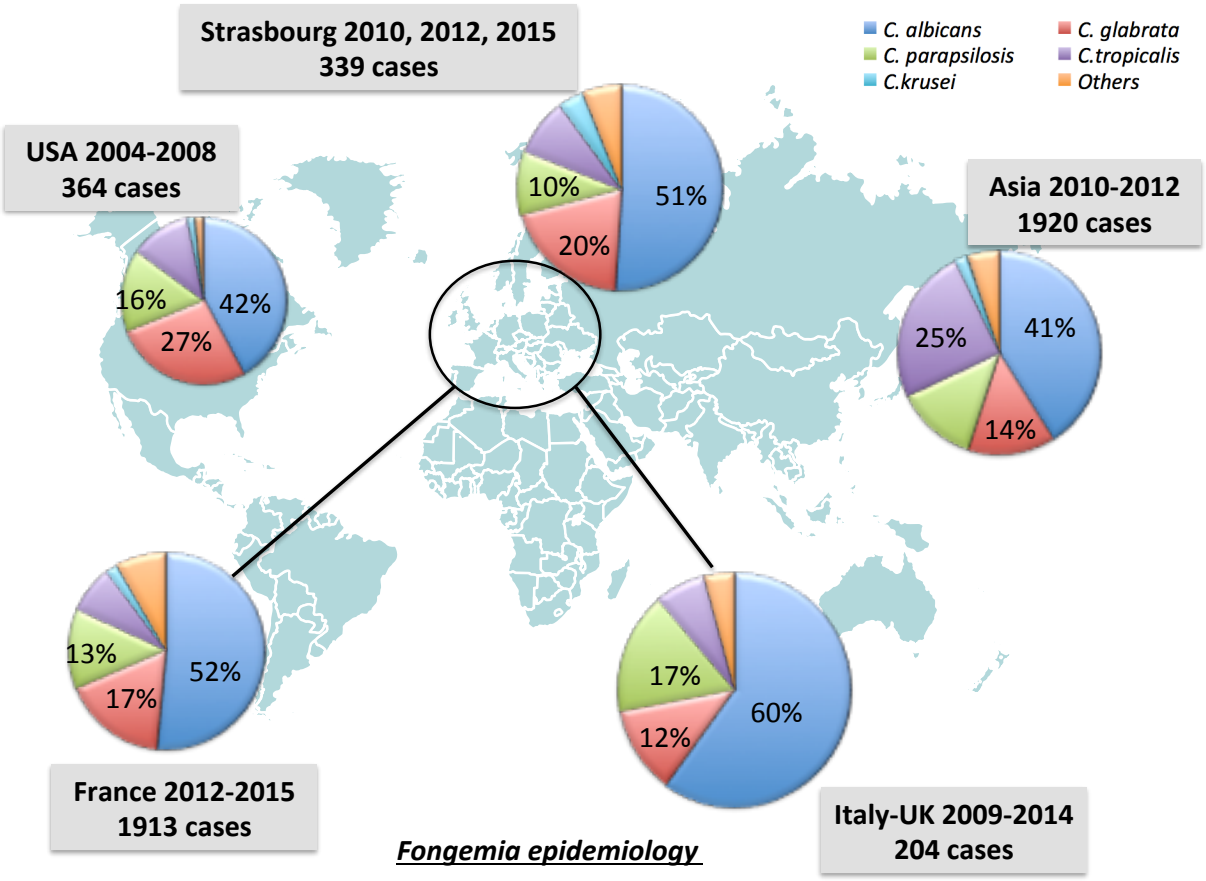


*FIGURE 5: FONGEMIA EPIDEMIOLOGY*

*Results from the following surveillance studies:Wisplinghoff, 2013, Diekema 2012, Pfaller et al., 2012, Tan, 2015, Bassetti, 2015, Cleveland , 2015*

*C. albicans* is also the species most often associated with biofilm formation. Biofilms are responsible for 65% of nosocomial infections (Lewis, 2007). The capacity to grow in this way on almost all medical devices and implants is extremely problematic, since studies show that more than 45 million medical devices are implanted each year in United States and more than 50% of nosocomial infections are related to these implants. Around 20% of these infections are caused by species from the *Candida* genus, and 8% from *C. albicans*, and these have a 40% mortality rate, which means that there are 400,000 deaths per year in the United States caused by *C. albicans* candidemia alone that are induced by medical device implantation. Furthermore, it is alarming that some types of *Candida* are becoming increasingly resistant to first-line and second-line antifungal medications, namely fluconazole and echinocandin drugs (anidulafungin, caspofungin, and micafungin).

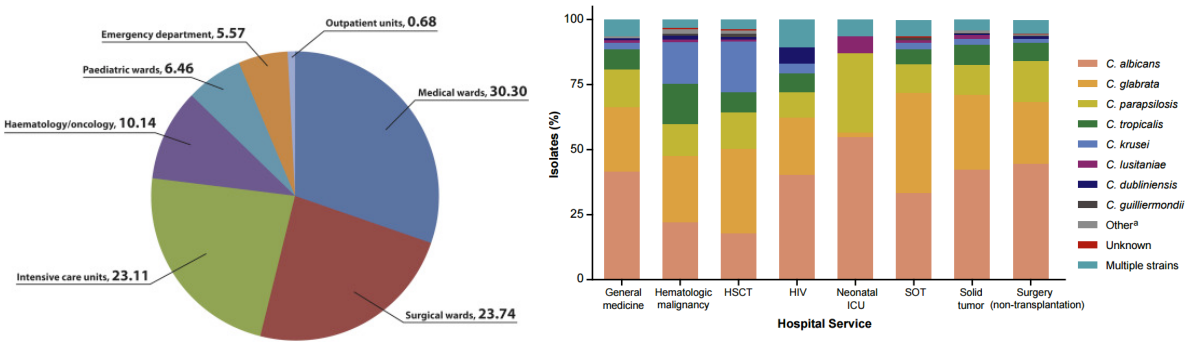


*FIGURE 6: DISTRIBUTION OF PATIENTS WITH CANDIDEMIA BY HOSPITAL SERVICE, NUMBER DENOTES % (TAN ET AL., 2015) AND RISKS FACTORS ASSOCIATED (PFALLER ET AL., 2012)*

In the United States, each case of candidemia is estimated to result in an additional 3 to 13 days of hospitalization and between $6,000 to $29,000 in healthcare costs (Morgan, 2005). This study correlates to a more recent one extended to North America and Europe which shows an increase of the cost for a minimum of 7700 € (Bloos *et al.*, 2014).

## 3. AVAILABLE ANTIFUNGAL DRUGS TO FIGHT *CANDIDA ALBICANS* AND ITS RESISTANCE MECHANISMS

Antifungal molecules were, for a long time, restricted to agriculture and plant treatment. It was only in 1939 that griseofulvin was discovered and it was finally used as a therapeutic agent in 1958 (Goldman *et al.*, 1960). In 1950, the polyene class was introduced with the first molecule, nystatin, followed five years later by amphotericin B. Two years after that, in 1957, the class of pyrimidine analogues was discovered and flucytosine was made available on the market. By the end of that decade, the azole class appeared with the emergence of miconazole, clotrimazole, and econazole. In 1983, the first triazole, ketoconazole, was discovered, followed by the discovery of a new class, allylamine, which had terbinafine as the first representative. After that, several triazoles were introduced on the market: fluconazole in 1990, itraconazole in 1993, voriconazole in 2002, and posaconazole in 2006. In a parallel manner, the echinocandin class appeared with caspofungin in 2002, anidulafungin in 2007, and micafungin in 2008 (Hincky-Vitrat, 2011).

Antifungal drugs are differentiated by their therapeutic uses: those used to treat topical or superficial infections administrated essentially locally, and those used to treat systemic mycoses (Lortholary, 1999).

Currently, there are several antifungal drugs suitable to fight *C. albicans* infections available, and they target the cell wall, the plasmic membrane, ergosterol, or RNA/DNA biosynthesis. They can include fungistatic agents, fungicide, or both.

### 1. POLYENES

This class is composed of natural antifungal molecules produced by some *Streptomyces* strains which have fungicide capabilities. The most known is amphotericin B (AmB), however nystatin or natamycin also exist and serve the same function. The ergosterol of the *C. albicans* cell wall is a component that is targeted by AmB and other polyenes. AmB binds irreversibly to the ergosterol complex within the fungal cell membrane, resulting in the depolarization of the membrane by an efflux of Na+ and K+ ions and the formation of pores. These pores permit leakage of intracellular contents and lead to the death of the yeast.

*C. albicans* has no natural resistance to AmB and other polyenes, however, the occurrence of a secondary resistance is rare but possible and already demonstrated. The mechanism of this resistance is not well elucidated today but there are several hypotheses that attempt to explain it. As polyenes do not need to interact at the intracellular level since they bind the external part of the plasmic membrane, they avoid metabolization and the efflux system. This means that the only possibility for resistance consists in deleting or substituting the target. Though essential for the yeast, substitutions are limited to quantitative or qualitative ergosterol modification related to erg2 and/or erg3 genes implicated in ergosterol biosynthesis, increasing of catalase activity, or accessibility decreased by cell wall modification (Granier, 2003). Despite these mechanisms and the fact that AmB has been used for a long time, no resistant *C. albicans* strains have been observed for now, although some studies do show that AmB creates an oxidative stress on *C. albicans* (Vandeputte, 2008).

Even with the larger spectrum of action in the antifungal arsenal, the problem with these drugs is the common general problem found in both antifungal and antiprotozoal drugs, a cross reaction due to the similarity of the target with the corresponding cell components in humans. Due to this, AmB has a cross reaction with cholesterol, the principal human sterol, so it is highly nephrotoxic, not to mention several other side effects, such as fevers, chills, and hypokalaemia.

## 2. PYRIMIDINE ANALOGS

This class is represented by the 5-flucytosine (5-FC) synthetic antifungal molecules which have fungistatic action. 5-FC is a pro-drug that enters the yeast and inhibits RNA and DNA biosynthesis. After penetration inside the cell, 5-FC is metabolized in 5-fluorouracyle (5-FU) by a cytosine deaminase. 5-FU is incorporated into the RNA instead of uracil which leads to an abnormal protein synthesis and a DNA synthesis alteration by thymidylate synthetase (TS) inhibition, leading to a halt in the development of the yeast.

In some regions, primary resistance is no longer rare for *C. albicans.* Due to the complex action of 5-FC, several mechanisms could explain the resistance: a mutation on one of the enzymes involved in the 5-FC metabolization, such as the *fur1* gene, to avoid 5-FU integration in mRNA; an overexpression of the *cdc21* gene that codes the TS; cytosine

permease modification (Vandeputte, 2008); a default in the 5-FC metabolization; and a loss of pyrimidine biosynthesis control (Lortholary, 1999).

Monotherapy always leads to therapeutic failure due to the fast selection of resistant cells, so 5-FC is almost always coupled to another drug (Granier, 2000). It is generally well tolerated by human organisms, explained by the quasi-absence of cytosine deaminase in mammalian cells, but there is a chance for hematological and renal toxicity if there is an overdose. 5-FC blood dosages are recommended if the treatment is associated with AmB, in order to adapt the posology (Delaunay, 2006). Even if this dosage is complicated and not possible everywhere, 5-FC is the most frequently associated with AmB (Vandeputte, 2008). 5-FC is currently used less and less since the development of azoles class.

## 3. AZOLES

This class is composed of synthetic antifungal molecules which have fungistatic and fungicidal capacities depending on the posology and administration mode. There are 2 subclasses: imidazoles such as miconazole and triazoles such as voriconazole and fluconazole. All of the representatives of this class share the same action plan. They block the active site of the lanosterol 14α demethylase (CYP51) enzyme from the P450 cytochrome of the fungal mitochondria, coded by the *erg11* gene (Granier, 2003). This enzyme normally catalyzes the transformation of lanosterol to ergosterol, through P450 cytochrome activation (Granier, 2000). This inhibition leads to an accumulation of diverse ergosterol precursors (Lortholary, 1999) and thus to an inhibition of the fungal development by depletion of ergosterol and abnormalities in the permeability of the membrane (Gubbins *et al.*, 2011).

For 50 years, azoles and their derivatives have been the most used antifungal drugs in clinics, and they are thusly the most studied drugs in relation to their formulation, their improvement, as well as the resistance mechanisms of fungi (Vandeputte, 2008). At the beginning, their use was restricted to topical treatment due to their high toxicity through oral administration, but with time, scientists improved the galenic formulation to allow for their use in the treatment of systemic infections.

The cholesterol biosynthesis in mammalian cells is also inhibited by azoles but with a superior dosage than that used for antifungal treatment, except for itraconazole, and that

explains the high hepatotoxicity of azoles (Hincky-Vitrat, 2011). One of the biggest problems with this class is the variability between their *in vitro* activity and their clinical efficiency; indeed, the viability of *in vitro* sensitivity determination of fungi is a major problem in mycology (Mimoz, 2000).

Of all antifungal drugs, azoles are the most involved in interactions with other drugs due to the cross inhibition of the human P450 cytochrome, whose many enzymes are involved in drug metabolization and cholesterol biosynthesis (Gubbins, 2011). Drug interactions are particularly dangerous in the case of transplant recipients and cancer or AIDS patients (Vandeputte, 2008). Azoles also have the effect of slightly modifying the cardiac rhythm, which in some cases can lead to death (Palairon *et al.*, 2011).

*C. albicans* does not have a primary resistance to azoles but its occurrence is not rare after treatment, and several studies have shown an increase of these resistances (Cleveland *et al.*, 2012; Lockhart *et al.*, 2012). Moreover, if there is not a complete resistance, *C. albicans* can become less susceptible to azoles (Mimoz, 2000). Resistance mechanisms occur due to different strategies: an overexpression or alteration of CYP51, or an overexpression of efflux systems and azole metabolization generally coupled to an AmB resistance due to the absence of ERG3 who inhibit the ergosterol biosynthesis.

## 4. ECHINOCANDINS

Also named candins, this class is composed of synthetic compounds derived from lipopeptides secreted by *Aspergillus* and *Zalerion* strains for the industrial production and originaly from *Arthrinium phaeospermum*, that have fungicidal action (Vandeputte, 2008). The most known compounds from this class are caspofungin and micafungin. Members of this class inhibit the (1→3)-β-D-glucan synthase, which is involved in the biosynthesis of the fungal cell wall (Hochart, 2008). The fungal cell wall is composed of several elements which have no equivalents in humans. (1→3)-β-D-glucan is specific to the cell wall, and is an essential component and the indirect target of echinocandins.

Cell wall integrity is essential for the yeast's survival since it is a physical protection, the center for many enzymatic reactions, and important for intercellular communication

(Vandeputte, 2008). If the cell wall loses its stability, osmotic instability appears and causes the lysis of the fungal cell (Herbrecht, 2005).

Echinocandins are an innovative class in the pharmacological field since they focus on a really specific target. They also have a low toxicity and have few drug interactions. They are well tolerated by humans and induce only a few side effects, such as fever, nausea, vomiting, hypercalcemia, and an increase of transaminase (Granier, 2002). Thanks to that, echinocandins, especially micafungin, are used as a prophylaxis of *C. albicans* infections in transplant recipients (Herbrecht, 2005).

Constitutive resistances are rare but have been observed since the beginning of echinocandin use. Several cases reported natural mutants of *C. albicans* resistant to caspofungin, and in a lot of others cases it seemed that after long treatments for transplant recipients or AIDS patients, there was a progressive loss of the echinocandin efficiency (Laverdière *et al.*, 2006). The resistance can come from different sources: an *fks1* or *fsk2* gene mutation that codes (1→3)-β-D-glucan synthase subunits or (1→3)-β-D-glucan synthase overproduction. Echinocandins are also substrates of a particular ABC transporter called CDR2, so the efflux system is also a way for *C. albicans* to resist this class.

# II. THE RIBOSOME, AN OLD TARGET FOR NEW THERAPIES

The ribosome is a macromolecular complex formed by ribosomal-RNA (rRNA) and ribosomal-proteins (r-protein) that is found in all living cells. It is the cellular machinery responsible for the fundamental process of protein biosynthesis and it is involved in the expression of genetic information. It is the translation mechanism for the cell, which means that it plays the role of the genetic code translator in order to create a bridge between messenger RNA (mRNA) and the protein. This macromolecular complex can be blocked by small molecules and other inhibitors such as antibiotics. Ribosome inhibition represents one of the major challenges for scientists who need a high comprehension of ribosome formation and structure, but also of translation mechanisms.

The ribosome formation mechanism, which can contain more than 300,000 atoms, has been presented as the biggest asymmetric macromolecular biological complex, and its structure can be analyzed using X-ray crystallography (Bokov and Steinberg, 2009). Even though many diverse structures have already been crystallized (there are more than 120,000 structures on Protein Data Bank, 107,000 of which were analyzed through crystallography; around 1200 pertain to the ribosome or part of it), the ribosome was one of the last complete structures to be solved due to its size and complexity. The resolution of the 3D structure is hard to obtain due to the difficulty of the production of a pure and complete complex that is crystallizable.

In bacteria, ribosomes can float freely in the cytosol, or are attached to the plasma membrane; in eukaryotes, ribosomes can float freely in the cytosol, or are attached to the endoplasmic reticulum membrane, or to the nuclear membrane. They can be found in mitochondria and chloroplasts, whose structure is close to that of prokaryotic ribosomes. They are also involved in the translation mechanisms of mitochondrial and chloroplastic genetic information. These facts are the basis for the endosymbiotic theory.

When translation is active at high levels, several ribosomes can be associated to the same mRNA at the same time. This simultaneous association is called a polysome.

"Palade particles" were discovered in the 1950s by George Emil Palade, who observed dense particles or granules within a cell using an electron microscope (Figure 7) (Palade, 1955), however, it was Richard B. Roberts who in 1958 proposed the term "ribosome" to designate ribonucleic protein particles ranging in size from 35 to 100S (Roberts, 1958). In 1974, the Nobel Prize in Physiology or Medicine, was awarded to Palade, Albert Claude, and Christian de Duve for the discovery of the ribosome.

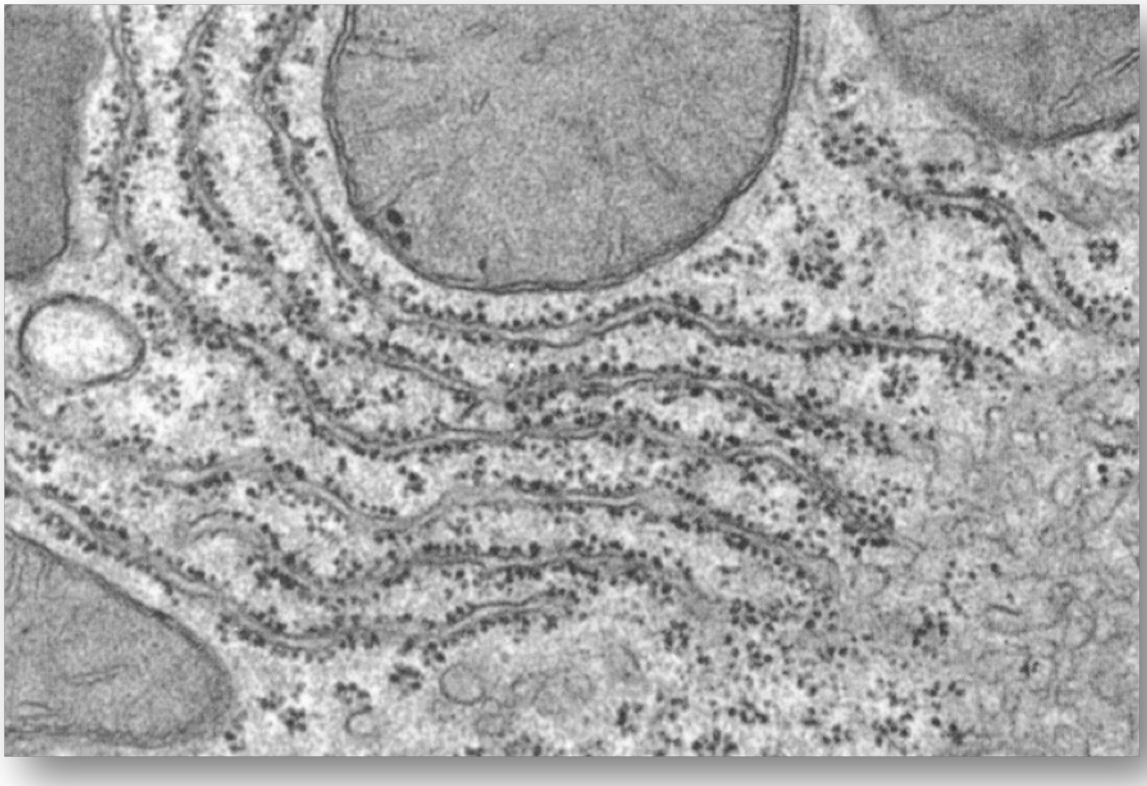

*FIGURE 7: PALADE PARTICULES OBSERVED BY ELECTRON MICROSCOPE (PALADE, 1955)*

A first draft of the complete ribosome structure was obtained by using cryo-electron microscopy (cryo-EM) (Frank *et al.*, 1988). In order to reach a better precision level, efforts were made to focus on X-ray crystallography, at that time the only technique able to approach the atomic level in such a large particle. The principal limitation of this technique resides in

the obtainment of macromolecule crystals able to diffract X-rays at a high resolution. Even though the technique proved successful in biomolecular structural analysis, adaptation to large macromolecular complexes such as the ribosome was unheard of, and its feasibility was seriously questioned. Because of the ribosome's large size and the difficulty faced in its experimental manipulation, ribosome crystallography needed developments. In the 1980s, the first ribosome subunit crystals were obtained (Yonath *et al.*, 1983), and soon after functional complexes with mRNA and tRNA (Trakhanov *et al.*, 1989; Yusupova *et al.*, 1991). Synchrotron radiation and cryo-EM development coupled with powerful computers and dedicated specific software contributed to speeding up of discoveries and research in this field. In 2000, several structures were published by different teams in the world; these structures presented the two subunits of archaeal (Ban *et al.*, 2000) and bacterial ribosomes (Wimberly *et al.*, 2000; Harms *et al.*, 2001) in a functional state with mRNA and tRNA (Yusupov at al., 2001; Yusupova *et al.*, 2001). Constant improvement has led this technique to reach near atomic precision in the complete ribosome (Selmer *et al.*, 2006; Jenner *et al.*, 2010). Thanks to these advances, different functional states have been observed, thus allowing a description of the fundamental mechanism of protein biosynthesis to be made (Schmeing & Ramakrishnan, 2009). In 2009, a second Nobel Prize, in Chemistry this time, was awarded to Yonath, Steitz, and Ramakrishnan for the discovery of the ribosome structure and mechanism.

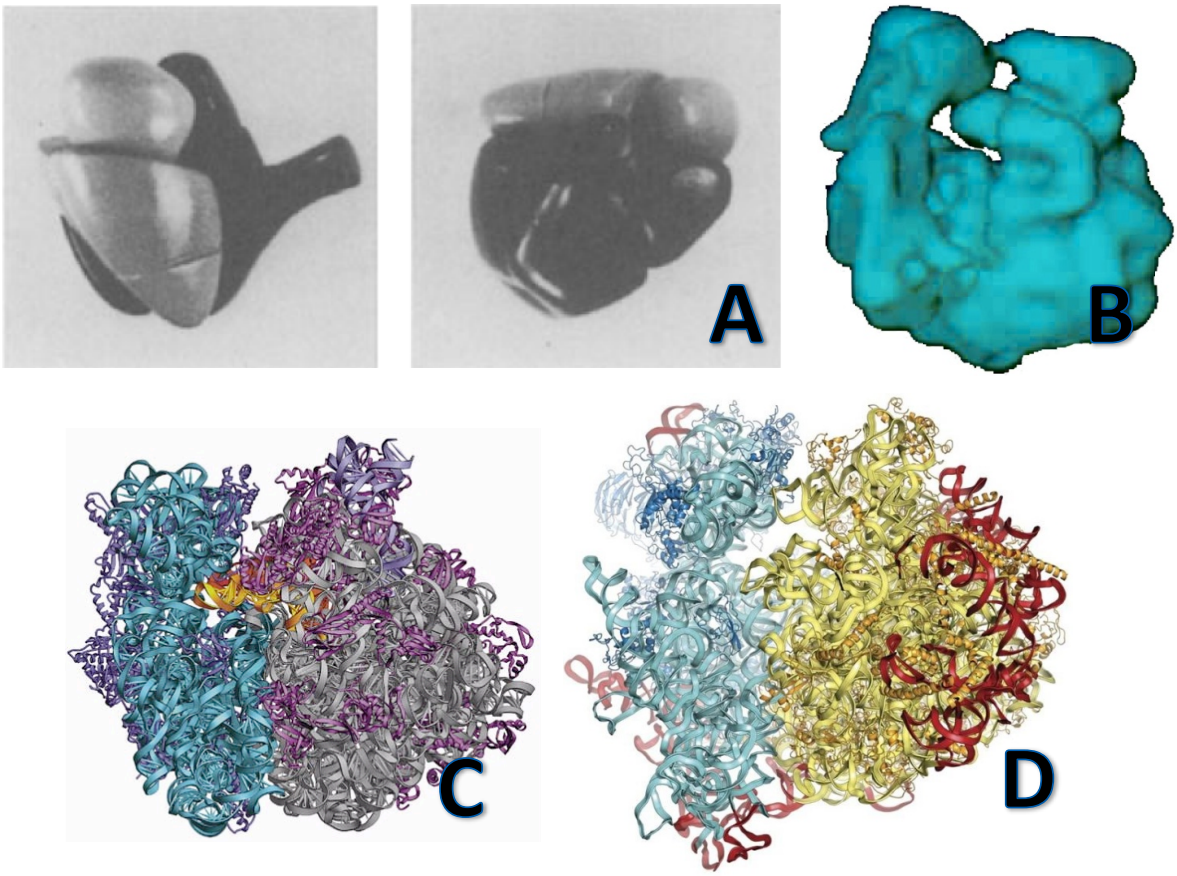


*FIGURE 8: EVOLUTION OF RIBOSOME STRUCTURE PRECISION FROM 1983 TO 2011*

*A: Escherischia coli, electron microscopy (Vasiliev et al., 1983); B: Escherischia coli, electron microscopy (Frank et al., 1996); C: Thermus thermophilus, Xray crystallograhiy (Yusupov et al., 2001); D: Saccharomyces cerevisiae (Ben-Shem et al., 2011)*

In parallel to this, the integration of all the near-atomic resolution structures of the ribosome in an electronic microscopy map paved the way for the functional analysis of ribosomal complexes and allowed scientists the opportunity to assemble step by step ribosome snapshots during translation.

All of these developments have also proven useful in the study of the eukaryotic ribosome. Cryo-EM was utilized to release a first draft of its general form, and through morphological comparison with the bacterial form, the presence of eukaryotic characteristics were exposed (Verschoor & Frank, 1990). Moreover, this technique has been used to visualize different functional states of ribosomes with tRNA, translation cofactors, or other natural ligands (Spahn *et al.*, 2004; Halic *et al.*, 2006; Becker *et al.*, 2009). However, despite

these studies, their results, and cryo-EM technique improvement, the limited resolution and the absence of a molecular model of the ribosome hindered an expanded analysis, and so the translation mechanism remained a mystery for ten years. It was in 2010 that the first 80S ribosome structure of *S. cerevisiae*, describing rRNA expansion segments and the conformational variations occurring during translation, was released (Ben-Shem *et al.*, 2010), and it was improved with a better resolution one year later (Ben-Shem *et al.*, 2011). This allowed scientists to observe movement between subunits, and also permitted cryo-EM scientists to use it as a model to fit in their cryo-EM maps. Since then, a considerable amount of eukaryotic ribosome structures have been solved by this technique. The *Homo sapiens* ribosome structures were obtained using cryo-EM in 2013 (Anger *et al.*, 2013) and improved two years later with a 3,6 Å resolution (Khatter *et al.*, 2015).

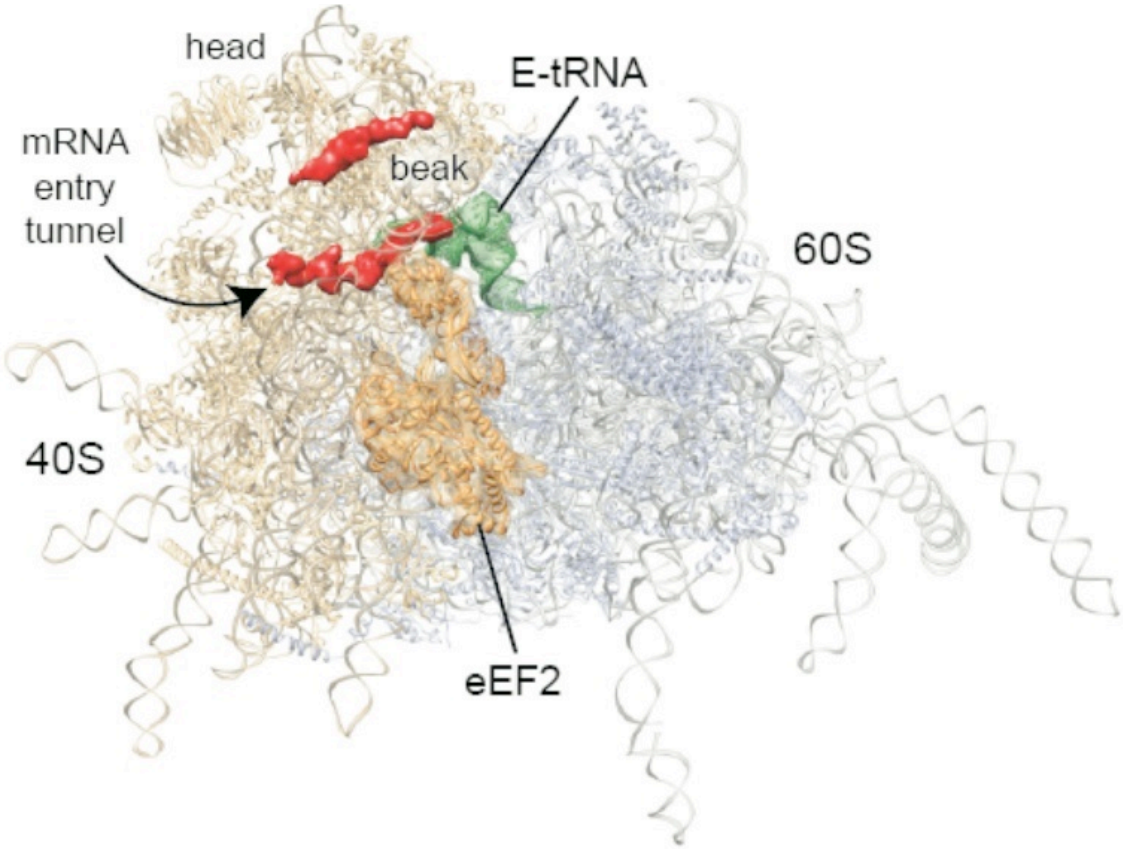


*FIGURE 9: FIRST CRYO-EM COMPLETE STRUCTURE OF HUMAN 80S RIBOSOME (ANGER ET AL., 2013)*

Due to all of these developments, several ribosome structures in pathogenic organisms have been solved (*Trypanosoma brucei* (Hashem *et al.*, 2003) and *Leshmania donovani* (Shalev-Benami *et al.*, 2016)) in order to reveal certain differences that create a resistance to drugs (Locke *et al.*, 2009) or that could be targetable by inhibitors, as in *Staphylococcus* (Eyal *et al.*, 2015). Some model organisms have been used to show inhibitors binding on the ribosome (Dunkle *et al.*, 2010 ; Garreau *et al.*, 2014) and this is considered by the scientific community as a contemporary challenge (Auerbach-Nevo *et al.*, 2016 ; Renaud *et al.*, 2016).

## 2. RIBOSOME COMPOSITION

The ribosome is present in all the different living kingdoms albeit with substantial differences. It is composed of two different entities: a large one named large subunit (LSU), and a smaller one named small subunit (SSU). The LSU is also identified according to its sedimentation coefficient: 50 Svedberg (S) for prokaryotic LSU and 60S for eukaryotic LSU, while the SSU is equivalent to 30S for prokaryotes and 40S for eukaryotes.

The closest phylogenetically known structure of the *C. albicans* ribosome is that of the *S. cerevisiae* ribosome. This structure has been described and its composition detailed: the LSU, equivalent to 2.8MDa, is composed of 46 r-proteins and 3 rRNA, 5S is composed of 121 bases, 5.8S is composed of 158 bases, and the 25S rRNA is composed of 3396 bases; the SSU, equivalent to 1.4Mda, is composed of 33 r-proteins, and the 18S rRNA is composed of 1800 bases (Woolford & Baserga, 2013).

When the two subunits are assembled within the ribosome function, they represent a molecular weight of 4.2 MDa with a sedimentation coefficient of 80S (70S for prokaryotes). Eukaryotic ribosomes are between 25 and 30 nm (250–300Å) in diameter, (20 nm for prokaryotes), with an rRNA-to-protein ratio closer to 1 than that of prokaryotic organisms.

Ribosomes consist of two subunits: a smaller one that reads the mRNA, and a larger one that is responsible for the polymerization of amino acids that forms the corresponding protein. Both ribosome subunits are built around a central heart of rRNA that possesses a highly compact structure around which r-proteins are attached. In this structure, rRNA create bonds and interactions that allow for the maintenance between the proteins of a ribosomal subunit as well as other subunits, and they also carry out catalytic activity.

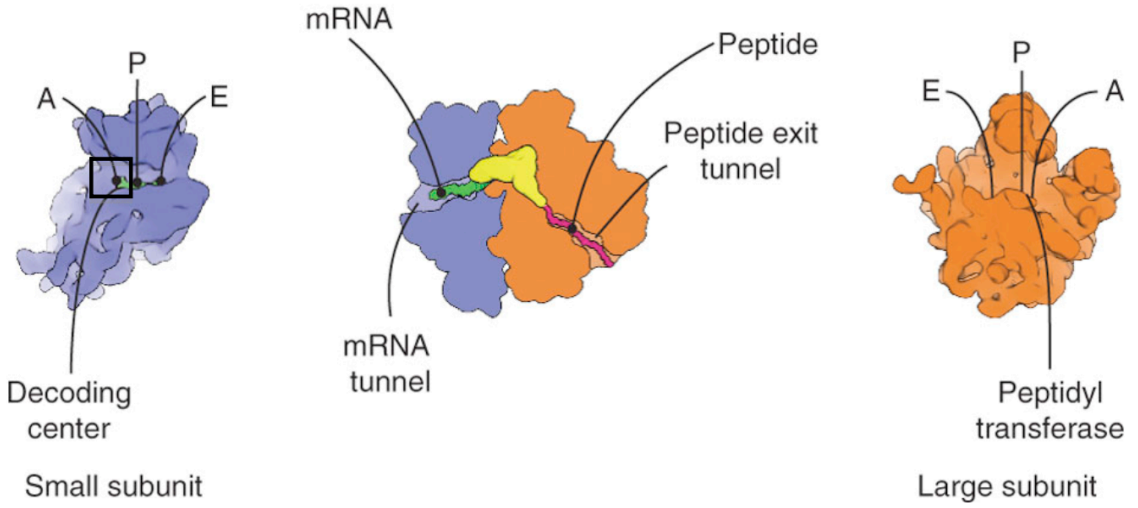


*FIGURE 10: CORE ACTIVITIES OF THE RIBOSOME (MELNIKOV ET AL., 2012)*

*The messenger RNA passes through the small subunit (30S or 40S) containing the tRNA binding sites on the mRNA. The large subunit contains the catalytic portion, called peptidyl-transferase center, which performs the synthesis of the peptide bond between the consecutive amino acids of the protein. The large subunit also contains a tunnel through which the protein chain leaves during synthesis. There are also the three large subunit sites that bind tRNAs carrying the amino acids during translation: the A-site (for aminoacyl tRNA), which is occupied by a tRNA carrying an amino acid awaiting be bound to the polypeptide chain; the P-site (for peptidyl-tRNA), which is occupied by a tRNA carrying an amino acid linked to the resulting polypeptide chain; finally, the E-site (for exit), which allows the release of deacylated tRNA that has delivered its amino acid. The ribosome is a molecular motor, which*

*advances on the messenger RNA by consuming the energy supplied by the hydrolysis of GTP. Several proteins, called elongation factors, are involved in this process, which is called translocation.*

The ribosome is the cellular machinery that performs, according to the correspondence with the genetic code, the translation of mRNA into proteins. A key stage of genetic expression in all living cells, the decoding of information carried by mRNA occurs due to two reactional sites on the ribosome: the decoding center (DC) and the peptidyl transferase center (PTC), as well as three active sites: the aminoacyl-tRNA site (A-site), the peptidyl-tRNA site (P-site), and the exit site (E-site). The A-site is where there is a tRNA carrying an amino acid, that has been selected due to its anti-codon through complementarity with the playing codon, waiting to be linked to the polypeptide chain; the P-site is occupied by a tRNA carrying an amino acid linked to the newly synthesized polypeptide chain; and the E-site performs the release of the tRNA that issued the amino acid (Steitz, 2008) (Figure 10). The ribosome uses the transfer RNA or tRNA as "adapters" between messenger RNA and amino acids.

## 4. TRANSLATION MECHANISM AND PROTEIN BIOSYNTHESIS

The translation mechanism is a ribosomal interpretation of mRNA codons in amino acids, according to a correspondence with the genetic code; this event occurs in the cytoplasm. During translation, ribosomes moving along the mRNA sustain important conformational modifications, and interact with tRNA and diverse proteic cofactors (Druzina & Cooperman, 2004; Dudzinska-Bajorek *et al.*, 2006; Peske *et al.*, 2004; Rodnina *et al.*, 2002). Several ribosomes can translate the same mRNA at the same time, and this resulting assembly is called a polysome. The speed of this mechanism is linked to the elongation of the polypeptide chain by a eukaryotic ribosome of three to five amino acids per second, ensuring the cellular protein biosynthesis in less than one minute for shorter ones and hours for the longer ones (Ingolia *et al.*, 2009). Translation can be divided into five principal phases: the ribosome binding to the mRNA, the initiation, the elongation, the termination of the translation, and the SU recycling.

The three reaction steps require different specific factors, called respectively

eukaryotic Initiation Factors (eIFs), Elongation Factors (EFs), and eukaryotic Release Factors (eRFs). Translation steps are conserved between the three life kingdoms and these steps will be described according to how this process occurs in *S. cerevisiae* given its phylogenetic proximity with *C. albicans* and the fact that it is the most well-studied eukaryotic ribosome (Lodish *et al.*, 2004).

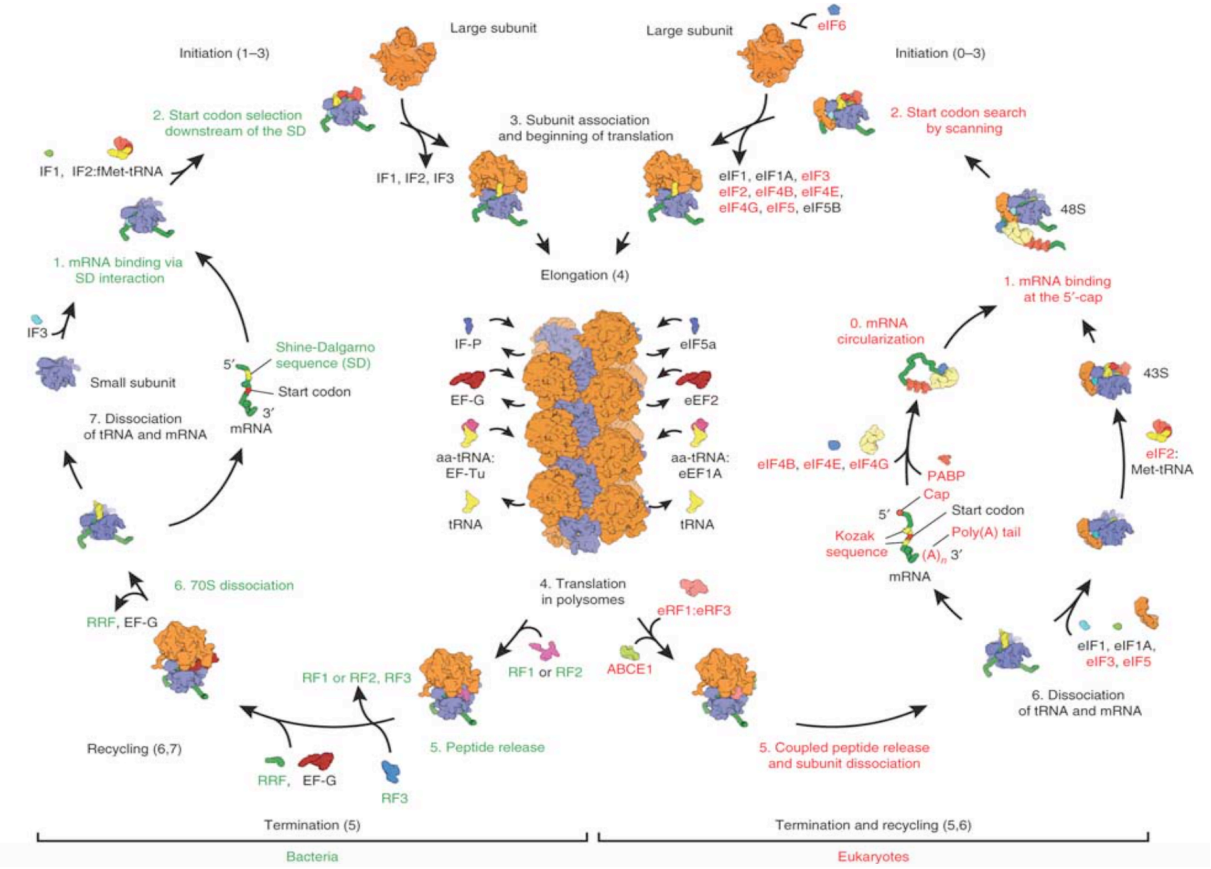


*FIGURE 11: THE TRANSLATION CYCLE IN BACTERIA AND EUKARYOTES (ADAPTED FROM MELNIKOV ET AL., 2012)*

*While key steps of protein synthesis are conserved in prokaryotes and eukaryotes, eukaryotic ribosome functions have many specifics. In bacteria, ten protein factors bind successively to the ribosome to catalyze various stages of translation, namely, initiation, elongation, termination, and recycling. In contrast, the mechanisms of protein synthesis in eukaryotes differ at many levels. For example, up to thirteen different factors are involved in the initiation step of translation in eukaryotes. Furthermore, the steps of termination and recycling operate differently and require the involvement of non-conserved factors in bacteria. The assembly of the eukaryotic ribosome is highly controlled and involves a hundred factors. Finally, apart from its major role in protein synthesis, the eukaryotic*

*ribosome and its constituents are actively involved in the regulation of gene expression.*

## 1. THE INITIATION

Translation initiation is the recognition mechanism of the first mRNA codon and which gives place to the positioning of the first aminoacyl-tRNA in the ribosome P-site. The first codon of an mRNA is most often an AUG codon, and the corresponding aminoacyl-tRNA is a methionyl-tRNA initiator (Met-$tRNA_{i)}$, and so the first aminoacyl of a neoprotein is a methionine (Li et Chang, 1995). Firstly, a preinitiation complex named 43S due to its sedimentation coefficient is formed (Figure 11), and it is constituted by the SSU, eFI1A and eIF3, and the ternary complex including the Met-$tRNA_i$, eIF2, and a GTP molecule. In parallel, the eIF4 complex recognizes the 5' cap ($m^7$Gppp) of an mRNA. The binding of the preinitiation complex to eIF4 leads to the 48S initiation complex formation. Subsequently, the 48S complex slides along the mRNA in 5' to 3' direction until the Met-$tRNA_i$ recognizes an initiation codon (Kozak, 1980). Helicase activity is carried out by eIF4A and needs energy obtained through ATP hydrolysis. Most of the time, the initiation codon is the first AUG found in the mRNA sequence, generally less than 100 nucleotides away from the cap. The selection of this site is facilitated by the nucleotide sequence neighboring the AUG codon; this sequence is called the Kozak consensus sequence (Kozak, 1978). Indeed, the initiation of the translation is favored by an adenine at the -3 position and a guanine at the +4 position. At this moment, eIF2 hydrolyzes the GTP molecule, which leads to the release of eIF1A, eIF3, and eIF4, and prevents all subsequent scanning possibilities. When the SSU is properly positioned on the translation initiation site, the LSU will bind in the order to form the functional 80S ribosome. The eIF5 GTPase activity is necessary at this step to link the 2 SU irreversibly so that the dissociation will only be possible after translation termination. The 80S ribosme – mRNA - Met-$tRNA_i$ complex, where the Met-$tRNA_i$, is located in the P-site is ready for the elongation process.

## 2. THE ELONGATION

The translation elongation step is an iterative process where the currently under

synthesis polypeptide chain is elongated following the mRNA template. Each amino acid added to the chain needs the peptidyl transferase activity of the ribosome. The necessary energy is produced by the hydrolysis of two GTP molecules performed by EF1 and EF2. In the A-site, the ribosome structure has a position where the aminoacyl-tRNA linked to EF1 can run into. Inside the A-site, aminoacyl-tRNA n+1 is oriented in such a way that the anticodon site of tRNA is positioned in front of the mRNA codon. If there is recognition between the anticodon and the complementary codon, aminoacyl-tRNA is stabilized in the A-site. Ribosomal conformational remodeling leads to the movement of the aminoacyl-tRNA to the P-site where the peptidyl-tRNA, to the effect that the residue n+1 to be incorporated is in nucleophile attack position on the chain's n residue. This action needs energy given produced by GTP linked to EF1 hydrolysis. The polypeptide chain which henceforth counts n+1 residues, is transferred to the tRNA n+1 on the A-site. A new ribosomal conformational remodeling, enhanced by the GTPase activity of EF2, leads to the sliding of three nucleotides along the mRNA in the A-site to the P-site direction. This movement follows the translocation of peptidyl-tRNA from the A- to the P-site and of tRNA n from the P- to the E-site. At the E-site, binding between tRNA n and mRNA is unstable and a gap allows the tRNA to be released into the cytoplasm. Those elongation steps are iterative since the ribosome arrives on a translation termination site.

## 3. THE TERMINATION

The translation termination is determined by the apparition of a stop codon in the mRNA sequence. Three stop codons exist (UGA, UGG, and UAG) for which the cell has no specific tRNA, which means that when one of these codons enters the ribosome A-site, elongation cannot progress anymore. The ribosome then makes a pause, during which eRF1 mimics a tRNA which will occupy the A-site. The eRF3-GTP GTPase binds to eRF1 and enhances the cleavage of peptidyl-tRNA in the P-site. The neoprotein, eRF1, and eRF3-GDP are released, and the 2 SU, the last tRNA and the mRNA are split by the intervention of other factors.

During evolution, the global ribosome structure was conserved. Despite this, the ribosome exhibits notable differences depending on the complexity level of the organism, even if it plays the same central role in the translation mechanism (Figure 12). This observation can be made thanks to all of the ribosome structures currently solved.

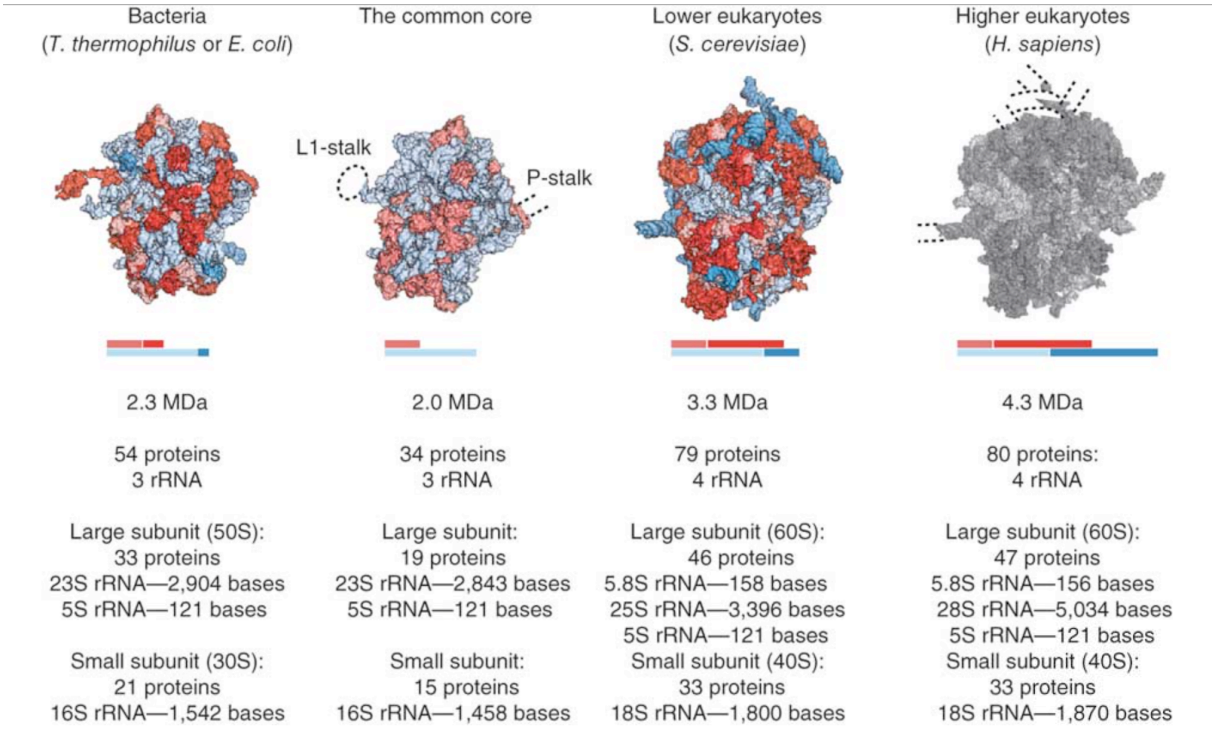


*FIGURE 12: BACTERIAL AND EUKARYOTIC RIBOSOME COMPOSITION (ADAPTED FROM MELNIKOV ET AL., 2012).*

*The conserved cores between bacterial and eukaryotic ribosomes are highlighted in light blue for rRNA and in light red for r-proteins. More than the core, ribosomes in each life domain contain their own set of r-proteins colored in red and rRNA extension segments colored in blue. This structure variation is shown also by a different molecular weight, since with around 3.3 MDa, the eukaryotic ribosome is 40% heavier than its bacterial homologe.*

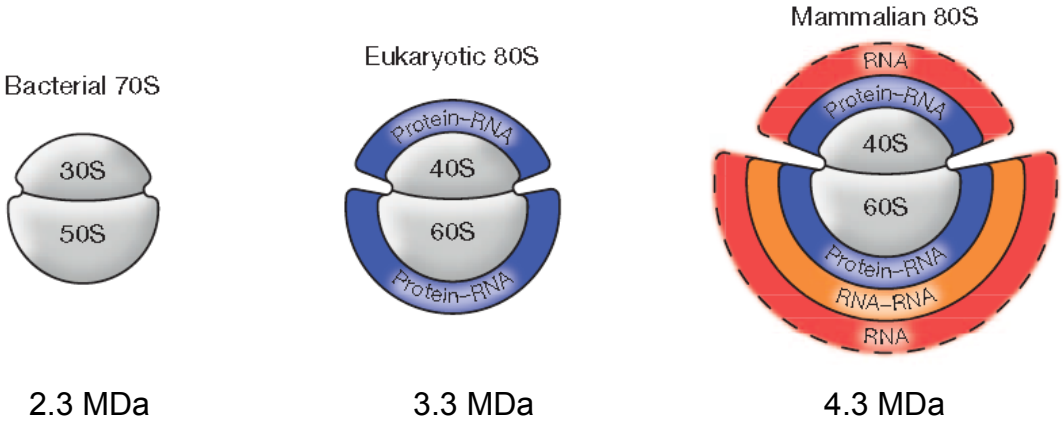


*FIGURE 13: EVOLUTION OF THE RIBOSOME (ADAPTED FROM ANGERS ET AL., 2013)*

*The 80S structure of several higher eukaryotes has been determined by both X-ray crystallography and cryo-EM and their cores are highly similar to the bacterial and yeast structures. The major distinctive feature in comparison with the yeast ribosome is the presence of long rRNA expansion segments (Angers et al., 2013).*

The major eukaryotic-specific elements are mostly found on the ribosome surface, forming a supplementary layer. They seem to have interactive properties with several other factor associated to the ribosome. This means that the ribosomal canonical function is conserved but also its core structure. *S. cerevisiae* is one of the best models upon which one can study the protein biogenesis and the eukaryotic ribosome biogenesis regulation, but it has shown limits in the supplementary function of the ribosome.

## 6. THE RIBOSOME AS AN INTERESTING THERAPEUTIC TARGET

The ribosome has been considered as a choice therapeutic target since the discovery of its implication in the gene expression mechanism at the translation level. A large number of molecules have been discovered as being potential inhibitors to the formation of ribosomes due to their actions which directly alter the structure, resulting in translation being impeded.

Even though a large number of molecules have had more or less beneficial effects on human health, there have been certain poisons partly composed of ribosome inhibitors related to the deaths of well-known people. A notable example is narciclasine, an extract of the Narcissus flower, that was used by certain royal families.

Though many recent discoveries describe ribosomopathies, which are illnesses related to the ribosome and its mutations, their implication in cancers (Goudarzi & Lindstrom, 2016), or in certain rare genetic diseases, the ribosome remains the primary target of choice in the majority of antibacterial treatments.

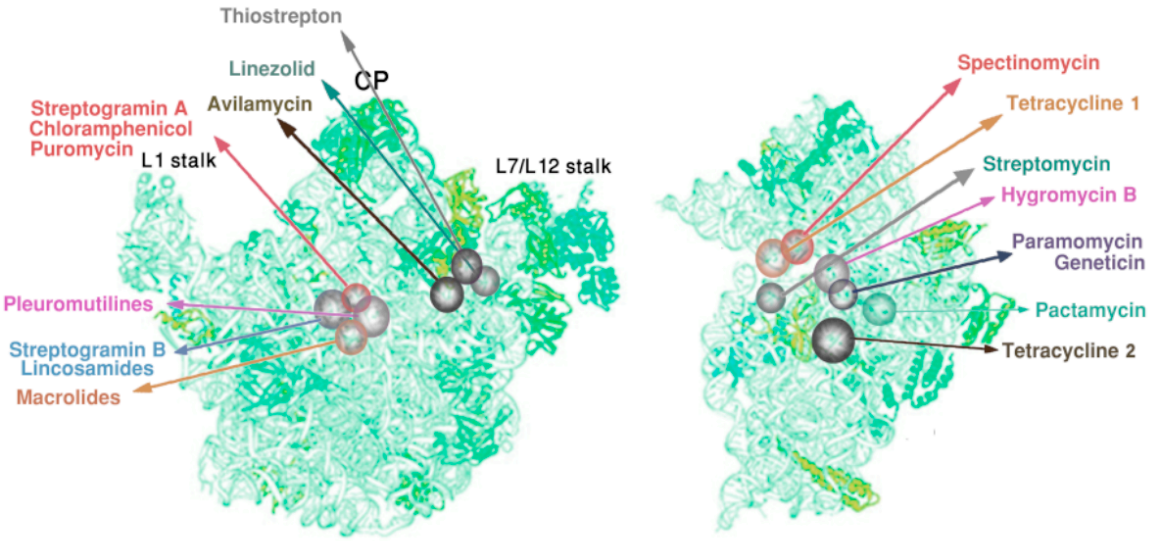


*FIGURE 14: MAIN ANTIBIOTICS BINDING SITES SHOWN ON THE SKELETONS OF THE LARGE (LEFT) AND THE SMALL (RIGHT) BACTERIAL RIBOSOME SUBUNITS (AUERBACH-NEVO ET AL., 2016)*

The ribosome is a major bacterial target for antibiotics. Drugs inhibit ribosome function either by interfering in messenger RNA translation or by blocking the formation of peptide bonds at the peptidyl transferase center. These effects are the consequence of the binding of drugs to the ribosomal subunits.

The antibiotics that unite ribosomes often show signs of prior large actions, with examples which include antibiotics used in laboratories to prevent the development of bacteria in eukaryotic cell cultures. Certain antibiotics, such as cycloheximide, react on both prokaryotic and eukaryotic cells, however others, such as aminoglycoside and chloramphenicol, are more specific to the prokaryotic kingdom, and do not have any effects on eukaryotic ribosomes.

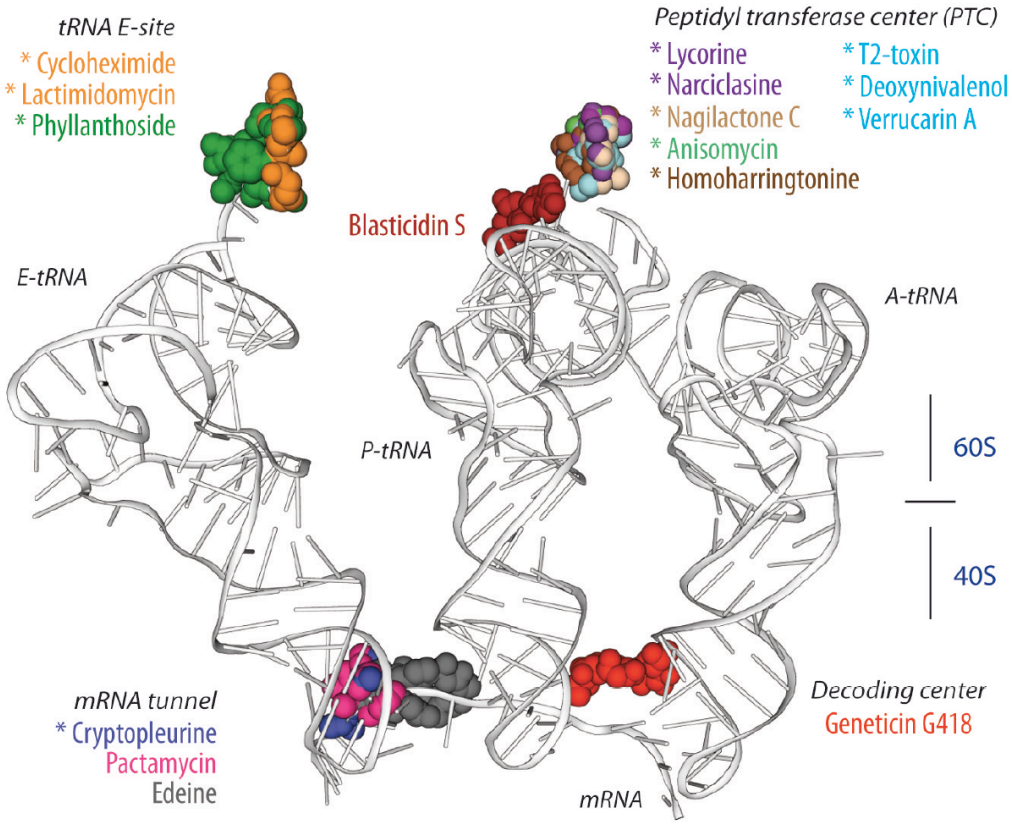


*FIGURE 15: BINDING SITES OF INHIBITORS ON THE YEAST RIBOSOME. (ADAPTED FROM GARREAU DE LOUBRESSE ET AL., 2014)*

*16 inhibitors of 12 different classes whose 4 broad-spectrum inhibitors and 12 eukaryote-specific.*

A large amount of eukaryote-specific inhibitors have been discovered by scientists, however, very few of them can be used in therapeutic treatments. In fact, the core of the ribosome which is almost perfectly maintained across all kingdoms rarely permits curative uses to be implemented. Cross reactions due to the similarity between the molecular targets that are binding sites and the high level of some molecules' toxicity greatly limit the development of new medicines.

Currently, it is necessary to develop new ribosome inhibitors, some of which are directed toward applications against cancer, in order to restore proteic expression levels to normal rates. A notable example is omacetaxine, which was approved by the United States Food and Drug Administration (FDA) in 2012. Other inhibitors could modulate translation by forcing the ribosome to prematurely decode certain codon stops related to certain genetic diseases; some aminoglycosides, such as gentamicin, are used to this effect.

Prior developments in the discovery of numerous translation inhibitors on both prokaryotic and eukaryotic (Garreau de Loubresse *et al.*, 2014) ribosomes notwithstanding, the ribosomal structures of pathogenic organisms have not been extensively studied and used in order to find new therapeutic targets.

# III. PROBLEMATIC AND EXPERIMENTAL APPROACHES

*Candida albicans* is an opportunistic and nosocomial agent that has become a cause of major health concerns. It has emerged as an important cause of morbidity and mortality in immunocompromised or immunocompetent patients, being responsible of unacceptably high mortality rates. Prevention has led to a widespread use of antifungal drugs, leading to the emergence of resistant strains. There is a need for new selective and less toxic antifungal molecules. Moreover, the drug companies' antifungal pipeline is mostly dry, urging for a different approach of exploring the target. The ribosome is an interesting target: it represents the cellular machinery responsible for protein biosynthesis and it can be blocked by small molecules such as antibiotics. The aim of our project is to solve the mystery of the *C. albicans* ribosome structure and to use it as a new model for future drug development. This approach has already been used successfully to develop new antibiotics based on crystallographic structures of the bacterial ribosome.

Although its functionality is universally conserved in the living world, the ribosome has major differences between the kingdoms (eukaryotic, prokaryotic, archaeal) but also within these realms (metazoan, protozoa, fungus). The study proposed in this thesis is particularly interested in the ribosome structure of *C. albicans*, which has never been resolved. Decryption of this structure will provide a solid basis for further studies concerning the translation mechanism in this organization that does not meet the universal genetic code.

In parallel, we conducted comparative studies between the bioinformatic structure of *C. albicans* and *S. cerevisiae* and those of *H. sapiens* to highlight specific sites in *C. albicans*. The study will highlight therapeutic pathways contributing to the development of new antifungals specifically directed against *C. albicans*.

Determining the structure of the ribosome of *C. albicans* was performed using two approaches:

- By bioinformatic modeling through the completion of alignment and modeling of protein sequences and ribosomal RNA
- By using an X-ray crystallography beam

The identification of potentially interesting target sites was initially carried out using a bioinformatic approach and then was confirmed by crystallography. The interest of these potential target sites will be tested through the inhibition test of realization and *in vivo* determination of minimum inhibitory concentration, using known inhibitors of the eukaryotic ribosome.

# IV. BIOINFORMATIC MODELING OF THE *CANDIDA ALBICANS* 80S RIBOSOME

## 1. AIM OF THE PROJECT

The ribosome is responsible for the translation of mRNA into protein. Given its size and complexity, it is one of the last complete structures to have been solved by crystallography. This macromolecular complex can see its action blocked by small molecules, especially at some of the known active sites, such as the A, P, or E-sites, the decoding center, and the tunnel of the mRNA. The ribosome is present in all areas of life, but it nevertheless has certain peculiarities in each area, and even between different species of the same phylogenetic family.

The strategy adopted during this project consisted initially of the search for and in some cases the reconstruction of r-proteins and rRNA sequencing of *C. albicans*, by homology with other species. These sequences were annotated and characterized, then assembled to model *in silico* the 80S ribosome of *C. albicans*.

This model was then characterized and areas specific to *C. albicans* have been identified and located. This model was also analyzed at the level of its active sites and compared with the *S. cerevisiae* vacuum structure, then with the *S. cerevisiae* structure associated with eukaryotic translation inhibitors already identified by our team. This allowed us to identify the different sites that could host an inhibitor in *C. albicans*.

In order to seek new antifungals directed specifically against *C. albicans*, when an interesting site was found, we compared the human ribosome structure with that of *C. albicans* to demonstrate the value of such a site with the idea of minimizing the maximum side effects in humans and the inactivity of the molecule on the normal flora of the host.

## 1. EXTRACTION AND RECONSTRUCTION OF RIBOSOMAL PROTEINS AND RNA SEQUENCE VIA MULTIPLE ALIGNMENTS OF SEQUENCES OF OTHER ORGANISMS

The sequences of r-proteins and rRNA of the SC5314 clinical isolate of *Candida albicans* used in all experimental manipulations of this study were based on data obtained from assembly 22 of the genome available at www.candidagenomedatabase.org, which currently contains the best characterizations of this strain (Muzzey *et al.*, 2013). Though several r-proteins were not available, we were able to reconstruct them based on the multiple alignments of r-proteins from several other organisms.

In order to identify homologous sequences, the complete proteomes of different organisms were downloaded from the UniprotKB database (www.uniprot.org), including metazoans such as *Homo sapiens*, *Mus musculus*, *Drosophilea melanogaster*, *Ceonarbitis elegans*; fungi such as *S. cerevisiae*, *Candida glabrata*, *Candida albicans* SC5314 strain, *Candida albicans* WO1 strain, *Aspergillus fumigatus*, and *Pneumocystis carinii*; and several protozoans such as *Plasmodium falciparum*, *Toxoplasma gondii*, *Trypanosoma brucei*, and *Cryptosporidium parvum*. A BLASTP database search was then performed, using each of the 80 ribosomal proteins from *Candida albicans* as the query and parameters were set to optimize the search for short sequences (Expect =200000, Word size = 2, Max matches = 0, Matrix = PAM30, Gap penalties = 9 and 1, No Adjustment for Complexity).

A multiple alignment was then constructed for each ribosomal protein, together with the homologous sequences detected by BLASTP, using the PipeAlign pipeline (Plewniak *et al*., 2003). PipeAlign is a tool for the automated analysis of protein families (Plewniak et al., 2003), which integrates a six step process, corresponding to six different sequence analysis programs, ranging from the search for homolog sequences in protein and 3D structure databases, to the construction of hierarchical relationships within and between families.

Based on the multiple alignments, potentially mispredicted sequences were identified manually and corrected by performing a TBLASTN search in the corresponding genome

sequence. TBLASTN was used to search translated nucleotide databases using a closely related protein as a query.

## 2. STRUCTURAL AND FUNCTIONAL ANNOTATION OF MULTIPLE PROTEIN SEQUENCE ALIGNMENT

The multiple alignments produced by PipeAlign were annotated with structural and functional information with the MACSIMS program (Thompson *et al.*, 2006). This information includes secondary structure elements, structural or functional domains, known functional motifs, or active sites. Then, based on these multiple alignments, regions conserved in all organisms, but also regions found only in a single clade or even more specifically only in *Candida albicans*, were identified with a new algorithm LEON-BIS (Vanhoutrève *et al.*, 2016), which uses Bayesian statistics to estimate the existing homologous relationships between the sequences in a multiple alignment.

The multiple alignments and their annotations, were visualized using the Jalview software (Clamp *et al.*, 2004) that allows quick viewing and editing of multiple sequence alignments.

## 3. MODELING OF THE 3D STRUCTURE OF THE RIBOSOME OF *CANDIDA ALBICANS*

The 3D structure of the ribosome of *C. albicans* was modeled by homology to the *S. cerevisiae* structure (PDB = 4V7R), which is similar in many points with that of *C. albicans* (Arnaud *et al.*, 2009).

The sequences of r-proteins used are those retrieved from the database www.candidagenome.org, one of which needed to be reconstructed through the multiple alignments unavailable in databases. Their 3D structure, in turn, was predicted *in silico* using the tool Phyre2 (www.sbg.bio.ic.ac.uk/phyre2).

The rRNA strands, available in the www.candidagenome.org database, were built using the tool Assemble2 (bioinformatics.org/s2s/), in collaboration with Fabrice Jossinet (IGBMC, Strasbourg) using the sequence of *S. cerevisiae a*s a model.

Finally, the individual r-protein and rRNA models were superimposed with their counterparts in the complete structure of *S. cerevisiae* via the Phenix tool (www.phenix-

online.org).

## 4. LOCALIZATION OF FUNCTIONAL SITES AND INHIBITORS OF THE EUKARYOTIC RIBOSOME

The A, E, and P-sites, the decoding center, and the mRNA of the tunnel were located on the 3D structure of *S. cerevisiae* through annotations of residues in the work of Nicolas Garreau Loubresse (Garreau Loubresse *et al.*, 2014). Then, in order to identify the corresponding sites on the structure of *C. albicans*, a superposition of the structures of *S. cerevisiae* and *C. albicans* was performed in Pymol. The same operation was subsequently carried out on the human ribosome. Finally, inhibitors (Table 2) that were already known and positioned in *S. cerevisiae* (Loubresse Garreau *et al.*, 2014) were positioned on the model of the *C. albicans* ribosome to allow a visual comparison of the antifungal sites between the two yeasts.

*TABLE 2: KNOWN EUCARYOTIC RIBOSOME INHIBITORS*

| Sites | Inhibitors |
|---|---|
| A-site | Anisomycine |
| P-site | Blasticidin S |
| E-site | Cycloheximide |
| Decoding center | Geneticine |
| mRNA tunnel | Cryptopleurine |

## 5. SPECIFIC RESIDUE CLUSTERING AND VISUALIZATION

In order to identify structural regions that are possibly specific in *C. albicans*, i.e. regions that might correspond to potential target sites for inhibitors, residues corresponding to post-translational modifications in the annotated MACSIMS files, and residues that are not found in the conserved blocks identified by LEON-BIS, were identified in the 3D model. Due to the large number of potential sites, a manual analysis was not possible. Therefore, the specific residues were clustered based on their 3D coordinates, using the "mixture models" method (*McLachlan, 1988)*, which is a statistical model to represent the presence of sub-populations within a global population**.** A cluster thus contains a set of residues that are located in the same spatial area within the ribosome. Finally, the cluster residues were annotated in the PDB format files corresponding to the *C. albicans* ribosome model.

These files in PDB format can be viewed by software dedicated to the visualization of 3D structures, such as Chimera or Pymol (www.pymol.org). Chimera is a program for visualization and analysis of molecular structures and related data, such as sequence alignments and this is one of the only free software that supports the loading of the complete structure of the ribosome. Pymol is an open-source visualization tool, which is easily expandable with the python programming language and that helped me identify overlays between ribosomes.

### 6. GLOBAL CHARACTERIZATION OF CHANNELS AND CAVITIES IN THE RIBOSOME

To calculate the volume of the different sites that could potentially host antifungals, a web server was utilized, the "Voss Volume Voxelator" (Voss and Gerstein, 2010) which takes a PDB file as input and calculates several types of volumes for a protein or RNA molecule. Thus, according to the tool used, one can obtain either the total volume of the surface at various resolutions, the volume of the solvent, or the channel volume, that is to say in our case all the places that could drag antifungals. Volumes are represented by density maps and saved to a file in an MRC format that allows viewing volumes identified with Chimera.

## 3. RESULTS

### 1. SEQUENCES OF RIBOSOMAL PROTEINS AND RNA AND MULTIPLE ALIGNMENTS WITH OTHER ORGANISMS

The four rRNA sequences that form 5S, 5,8S, 18S and 25S were found easily on the database at www.candidagenomedatabase.org. It was slightly harder for the 80 r-proteins. Indeed, though some of them were already annotated as ribosomal proteins, others were identified as “likely cytosolic proteins”, while most of them were identified as simple ORFs, and finally a few of them were missing on the database. For this last category, the multiple

alignment was helpful to find the different constitutive exons on the genome and to reassemble them together in order to obtain the missing r-protein sequences; furthermore this multiple alignment also allowed us to identify other tracks on which to find interesting targetable differences (Figure 16). All of the r-proteins and rRNA used for this work are listed in Annex as named by universal nomenclature (Ban *et al.*, 2014).

The multiple alignment of the 80 r-proteins from different organisms allowed us to find the 35 r-protein component of the ribosomal SSU and the 44 r-protein component of the ribosomal LSU. Normally, 45 r-proteins are found in the eukaryotic ribosomal LSU, but it was impossible to find the sequence of the eL41 r-protein. Moreover, we did not find the corresponding genomic sequence in the *Candida albicans* SC5314 genome either. It is impossible to assume that this r-protein is not present in the *C. albicans* ribosome; indeed, its length is only around 25 amino acids in other organisms. Since this r-protein is oriented toward the solvent side of the ribosome and not located deeply inside the structure, the modeling was done without it.

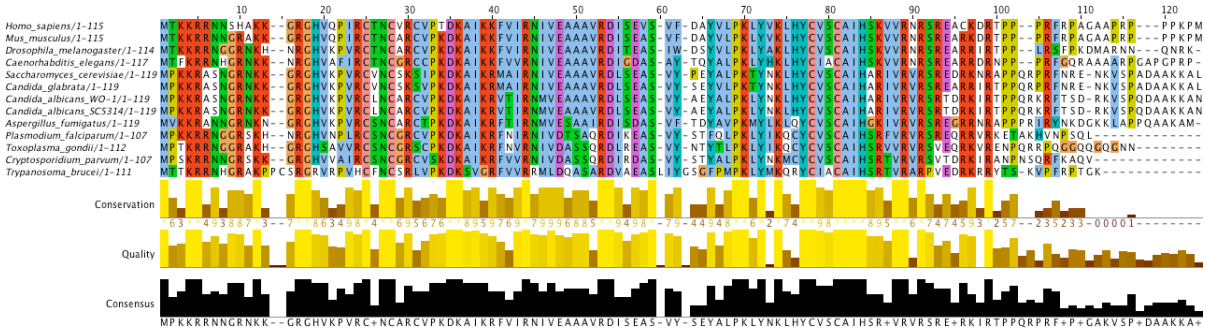


*FIGURE 16: ES26 R-PROTEIN ALIGNMENT VISUALIZED USING THE JALVIEW 2.8.2. EDITOR*

*The three groups of organisms aligned show an extremely high level of conservation of all the r-proteins. Conserved positions in the alignment are highlighted by residue coloring and different conservation scores shown beneath the alignment. Insertions are often observed, for example in the Trypanosoma brucei eS26 r-protein sequence (columns 13-14, 60, 63). Also, the three groups present some specific features shared between their members. In this particular case, the protozoan group has shorter sequences than the metazoan and the fungi groups. Similarly, we observe that the fungi sequences share the same C-terminal region, which is different from the metazoan taxa. Differences are observed inter-group, but also intra-group.*

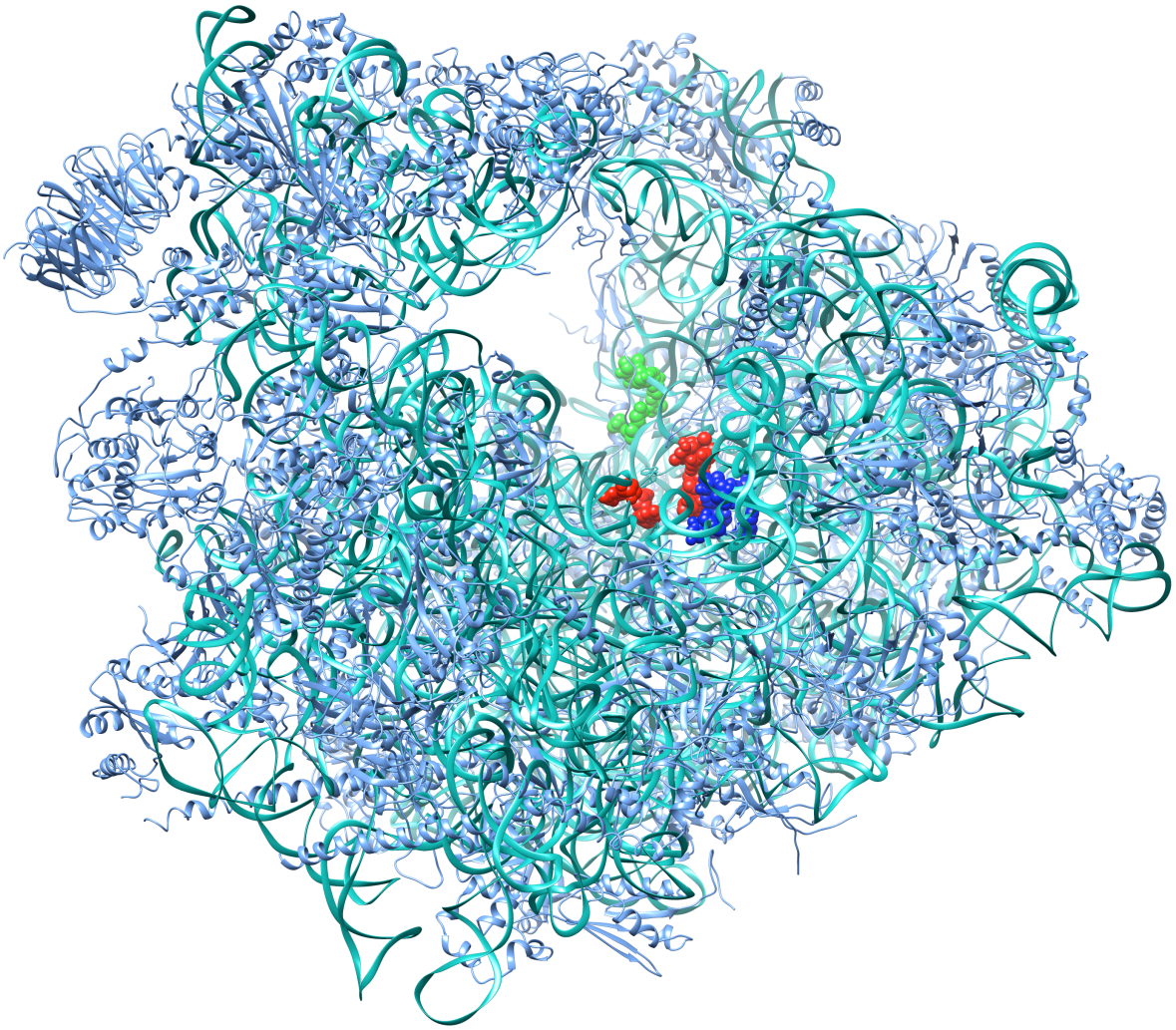

*FIGURE 17: CANDIDA ALBICANS 80S RIBOSOME MODEL*

*The positions of the three active sites are highlighted in color; A-site in blue, P-site in red, E-site in green. The r-proteins are colored dark blue and rRNA are colored in light blue.*

Modeling of the *C. albicans* ribosome allowed us to evaluate its molecular weight as around 3.2 MDaltons with an rRNA/r-protein ratio of 1.27 (Annex). 44 r-proteins are found in the large sub-unit (LSU) and 35 in the small sub-unit (SSU). By comparison of the sequences of r-proteins and rRNA of *C. albicans* with those of the *S. cerevisiae* ribosome, we identified a high level of similarity. Though the eL41 r-protein is missing, the A, E, and P-sites are identified on the *C. albicans* ribosome model (Figure 17) by structure superposition with the *S. cerevisiae* ribosome structure (PDB 4V7R). This allows us to identify residues involved in these three active sites (Table 3).

| Sites | Residues | *S. cerevisiae* | *C. albicans* | *H. sapiens* |
|---|---|---|---|---|
| A | 25S rRNA | G2403 | G2382 | G3907 |
| | | G2816 | G2789 | G4393 |
| | | A2820 | A2793 | A4397 |
| | | C2821 | C2794 | C4398 |
| | | U2873 | U2846 | U4450 |
| | | U2875 | U2848 | U4452 |
| P | 25S rRNA | C2405 | C2384 | C3909 |
| | | C2406 | C2385 | C3910 |
| | | C2407 | C2386 | C3911 |
| | | G2619 | G2592 | G4196 |
| | | G2620 | G2593 | G4197 |
| | | U2807 | U2780 | U4384 |
| | | A2808 | A2781 | A4385 |
| | | A2969 | A 2942 | A4546 |
| | | C2970 | C 2943 | C4547 |
| E | 25S rRNA | C2764 | C2737 | C4341 |
| | | G2793 | G2766 | G4370 |
| | | G2794 | G2767 | G4371 |
| | eL42 Protein | 43 TYR | 43 TYR | 41 TYR |
| | | 55 LYS | 55 LYS | 53 LYS |
| | | 56 PRO | 56 GLN | 54 PRO |
| DC | 18S rRNA | A1755<br>A1756 | A1742<br>A1743 | A1824<br>A1825 |

*TABLE 3: COMPOSITION OF THE THREE ACTIVE SITES OF S. CEREVISIAE (PDB 3J77), THE C. ALBICANS MODEL, AND THE H. SAPIENS (PDB 4UG0) 80S RIBOSOME.*

*The A-site is composed of six nucleotides located on the 25S rRNA. The P-site is composed of nine nucleotides located on the 25S rRNA. The E-site is composed of three nucleotides located on the 25S rRNA and three amino acids located on the eL42 protein. The decoding center is composed by two consecutive nucleotides located on the 18S rRNA.*

Though the A and P-sites are conserved in these three organisms, there is a difference in the composition of the E-site on the *C. albicans* ribosome. On the eL42 protein, amino acid 56 in *S. cerevisiae* and amino acid 54 in *H. sapiens* are both prolines, but in the *C. albicans* ribosome, we observe a glutamine. The decoding center constituted by two nucleotides located on the 18S rRNA is conserved (Table 3).

## 3. ANALYSIS OF BINDING POCKETS FOR THE KNOWN INHIBITORS OF THE EUKARYOTIC RIBOSOME

The identification of antifungals already positioned in *S. cerevisiae*, the aminoglycoside family, glutarimides, and others described in the works of Nicolas Garreau (Garreau de Loubresse *et al.*, 2014), prompted us to compare target pockets of *S. cerevisiae* and *C. albicans*. These may be solutions or at least the first steps in studies to find one or more target sites for potential drug candidates to block the action of the ribosome of *C. albicans*. One inhibitor of each site described was chosen arbitrarily.

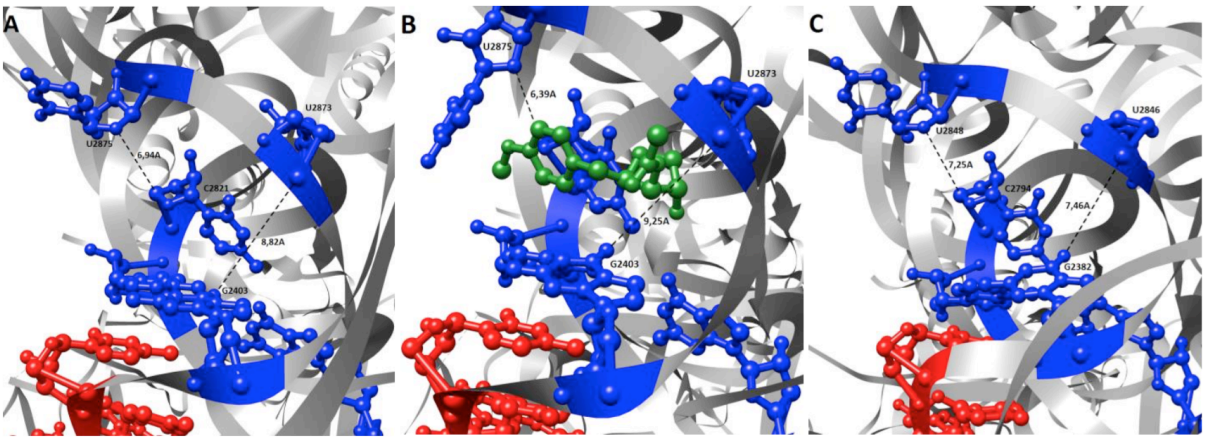


*FIGURE 18: COMPARISON OF A-SITE BINDING POCKETS OF SACCHAROMYCES CEREVISIAE AND CANDIDA ALBICANS.*

*The A-site is colored in blue, the P-site in red, and anisomycin in green. Image A shows the vacant A-site of S. cerevisiae; B shows the anisomycin binding in the A-site of S. cerevisiae; and C shows the vacant A-site of C. albicans. Distances between important residues are indicated to better evaluate the volume of the binding pocket and to identify changes occurring after drug binding.*

The A-site is composed of the same residues in both *S. cerevisiae* and *C. albicans* (Table 3). Images A and C (Figure 18) show the structures of the vacant A-site in both yeasts and allow for a comparison between them. They look highly similar; indeed, the atomic distances indicated between important residues are similar. Image B shows the binding of the anisomycin (ANM) in the A-site of *S. cerevisiae*. ANM is a known inhibitor of the ribosome that binds on the A-site, and is by extension an inhibitor of the eukaryotic translation. Indeed, it inhibits the peptidyl transferase, and thus the formation of the peptide bond between the peptide chains during synthesis and the new amino acid to be incorporated. The ANM binding in *S. cerevisiae* induces a major conformational modification of two residues, U2875 and C2821 (Garreau de Loubresse *et al.*, 2014).

As described previously, the A-site binding pocket is highly similar between *C. albicans* and *S. cerevisiae*, in both important residues and structures, and this similarity implies a high probability of ANM binding in the *C. albicans* A-site. It seems to be a relatively interesting site in view of all the inhibitors already known to bind the A-site in *S.*

*cerevisiae*. A comparison with *H. sapiens* should be carried out to determine if the human A-site is different enough in order to specifically target that of *C. albicans*.

## 3. 2. THE P-SITE

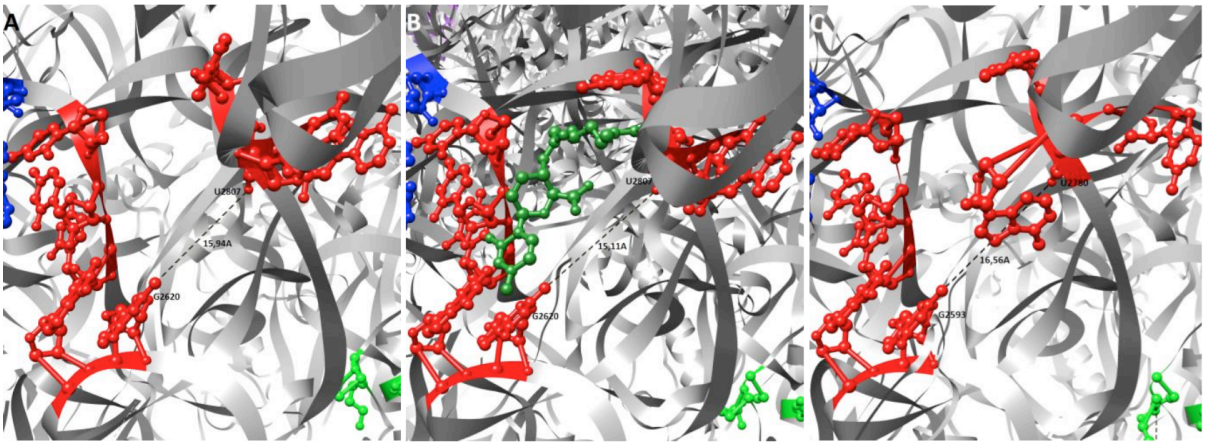


*FIGURE 19: P-SITE BINDING POCKET COMPARISON BETWEEN SACCHAROMYCES CEREVISIAE AND CANDIDA ALBICANS.*

*The A-site is colored in blue, the P-site in red, blasticidin in dark green and the E-site in light green. Image A shows the vacant P-site of S. cerevisiae; B shows the blasticidin binding in the P-site of S. cerevisiae; and C shows the vacant A-site of C. albicans. Distances between important residues are indicated to better evaluate the volume of the binding pocket and to identify changes occurring after drug binding.*

The P-site is composed of the same residues in both *S. cerevisiae* and *C. albicans* (Table 3). Images A and C (Figure 19) show the structures of the P-site in both yeasts and allow for a comparison between them. They appear to be different because there are two missing nucleotides in the modeling of the 25S rRNA of *C. albicans*; even if those nucleotides are identical to those of *S. cerevisiae*, we observe a visual obstruction created by the Chimera software that voids these missing nucleotides, A2942 and C2943.

Image B shows the binding of the blasticidin (BLC) in the P-site of *S. cerevisiae*. BLC is a known inhibitor of the ribosome that binds on the P-site, and is by extension an inhibitor of the eukaryotic translation. Indeed, it inhibits the termination step of the translation by inhibition of the neopeptide release. The BLC binds in *S. cerevisiae* without inducing any conformational modifications of P-site residues (Garreau de Loubresse *et al.*, 2014).

As described previously, the P-site binding pocket is highly similar, in both important residues and structure, between *C. albicans* and *S. cerevisiae*, and this similarity implies a high probability of BLC binding in the *C. albicans* P-site. It seems to be a relatively

interesting site in view of all the inhibitors already known to bind the A-site in *S. cerevisiae*. A comparison with *H. sapiens* should be carried out to determine if the human A-site is different enough in order to specifically target that of *C. albicans*.

## 3. 3. THE E-SITE

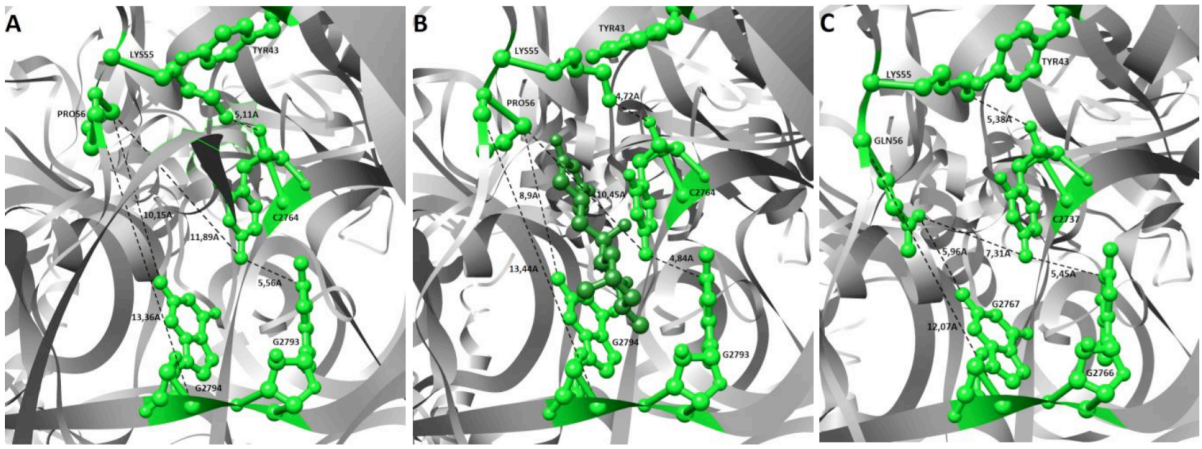


*FIGURE 20: E-SITE BINDING POCKET COMPARISON BETWEEN SACCHAROMYCES CEREVISIAE AND CANDIDA ALBICANS.*

*The E-site is colored in light green and the cycloheximide in dark green. Image A shows the vacant E-site of S. cerevisiae; B shows the cycloheximide binding in the E-site of S. cerevisiae; and C shows the vacant E-site of C. albicans. Distances between important residues are indicated to better evaluate the volume of the binding pocket and to identify changes occurring after drug binding.*

The E-site is composed of the same residues, except one amino acid located on the eL42 r-protein, in both *S. cerevisiae* and *C. albicans* (Table 3). Images A and C (Figure 20) show the structures of the E-site in both yeasts and allow for a comparison between them. The structure of the E-site is identical, but the space is reduced by the modification of residue 56 of the eL42 r-protein. Residue 56 in *S. cerevisiae* is a proline, but in *C. albicans* it is a glutamine. The side chain of the glutamine is involved in the occupancy of the E-site pocket, and the reduction of the available space there.

Image B shows the binding of the cycloheximide (CHX) in the E-site of *S. cerevisiae*. CHX is a known inhibitor of the ribosome that binds on the E-site, and is by extension an inhibitor of the eukaryotic translation. Indeed, it inhibits the mRNA translation mechanism by

stalling translating ribosomes on mRNA, and it has been described by crystallography. It blocks the release of tRNA after their delivery of the new amino acids. The CHX binds in *S. cerevisiae* without inducing any strong conformational modifications of E-site residues (Garreau de Loubresse *et al.*, 2014).

As described previously, the E-site binding pocket is slightly different in both important residues and structure between *C. albicans* and *S. cerevisiae*, an observation that could explain the resistance of *C. albicans* to CHX (Goldway *et al.*, 1995). We note that the size of the binding pocket is smaller due to a modification to amino acid 56 of the eL42 r-protein. The replacement of a proline in *S. cerevisiae* by a glutamine in *C. albicans* does not induce a charge modification, but rather a steric clash that is certainly implicated in this CHX resistance. It seems to be an interesting site in view of the two other inhibitors already known to bind the E-site in *S. cerevisiae*, lactimidomycin (LAC) and phyllantoside (PHY).

The LAC and PHY which are positioned in the same place, certainly suffer the same effect this transformation entails. Indeed, CHX causes a static inhibition; it can bind and unbind the ribosome, since it is non-covalently linked. However, when LAC and PHY bind to the ribosome they lead to a type of lethal inhibition; once linked to the E-site, they do not come off and therefore lead to a halt of the translation. However, in order to do this they need to be able to bind to this site. In the case of *C. albicans*, either the binding pocket is smaller, to the point that CHX cannot bind, or CHX is proportionally smaller than LAC and PHY. We can hypothesize that the mutation confers *C. albicans* not just a resistance against the CHX but also against LAC and PHY.

This mutation, when present in *S. cerevisiae*, confers resistance to the LAC, so our hypothesis would be verified for this inhibitor. The question remains to be clarified regarding the PHY. Finally, a comparison with *H. sapiens* should be performed to determine if the human E-site is different enough in order to specifically target *C. albicans*.

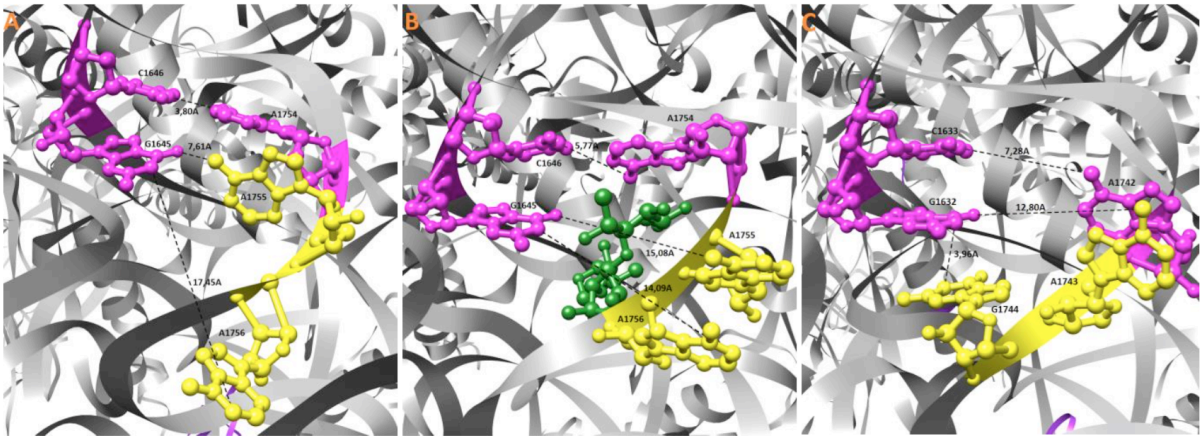


*FIGURE 21: DECODING CENTER BINDING POCKET COMPARISON BETWEEN SACCHAROMYCES CEREVISIAE AND CANDIDA ALBICANS.*

*The decoding center is colored in yellow, geneticin in green and important nucleotides implicated in its binding are in violet. Image A shows the vacant decoding center of S. cerevisiae. B shows the geneticin binding in the decoding center of S. cerevisiae; and C shows the vacant decoding center of C. albicans. Distances between important residues are indicated to better evaluate the volume of the binding pocket and to identify changes occurring after drug binding.*

The decoding center (DC) presents no difference in residue composition in *S. cerevisiae* and *C. albicans* (Table 3). Images A and C (Figure 21) show the structures of the DC and the steric dispositions of important residues implicated in the binding of geneticin (GEN) in both yeasts which allows for a comparison between them. According to the image, the binding pocket seems smaller for *C. albicans*. Even though there are the similarities in both yeasts, important residues are not oriented in the same way, even if they are the same. There is a steric obstruction created by guanine 1744 which occupies this space, and due to this the GEN binding seems relatively difficult.

Image B shows the binding of the GEN in the DC of *S. cerevisiae*. GEN is a known inhibitor of the ribosome that binds on the DC, and is by extension an inhibitor of the eukaryotic translation. Indeed, it inhibits mRNA decoding by preventing tRNA selection and its fixation. The GEN is positioned between residues by inducing a large change in their conformation. This is also observed by visualizing a movement called flipping-out, where nucleotides forming the DC move outward in order to host the GEN.

As described, the two DC are very different, but even if the *C. albicans* DC seems obstructed by the G1744, the flipping-out mechanism described during the GEN binding in *S. cerevisiae* could also happen in the *C. albicans* DC. The only restriction is that this hypothesis would create an overwhelming tension in the chain of 25S rRNA, thus not allowing the GEN binding to occur.

## 3. 5. THE MESSENGER RNA TUNNEL

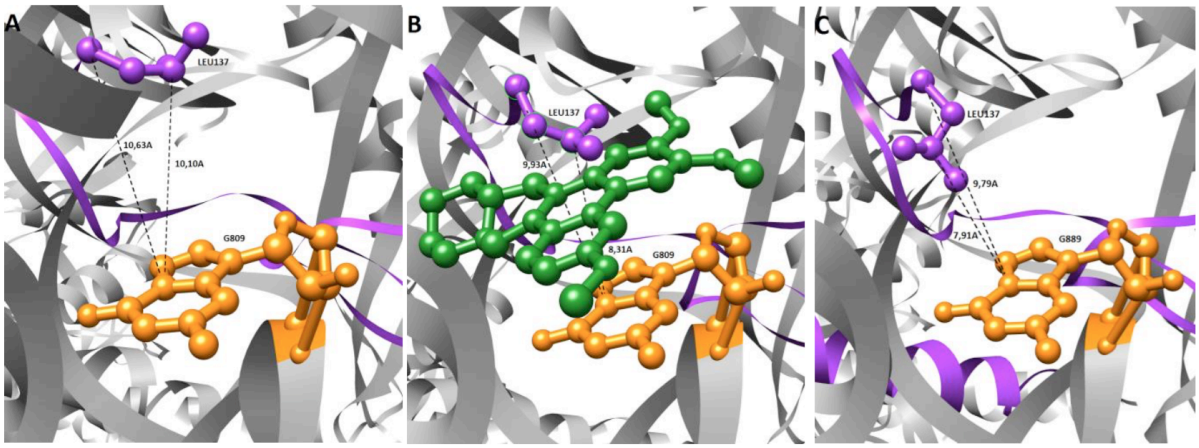


*FIGURE 22: CRYPTOPLEURINE BINDING POCKET IN A PART OF THE MRNA TUNNEL, COMPARISON BETWEEN SACCHAROMYCES CEREVISIAE AND CANDIDA ALBICANS.*

*This part of the mRNA tunnel represents the binding pocket of the cryptopleurine. It is composed of nucleotide 904 of the 18S rRNA colored in orange; cryptopleurine in green; and r-protein uS11 and its important C-terminal amino acid leucine 137, implicated in the binding of cryptopleurine and modeled here as sticks, are colored in violet. Image A shows the vacant binding pocket of S. cerevisiae; B shows the cryptopleurine binding this particular pocket in S. cerevisiae; and C shows this vacant binding pocket in C. albicans. Distances between important residues are indicated to better evaluate the volume of the binding pocket and to identify changes occurring after drug binding.*

The mRNA tunnel binding pocket is composed of the same residues in both *S. cerevisiae* and *C. albicans*. Images A and C (Figure 22) show the structures of the A-site in both yeasts and allow them to be compared. They look slightly different due to the placement of leucine 137 (LEU137); indeed, in the case of *C. albicans*, LEU137 is located in the binding pocket and therefore reduces the available space there. The atomic distances indicated between important residues show that the binding pocket is smaller in *C. albicans*. Image B

shows the binding of the cryptopleurine (CRY) in the binding pocket of *S. cerevisiae*. CRY is a known inhibitor of the ribosome, which binds in a part of the mRNA tunnel and is by extension an inhibitor of the eukaryotic translation. It inhibits the translocation mechanism which permits the release of deacetylate tRNA. CRY binds the ribosome SSU between those residues by inducing a light modification of the LEU137 conformation which is more oriented in the inhibitor direction (Garreau de Loubresse *et al.*, 2014).

The binding pocket is relatively smaller in *C. albicans* due to the orientation of the last amino acid of protein US11 (image C, Figure 22), which leaves less space and therefore makes a possible binding of the CRY more difficult. It is important to note, however, that the last amino acid of a protein will be more mobile than an amino acid in the middle of a polypeptide chain. Thus, this space difference can possibly be compensated for by a greater mobility of this residue, leucine 137, which will then allow for the binding of the CRY.

## 4. SPECIFIC RESIDUE IDENTIFICATION IN MULTIPLE ALIGNMENTS AND 3D VISUALIZATIONS

From multiple alignments for each ribosome protein built, we identified two types of residues that may represent potential targets for antifungal agents. We define “specific residues” as those that are not conserved between the different organisms in the multiple alignment, as well residues with a post-translational modification (PTM). Using a statistically robust algorithm, LEON-BIS (Vanhoutrève *et al.*, 2016) that was developed and tested during the course of this work, we were able to identify 112 specific residues and 80 PTMs in *C. albicans*.

After this, a clustering of the different sets of residues was carried out, based on their 3D coordinates. These identified clusters of residues are spatially close and therefore potentially interesting for the study. We obtained 18 clusters for the combined 192 specific residues and PTMs.

Due to a lack of time, the complete and detailed study of these clusters could not be completed, but an interesting cluster was identified based on its distance to the active sites (Figure 23 & 24). It lies on the eL18 r-protein, which is in the large subunit and has a length of 186 amino acids. It is at 15.74 Å from the E-site, at 47,86 Å from the A-site, and at 43,20 Å

from the P-site. It consists of two amino acids: 185, which is a lysine (Lys, L), and 186, which is a valine (Val, V). It is observed that these two amino acids are identical in *S. cerevisiae* and *C. albicans*, but not in humans, in whom asparagine 186 (Asn, N) is observed. This amino acid is the closest to the active sites that is different between the two yeasts and humans.

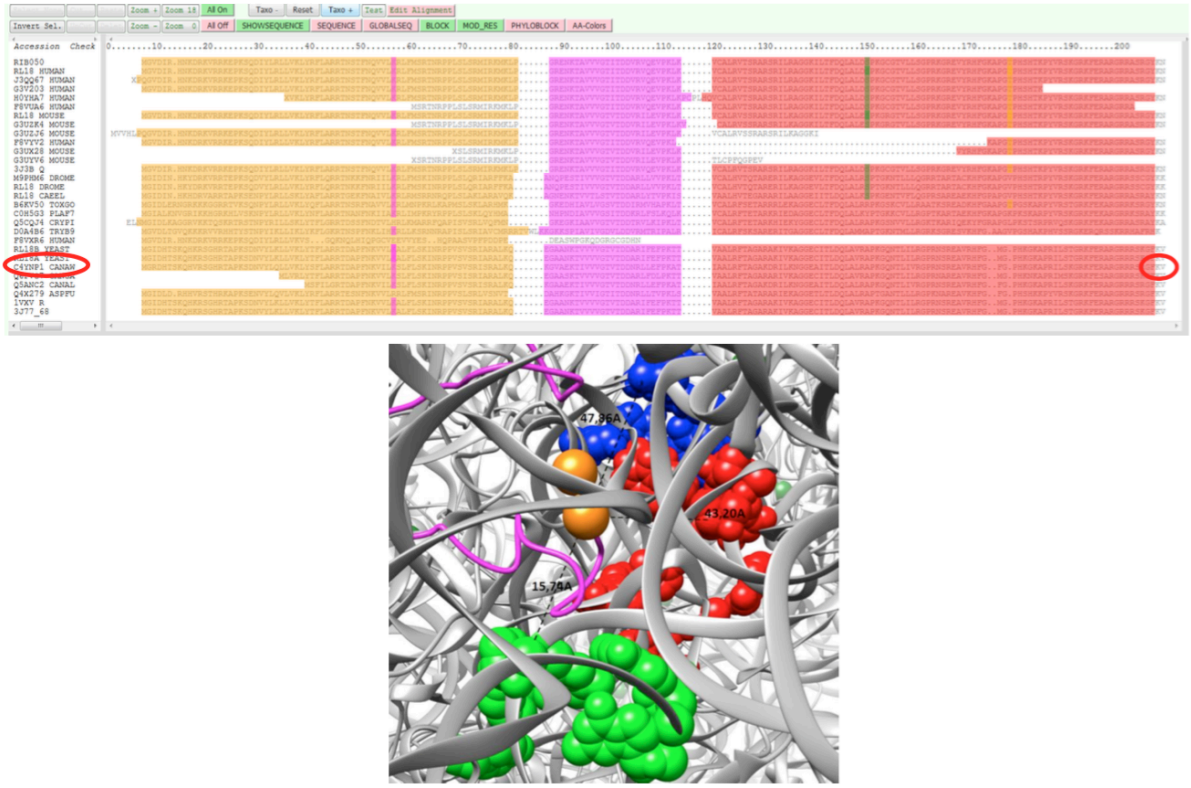


*FIGURE 23: EL18 R-PROTEIN ALIGNMENT VIZUALIZED USING THE WALI SOFTWARE (A) AND A ZOOM ON THE IDENTIFIED CLUSTER ON THE CANDIDA ALBICANS RIBOSOME (B).*

*(A) Visualization of the eL18 r-protein multiple alignment with conservation blocks (in orange, violet, and red) and PTM residues (dark green). The red circle corresponds to the interesting cluster on its r-protein.*

*(B) Visualization with Chimera of the cluster lying on the eL18 r-protein colored in violet. amino acids that are not located in conservation blocks are colored in orange.*

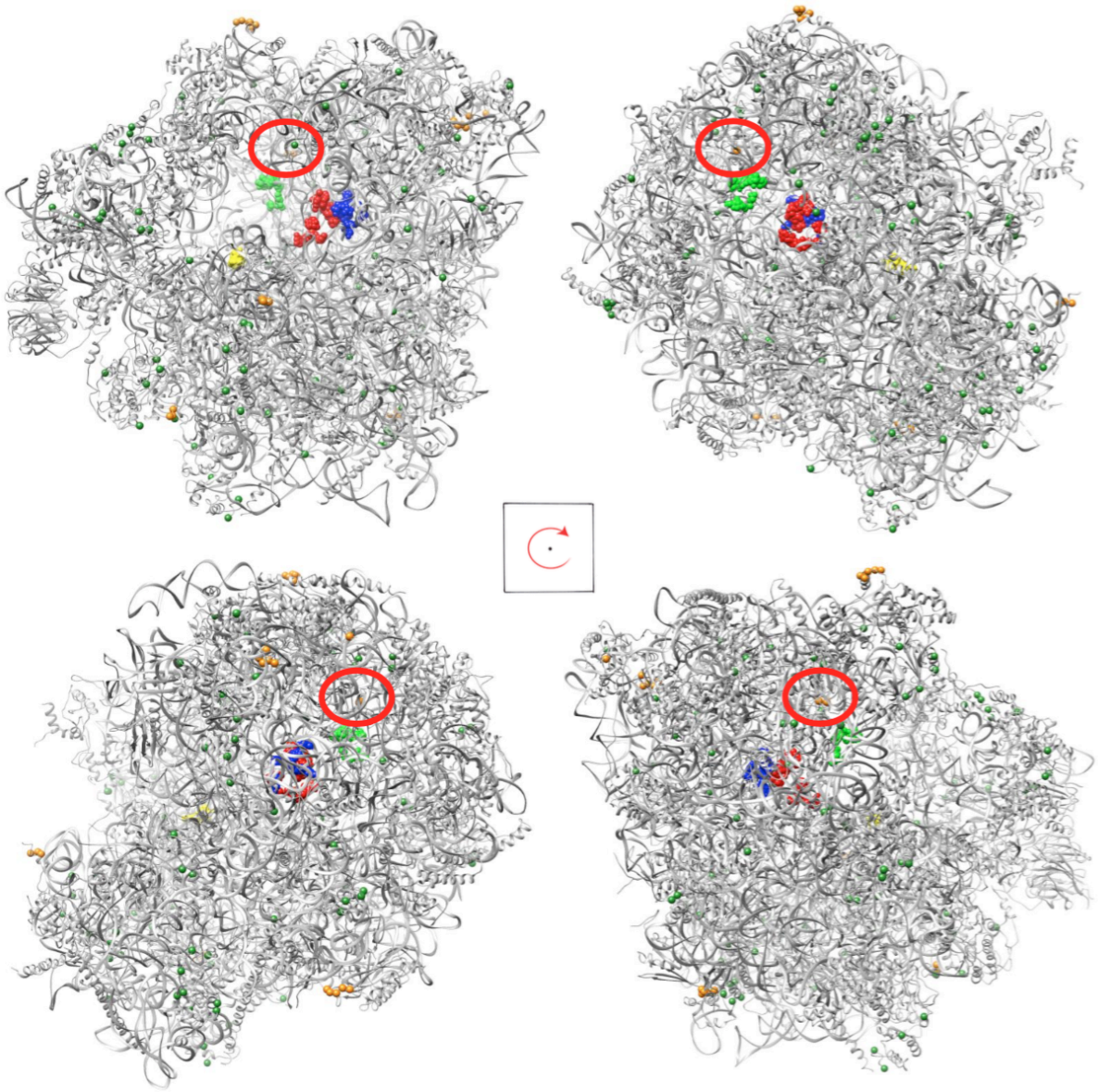

*FIGURE 24: CLUSTER VIZUALISATION ON THE CANDIDA ALBICANS RIBOSOME*

*The C. albicans ribosome viewed on Chimera with a 90° rotation and the active sites. The P-site is in red, the E-site in light green, the A-site in blue, and the decoding center in yellow. The visual result of the program with dark green residue modifications (type "MOD_RES of MACSIMS) and orange residues that are outside of the conservation blocks. The red circles correspond to an interesting cluster on the r-protein eL18.*

## 5. VISUALIZATION OF CHANNELS AND CAVITIES, SPATIAL CHARACTERIZATION OF THE RIBOSOME

To identify and characterize all the cavities and channels of ribosomes, the internal volumes of *C. albicans* and *S. cerevisiae* ribosomes were determined with the webserver tools *3V* (Voss and Gerstein, 2010).

A first tool, range volume, allows us to explore the surface of the structure according to probes of different radii. These probes each correspond to a radius a probe may have in order to enter the macromolecule. The calculated volume corresponds to the volume of the structure accommodating the probes of a radius less than the specified radius. Thus, for a probe radius of 0A, which is the Van der Waals radius (Voss and Gerstein, 2010), we obtain a volume of 2,376,493 $Å^3$ for a surface of 1992174 $Å^2$ in *C. albicans*. Table 4, details the volumes and surfaces obtained for various probes, as well as the comparison with *S. cerevisiae*. An overall comparison of the two structures reveals that the *C. albicans* ribosome seems to have a smaller size than that of *S. cerevisiae*.

*Table 4: Volume and the surface comparison obtained with 3V and its different tools.*

| | ***C. albicans*** | | ***S. cerevisiae*** | |
|---|---|---|---|---|
| **Tool + Radius of the probe** | **Volume** | **Surface** | **Volume** | **Surface** |
| **Volume range for 0Å** | 2 376 493 $Å^3$ | 1 992 174 $Å^2$ | 2 495 683 $Å^3$ | 2 192 978 $Å^2$ |
| **Volume range for 3Å** | 4 244 578 $Å^3$ | 627 373 $Å^2$ | 4 614 523 $Å^3$ | 650 557 $Å^2$ |
| **Volume range for 9Å** | 5 425 424 $Å^3$ | 281 485 $Å^2$ | 5 797 654 $Å^3$ | 299 698 $Å^2$ |
| | | | | |
| **Solvent extract from 3 to 9Å** | 917 353 $Å^3$ | 441 578 $Å^2$ | 908 444 $Å^3$ | 449 014 $Å^2$ |
| | | | | |
| **Channel found from 3 to 10Å** | 333 106 $Å^3$ | 131 507 $Å^2$ | 340 769 $Å^3$ | 133 137 $Å^2$ |
| **Channel found from 3 to 10Å** | 45 609 $Å^3$ | 15 425 $Å^2$ | 53 610 $Å^3$ | 19 841 $Å^2$ |

Subsequently, the extracted solvent volume was calculated (Table 4) by subtracting the excluded volume with the solvent (9 Å) from the shell volume (3 Å), with the tool *Solvent extract*. This volume can be divided into two types: the cavities and the channels. The cavities are large enough in volume to accommodate solvent molecules, but they are not connected to the outside. In contrast, the channels are connected to the surface, and thus include pockets, surface invaginations, the grooves, and tunnels (Voss and Gerstein, 2010). This volume corresponds to the volume of the solvent that the macromolecule may contain, including the cavities and tunnels (Figure 25). The comparison between the two bodies indicates that the *C.*

*albicans* ribosome contains more solvent than that of *S. cerevisiae*.

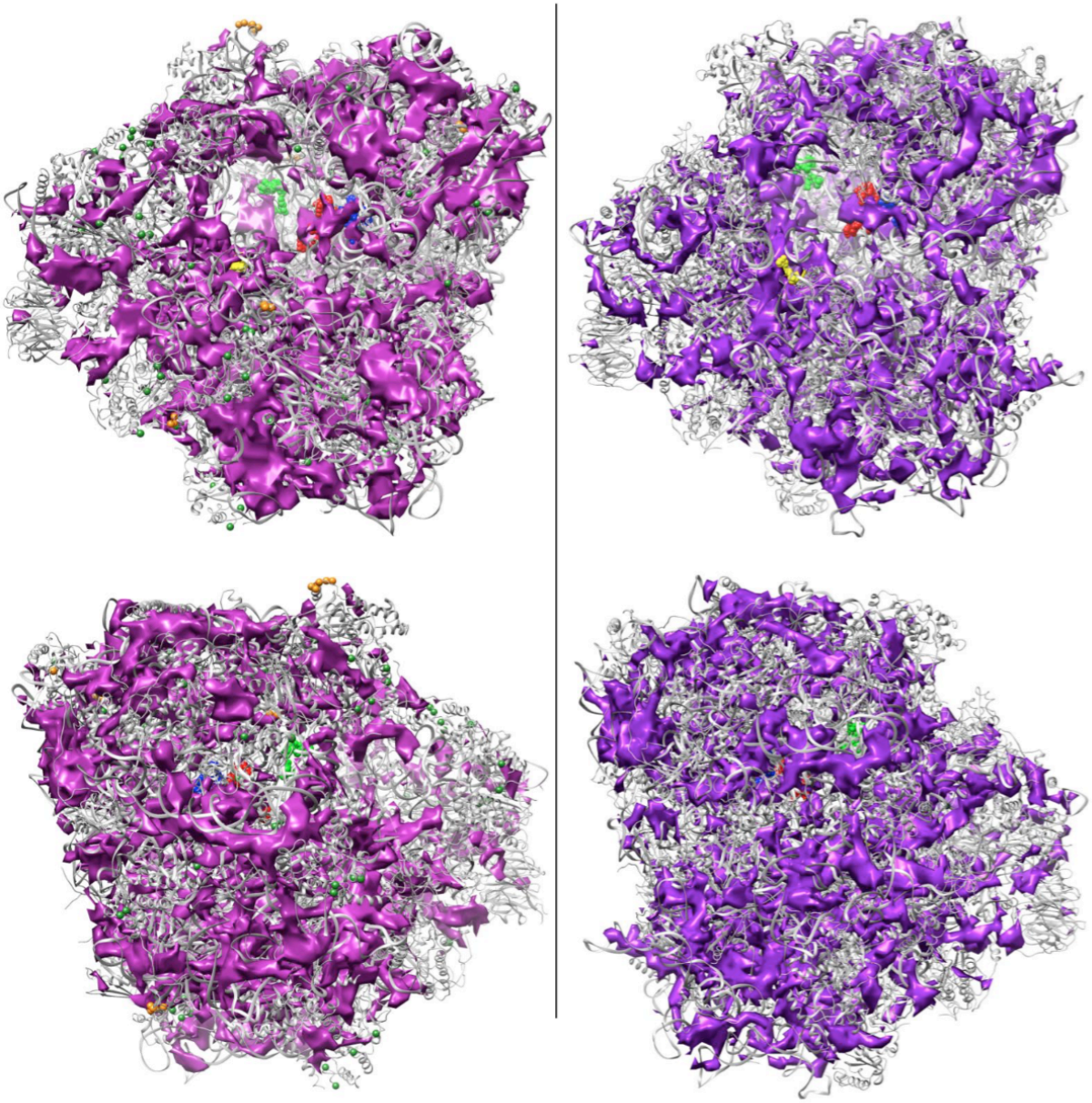

*FIGURE 25: SOLVENT VOLUME INSIDE THE CANDIDA ALBICANS AND SACCHAROMYCES CEREVISIAE RIBOSOMES*

*C. albicans ribosome on the left and S. cerevisiae ribosome on the right with a 180° rotation between the top image and the bottom one. The A-site is colored in blue, the P-site in red, the E-site in green, and the decoding center in yellow. Purple indicates the volume of solvent found with the tool Solvent Extract from 3V.*

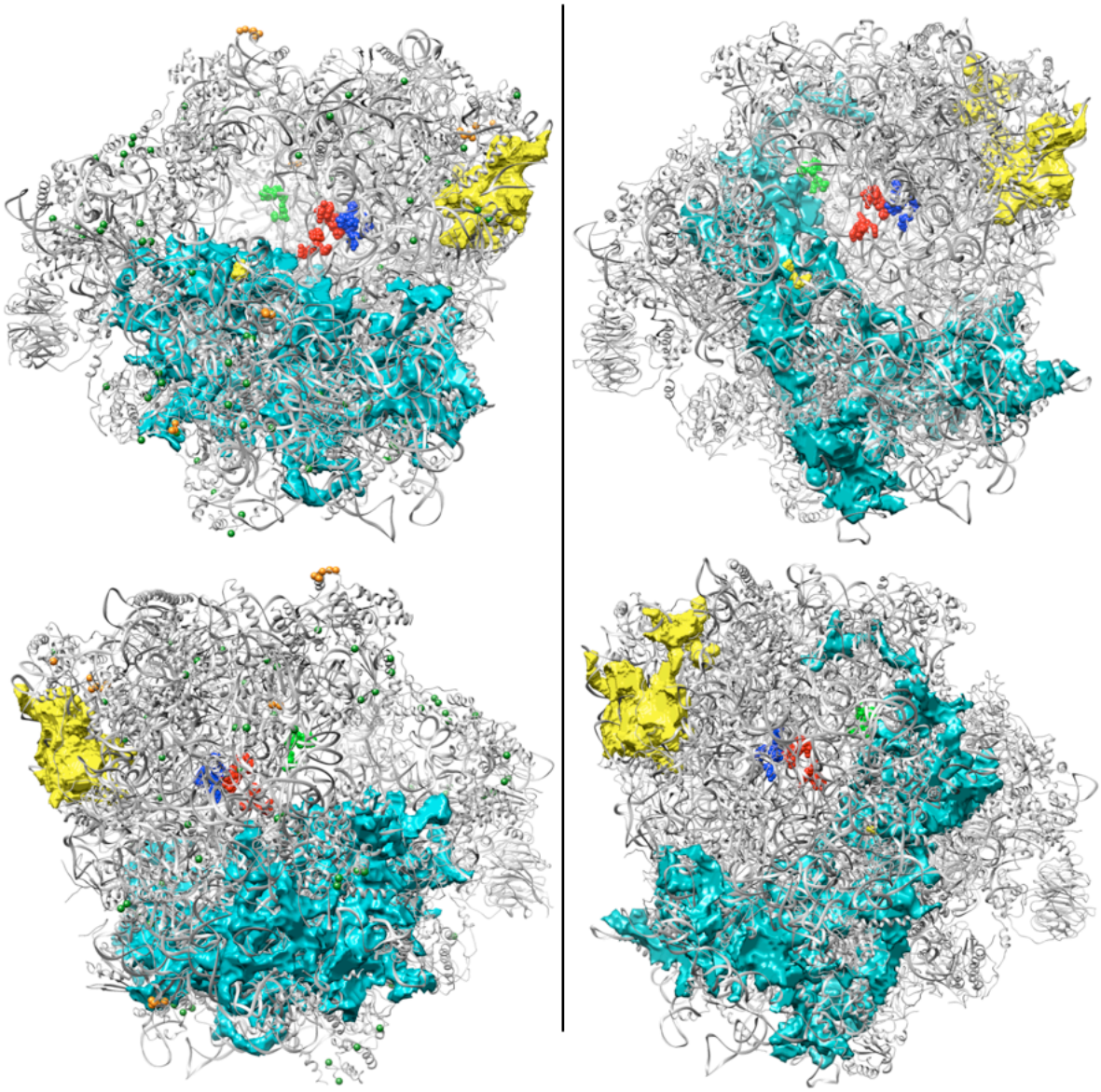

*FIGURE 26: VOLUME AVAILABLE TO ACCOMMODATE SPHERICAL PROBES CONNECTED TO THE OUTER SURFACE ON CANDIDA ALBICANS AND SACCHAROMYCES CEREVISIAE RIBOSOMES*

*C. albicans ribosome on the left and S. cerevisiae ribosome on the right with a 180° rotation between the top image and the bottom one. The A-site is colored in blue, the P-site in red, the E-site in green, and the decoding center in yellow. Light blue and light yellow represent the volume of both channels found with the tool "Channel Find" 3V.*

A final tool was used to find channels with two parameters: the number of channels to search for (2) and a radius of 3 to 10 Å. The volume obtained represents the solvent volume minus the volume of the cavities; given this, we obtain the sufficient size and volume available to accommodate spherical probes connected to the outer surface. Thus, we identified

the two larger channels (Table 4), which corroborates the results determined using the solvent extract. The largest volume is in the small subunit, while the second volume is at the level of the large subunit (Figure 26). This could certainly be related to the fact that the small subunit is much more mobile and flexible than the large ribosomal subunit.

# 4. DISCUSSION

## 1. KNOWN BINDING POCKETS

Most of the drugs that target the ribosome bind to it in one of the four sites, which are the three active sites A, P, E, and a reactional site, the decoding center (Loubresse Garreau *et al.*, 2014). These four sites are highly conserved in all organisms, with only one amino acid located in the E-site differing between *S. cerevisiae*, *H. sapiens* and *C. albicans*. Highlighting them in the 3D structure allows for an observation of specific residues in the space near to those sites, indicating a potential targetable spot.

*C. albicans* is known empirically in hospitals to be resistant to CHX, which binds to the E-site (Goldway *et al.*, 1995), and although this was identified at the protein level, it had never been demonstrated in a structural way. Comparing the *S. cerevisiae* and *C. albicans* ribosomes, some aspects were different; the volume of the binding pocket is smaller, and the important residues involved in the binding of an inhibitor CHX are not all similar. Indeed, in *C. albicans*, residue 56 of the eL42 r-protein is not a proline, as in *S. cerevisiae*, but a glutamine. This prevents the binding of CHX, driven by steric hindrance. This probably also blocks the binding of the LAC and hypothetically the PHY. Here, there is a particularly interesting site with its own specificity in *C. albicans* (eL42: P56Q); in fact, this resistance exists neither in *S. cerevisiae* (except in rare mutant strains) or in humans, who are both very sensitive to cycloheximide.

The A-site is where most inhibitors have been identified on the model of *S. cerevisiae* (Loubresse Garreau *et al.*, 2014), and given the similarities with the A-site of *C. albicans*, this would seem to be a relatively good site in terms of a possible inhibition with these previously known inhibitors. However, analyzing the residues involved in the formation of the A-site in humans, we realize that it is identical in terms of residues (Table 3). This would mean that, as in the case of using cycloheximide in humans, there would be a high toxicity because the

binding site is very similar to that of *S. cerevisiae*. The A-site, although very interesting on a pharmacological level, is finally not different enough between the three compared organisms and therefore is not specific enough to *C. albicans*.

By comparing the ribosome P-site of *S. cerevisiae* and *C. albicans*, we saw in the given sequences that nothing was different, and we reached the same conclusion for humans. So although modeling is not complete for this site, we can assume that the BLC will bind to the *C. albicans* ribosome. Nonetheless, the site does not seem to be the most interesting in this report, since it is effectively similar to human residues in its composition, and this site is conserved too much between the three organizations to find a specific target to focus on.

When comparing the *S. cerevisiae* and *C. albicans* DCs, many things were different: the volume of the binding pocket is smaller; even if the important residues involved in the binding of an inhibitor, in this case the GEN, are all similar; and most surprisingly, they are not at all in the same spatial positions. Indeed, in *C. albicans*, important nucleotides has a spatial position that appears to create a steric hindrance that is not present in *S. cerevisiae*. This would prevent the binding of GEN, due to the steric hindrance that results. Furthermore, the *S. cerevisiae* DC residues A1755 and A1756 perform a flipping-out when there is a binding of an inhibitor, so it can be assumed that it could also possibly take place in *C. albicans*. It will be interesting to see if this flipping-out can happen and if possible, if it can be done in a way such that GEN can bind to the *C. albicans* DC.

By comparing a specific portion of the mRNA tunnel between *S. cerevisiae* and *C. albicans*, only the residue in position 137, a leucine located at the N-terminal r-protein uS11, changes according to the organisms. It seems that there is a steric hindrance with a shorter distance in view of its position in *C. albicans*. There is also a changing in spatial position of this leucine between a vacant *S. cerevisiae* and an *S. cerevisiae* with an inhibitor, so it is conceivable that *C. albicans* may also have a change in spatial position of the residue, thus allowing the establishment of an inhibitor such as the CRY. However, though it has been identified as a eukaryotic specific inhibitor with a broad spectrum, CRY does not seem to be the inhibitor of choice for targeting *C. albicans*, particularly since it also interacts with the binding pocket described in the human ribosome.

## 2. IDENTIFICATION OF NEW POTENTIAL DRUG BINDING SITES

Despite the fact that most antifungal drugs that target the ribosome bind on the four most known functional sites, one could consider targeting other structural or functional regions with new inhibitors that would not affect humans. It can be hypothesized, for example, that it is possible to block the formation of the *C. albicans* ribosome, thereby preventing the translation process. The punctual mutation in the r-protein eL3 (Ban *et al.*, 2014) of the large ribosomal subunit of *S. cerevisiae* results in a phenotype resistant to anisomycin (Mailliot *et al.*, 2016). Depending on the binding site of the inhibitor, structural rearrangements within the ribosome may be different and either larger or smaller in size. The majority of eukaryotic specific inhibitors bind to the large ribosomal subunit. These inhibitors induce structural changes within 15Å from the binding site. For example, when binding to the A-site, the anisomycin causes the rupture of the pair U2875- G2952 and reorientation of the U2875 (Garreau Loubresse *et al.*, 2014). To identify such potentially pharmacologically interesting areas, we highlighted all the residues and the PTM specific to *C. albicans* and we localized specificity clusters within its 3D structure. Given the proximity of the identified cluster, consisting of amino acids of the r-protein eL18, the A-site shown in Figures 23-24 proves to be an interesting target taking into account the existing literature on the subject.

The identification of all the channels and cavities of the structure is very interesting as it allows us to access specific pockets in *C. albicans*. Thus, we have located in Figures 25 and 26 specific residues with respect to solvent volumes. This allows us to determine the accessibility of these molecules to specific areas and therefore the interest for chemists, for example, to use them in the design of new bioactive molecules.

For a more fundamental approach, the comparison between *S. cerevisiae* and *C. albicans* volumes allows us to provide differential information concerning the volume of solvent that the ribosomes of these two yeasts contain respectively. This information can be very useful in a study using radiocrystallographic approach since it provides important information about physicochemical parameters for different crystallization techniques currently used and developed.

# 5. CONCLUSION AND PERSPECTIVES

This study first described the *C. albicans* ribosome, which until now was not studied in its 3D structure. Active sites have been identified, located, and described. Secondly, the

specificities of *C. albicans* were highlighted through multiple approaches. This helped to identify possible sites to target in the case of use or design of specific inhibitors.

The A-site is very interesting in terms of its similarity with that of *S. cerevisiae*, and the inhibitors that target it, but it is too close to that of humans, which therefore makes it not specific enough. The P-site of *C. albicans* was shown to be different and specific, but since it is not yet properly modeled, it does not allow us to draw tangible conclusions. The decoding center and the portion of the mRNA tunnel described showed interesting possibilities given the structural differences highlighted in the figures comparing the two yeasts of interest. It would be interesting to check the position of these residues in humans. Finally, the E-site proved the most interesting in terms of specific characteristics of *C. albicans*. The modification of an amino acid effectively gives *C. albicans* resistance to an inhibitor and possibly two other drugs; this mutation is not present in neither *S. cerevisiae* nor humans. Thus, this is an extremely interesting target for performing work of drug design.

Specificities have been identified outside of these previously known sites, even though they can be close and therefore be targeted by inhibitors that set off a possible domino effect that disrupts or undermines the actions of these sites. For specific areas that are more remote from the active sites, it would be interesting to identify whether this part of the ribosome is involved in setting a cofactor involved in the translation mechanism or if it intervenes in other roles that the ribosome can have.

In order to verify the predictions made by the bioinformatics study, *in viv*o inhibitory studies are currently being developed. These studies will help demonstrate whether or not the inhibitors have an effect on *C. albicans*. Indeed, before reaching the ribosome, the molecules must pass through the fungal cell wall and plasmic membrane.

If these studies prove successful, this is to say, if at least one of the inhibitors of the ribosome stops the growth of the strain, then it will be important to verify the non-toxicity of this or these molecules on human cell cultures in order to obtain a new drug candidate, which will be a specific antifungal against *C. albicans*.

During this study, it was often difficult to find software that can run on large molecules, such as the ribosome, so it would be interesting to develop specific software for this purpose or to allow existing ones to support such a macromolecule. This predictive bioinformatics study is currently specified and correlated by a determination of the *C. albicans* ribosome structure performed by X-ray crystallography.

# V. *CANDIDA ALBICANS* RIBOSOME STRUCTURE DETERMINATION VIA X-RAY CRYSTALLOGRAPHY

## 1. AIM OF THE PROJECT

Predictive bioinformatics were useful to obtain information from a standpoint of r-proteins and rRNA sequences as well as bioinformatics ribosome modeling. This *in silico* model and the observations made on it can be confirmed or invalidated by a structural determination via X-ray crystallography. This process was carried out by our team who has a mastery in crystallography skills, and focused on a new organism which is very close to *S. cerevisiae*. The X–ray crystallography required:

- Establishing a protocol of culture and biomass production
- The establishment of a ribosome purification protocol
- Determining the crystallization parameters of the ribosome
- Determination of dehydration and cryopreservation conditions and crystal freezing
- The establishment of diffraction data collection parameters
- The integration of diffraction data obtained

The resolution of the structure via this approach is still ongoing but has produced sufficiently accurate results to allow for some initial descriptions of the decoding center, found later in this chapter.

Once the determination of the *C. albicans* 80S ribosome structure is complete, the establishment of a stable and reproducible protocol will allow us to conduct studies on the mechanics of translation in this particular organism since it does not follow the universal genetic code. We will also be able to study the binding of inhibitors in the *C. albicans* ribosome *in vitro*, instead of *in silico* (Chapter IV).

## 2. MATERIAL AND METHODS

The procedures utilized follow the previously developed protocols for the *S. cerevisiae* 80S ribosome purification and crystallization (Ben-Shem *et al.*, 2010), which have been improved since. Even if *S. cerevisiae* and *C. albicans* are close phylogenetically, several parameters had to be reset in order to produce a sufficient amount of pure *C. albicans* 80s ribosomes in order to purchase crystallization and crystallography studies.

### 1. PURIFICATION OF THE 80S RIBOSOME

The *C. albicans* strain SC5314 was provided by Dr. Sadri Znaidi (Institut Pasteur, Paris, France) (Gillum et al., 1984). It is a wild strain type of *C. albicans* isolated from a patient with a generalized infection (description on I. 1. 4.).

As *C. albicans* is classified as a biosafety level 2 pathogen, we were not allowed to produce the necessary biomass for the ribosome production at the IGBMC, since it is not equipped with a P2 lab accessible for yeast experiments. Thus, this and all prior steps such as strain maintenance, observation, and pre-cultures were performed at the *Institut de Parasitologie et de Pathologie Tropicale de Strasbourg* in the virology department of Professor Olivier Rohr.

The yeast culture is performed overnight in flasks containing standard YPD media at 34°C from a fresh single colony pre-culture. The culture requires constant attention since only colonies in white phase are selected (description in I. 2. 3.) for ribosome production. Cells are harvested by centrifugation when $OD_{600}$ reaches 1.0 to 1.2 maximum and are subjected to the glucose starvation treatment. Glucose starvation is used to homogenize ribosome population *in vivo* as much as possible by rapidly and reversibly inducing translation inhibition. After only a few minutes, all translating ribosomes in polysomes are transferred to inactive 80S monosomes (Ashe *et al.*, 2000). Practically, the treatment requires a resuspension of the pellet in YPA media (YPD without glucose) and an incubation of the flasks at 34° C for 12 minutes. The pellet is then recovered by centrifugation and all further steps are performed at 0 to 4°C. Cells are washed with buffer M (30mM Hepes-KOH pH 7.5, 50 mM KCl, 10 mM $MgCl_2$, 8.5% mannitol, 2mM DTT, 0.5 mM EDTA). Typically, 4 to 5 grams of cells are obtained from 4L culture.

After the washing steps, cells are prepared for lysis. The pellet is resuspended in 6.5

ml of buffer M supplemented with an additional 1200 µL of protease inhibitor cocktail (PIC, Roche), 200 µL RNasin (Promega), 240 µL Pefablock 100 mM, 535 µL KCl, 22 µL DTT and 60 µL of heparin 100 mg/ml. Heparin concentrations are found to participate in ribosome solubility thus affecting the amount of PEG required at later steps to precipitate the ribosomes. Cells are disrupted with glass beads by vortex shaking the tube 9 times for 1 minute with 1 minute breaks on ice between each shake. This step needed to be adapted since the cell wall of *C. albicans* seemed to be stronger than that of *S. cerevisiae*. Proteases and RNases inhibitor amounts are increased, since the *C. albicans* strain is not engineered as the *S. cerevisiae* strain, due to the selected deletions of particulars proteases and RNases (ref). After this, the obtained lysate is filtered on a 0.45-micron membrane (Stericup, Milipore) in order to obtain a sample free of any live *C. albicans* cell; this step allowed us to go back to the IGBMC and to perform the following steps of the purification there. The transport of the cells needs to be as quick as possible.

The lysate is clarified by centrifugation (30,000g during 10 minutes) before being subjected to a differential precipitation by 20,000 polyethylene glycol (PEG, Hampton Research). This step is used to quickly fractionate the lysate in order to recover the ribosome-containing fraction. Thus, PEG 20K is added from a 30% w/v stock to a final concentration of 4.5% w/v for the first fractionation. The solution is clarified by centrifugation (20,000g during 5 minutes), the supernatant is recovered, and the KCl concentration is adjusted to a 130 mM final concentration. PEG 20K concentration is increased to 8.5% for the second fractionation. Ribosomes are pelleted (20,000g during 10 minutes) and the supernatant is discarded. The ribosome pellet is resuspended in buffer M+, which is composed of buffer M with a KCl concentration adjusted to 150 mM and supplemented with protease inhibitors, DTT, and heparin. At this stage, typically 25 to 32 mg of ribosomes are obtained from 4 to 5 grams of yeast cells.

Ribosomes are further purified by a 10-30% sucrose gradient in buffer A (20 mM Hepes-KOH pH 7.5, 120 mM KCl, 8.3 mM $MgCl_2$, 2 mM DTT, 0.3 mM EDTA) using the SW28 rotor (18,000 rpm during 15 hours). The appropriate fractions are pooled and both KCl and $MgCl_2$ concentrations are adjusted to 150 mM and 10 mM respectively. In order to precipitate ribosomes, PEG 20K is added to a final concentration of 7% w/v. Ribosomes are pelleted by centrifugation (20,000g during 10 minutes). The white pellet is gently suspended in buffer G (10 mM Hepes-KOH pH 7.5, 50 mM KOAc, 10 mM $NH_4Cl$, 2 mM DTT, 5 mM $Mg(OAc)_2$) to obtain a final concentration of 21 mg/mL and can be frozen and stored at -

80°C, Usually, 8 to 11 mg of pure ribosomes are obtained from 4 to 5 grams of cells.

## 2. BIOCHEMICAL, BIOPHYSICAL, AND MASS SPECTROMETRY ANALYSIS OF *CANDIDA ALBICANS* 80S RIBOSOME

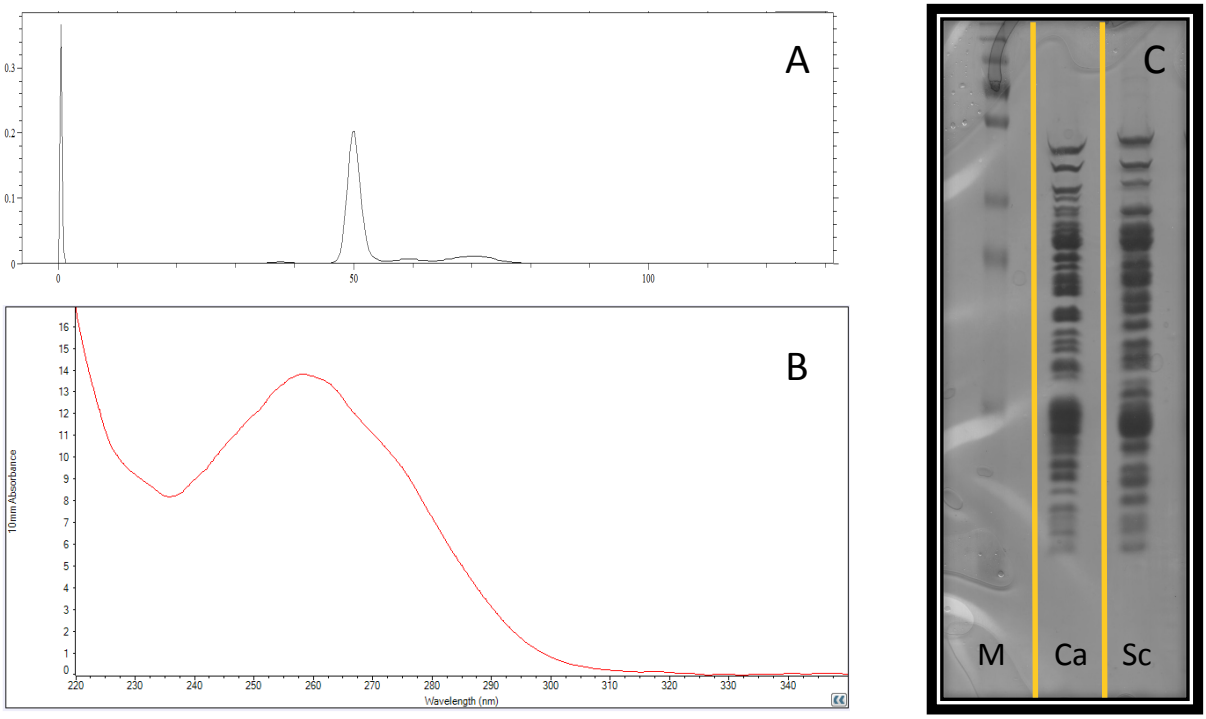


*FIGURE 27: BIOCHEMICAL AND BIOPHYSICAL ANALYSES OF THE CANDIDA ALBICANS 80S RIBOSOME*

*A: Analytical ultracentrifugation of Candida albicans RS in Buffer G; the main peak corresponds to 79.9S. B: Candida albicans ribosome absorbance spectrum; the maximal absorbance is observed at a wavelength of 260nm. C: Electrophoresis gel of r-proteins; M stands for the ladder, Ca for Candida albicans and Sc for Saccharomyces cerevisiae; visual comparison of r-protein composition of both yeasts.*

Though the sedimentation coefficient and the absorption spectrum are extremely similar between *C. albicans* and *S. cerevisiae*, a simple comparative r-protein electrophoresis gel allowed us to observe important differences at least in the size of r-proteins in both yeasts. In order to identify the *C. albicans* ribosome sample composition and to be sure that all of the r-proteins are present, we performed a mass spectrometry analysis known as MudPit which stands for *multidimensional protein identification technology*, a combination of liquid chromatography separation and mass spectrometry measurements (Washburn *et al.*, 2001).

First, the sample to analyze is desalted, then denatured and digested by endoproteases LysC (Wako) and trypsin (Promega). The digested mixture is loaded on a chromatography system for a two-step separation using a strong ion exchange followed by a reversed phase in a microcapillary column. Elution is performed gradually and iteratively to generate bundles of peptides that are immediately ionized and enter the tandem mass-spectrometer (MS/MS). Spectra are generated and queried against two protein databases to determine their protein origin (assembly 22 on www.candidagenomedatabase.org and the database sp Tr-EMBL). The MudPit experiment was performed on Orbitrap ELITE by Adeline Page and Mathilde Joint at the IGBMC proteomics facility. 30 to 60 r-proteins are found depending on which *Candida albicans* strain (WO-1 or SC5314) we use for database comparison. Ribosomal proteins, likely cytosolic ribosomal proteins, uncharacterized proteins, or even putative uncharacterized proteins, are identified by the databases, however some of the r-proteins of the *C. albicans* ribosome are still not known in the database and are thus not available for mass spectrometry results analysis. The eL41 r-protein is not found, though predictive bioinformatic results were identified with a very high score. The large difference between high scores observed for ribosomal proteins compared to very low scores for other protein possible contaminants, such as initiation, elongation, and termination factors of translation, confirms the high purity of our samples (Annex). There is one exception for the uncharacterized protein C4YQN5, as it is a non-ribosomal protein with a very high score. It is the homologous protein of Stm1p, a stress response protein known to bind the ribosome of *S. cerevisiae*. C4YQN5 seems to bind the purified 80S ribosomes.

## 3. CRYSTALLIZATION

Several large screenings, commercial and in-house, have been performed. Some of them were carried out by robots (Formulatrix, CBI facilities, IGBMC), and the rest by hand. They were then tested in several crystallization systems: microbatch, micro- and macroseeding, recrystallization, hanging, and sitting drop. An summary of cristals shape evolution in hanging drop system is in annex. The best crystallization condition is the following.

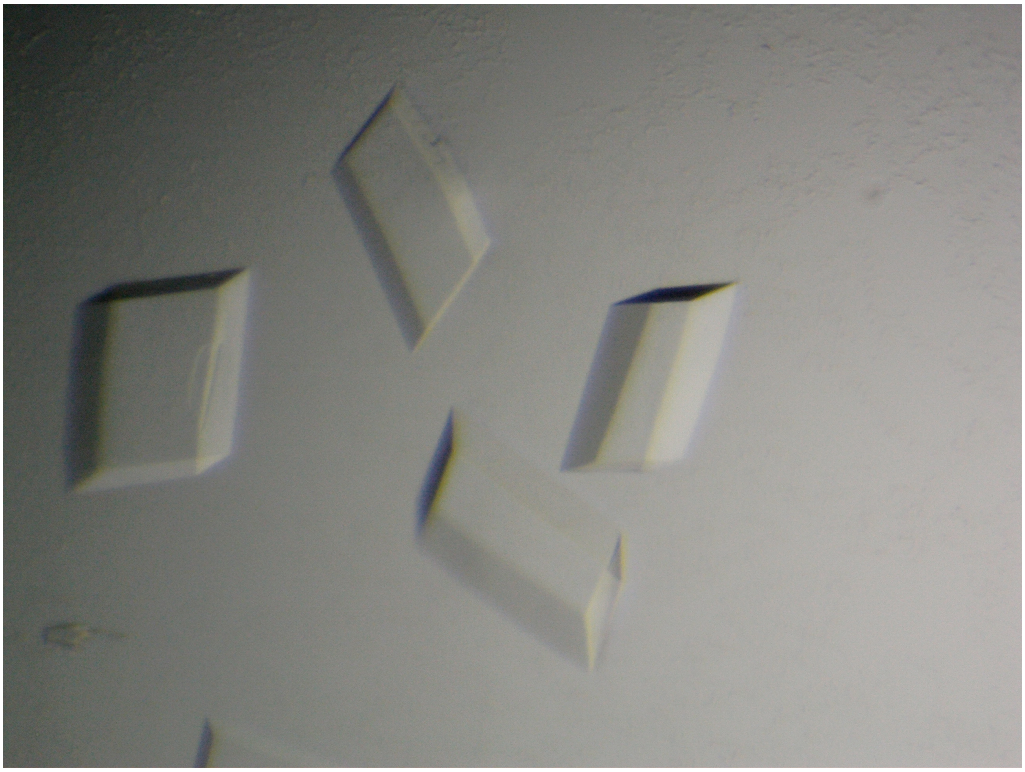

*FIGURE 28: LARGE CANDIDA ALBICANS RIBOSOME CRYSTALS WITH APPARENT DEFECTS*

F

or crystallization, the ribosome sample, defrosted slowly on ice, was prepared as following: 5 mg/mL ribosomes in buffer G, 2.5 mM Hepes-KOH pH 7.5, 2.5 mM $NH_4Cl$, 3.33 mM $Mg(OAc)_2$, 1.6 mM DTT, 0.055 mM EDTA, 2.8 mM Deoxy Big Chap, 40 mM KOAc, 5.5 mM $NH_4OAc$, 5.5 mM Tris-Acetate pH 7.0. The ribosome solution is incubated at 37°C for 10 minutes and left to cool down for at least 45 minutes in the cold room before crystallization. Ribosomes are crystallized using the hanging drop method at 4°C by mixing 2 µL of ribosome solution with 1.6 µL of reservoir solution (100 mM BisTris-Acetate pH 7.0, 250 mM KoAc, 100 mM KSCN, 3 mM $Mg(OAc)_2$, 20% glycerol, 3,8-4.3% w/v PEG 20K, 5 mM spermidine). Typically, crystals appear in a reproducible way after 5 days and reach their full size after 3 additional weeks. Large crystals with apparent defects were found to give the best diffraction limit, most likely due to their thickness (Figure 28), but it also seems that the shape of the crystal has an impact on the limit (Figure 29).

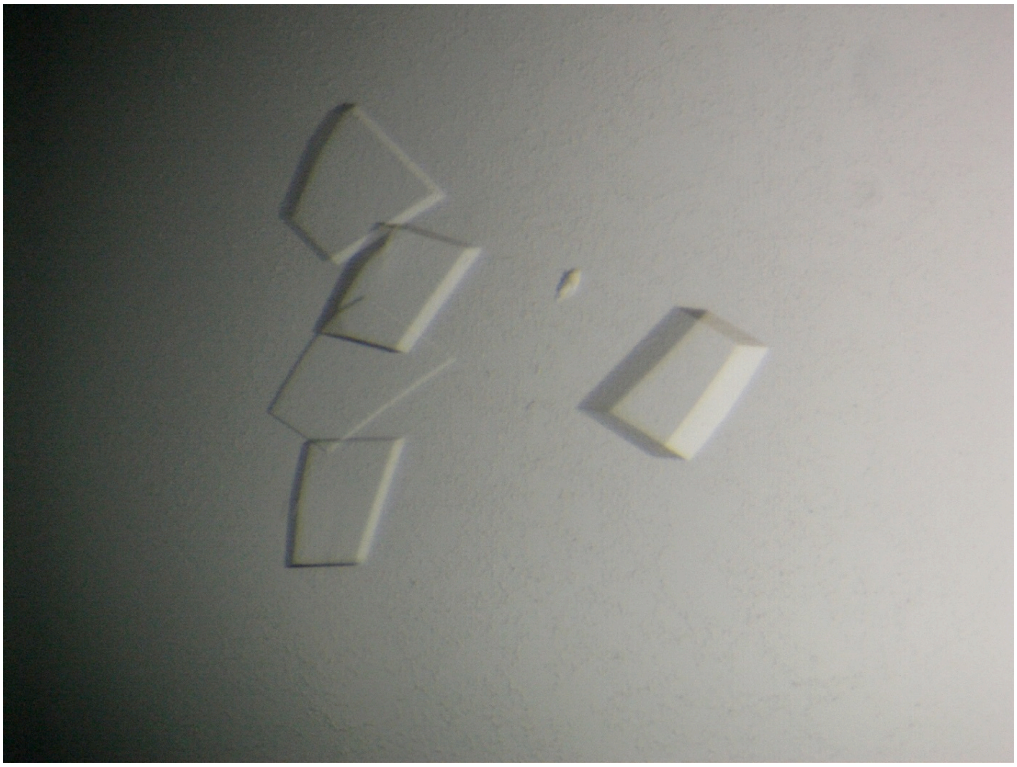

*FIGURE 29: CANDIDA ALBICANS 80S RIBOSOME CRYSTALS*

## 4. POST-CRYSTALLIZATION TREATMENTS

Post-crystallization treatments are used to improve crystal stability and diffraction. It is known that the reduction of the solvent content inside the crystal produces internal strengthening which often leads to an improvement of the diffraction limit and lifetime. This strategy, known as dehydration treatment, was used successfully for a number of proteins with drastic effects (Heras and Martin, 2005). The fact that cryo-protected 80S ribosome crystals diffract very poorly (at a resolution higher than 30 Å), even worse than the *S. cerevisiae* crystals well known in our lab, has forced us to consider the implementation of this approach. Empiric investigations reveal that different dehydration agents and variations in the treatment scheme result in different forms of the 80S crystals. The first experimentations carried out consisted in attempting to reproduce the same treatment as that established for *S. cerevisiae* crystals. Since it was directly adaptable, several different ways were investigated, each with the same pattern: a slow and step-wise increase of smaller PEG than the 20K used for the purification and crystallization process. Depending on which PEG was used, the cell parameter changed and also induced a conformational change in the degree of rotation of the 40S SU. In addition, osmium hexamine was conserved as an anomalous scatter for SAD experiments based on its property to bind RNA by mimicking fully hydrated magnesium

(Cate & Doudna, 1996). The crystals could diffract to high resolutions, and indeed spots are found on diffraction patterns up to 3.0 Å.

Optimization of this treatment allowed crystals to yield high-resolution diffractions in a reproducible way. The final scheme of treatment is described in Figure 30. The hanging-drop cover-slip was placed in a small Petri dish and the mother liqueur was first replaced by a solution with slightly higher concentration of PEG 20K (80mM BisTris-Ac pH 7.0, 70 mM KSCN, 10mM $Mg(OAc)_2$, 20% v/v Glycerol, 5% w/v PEG 20K, 6.5 mM spermidine, 7.5 mM NH4OAc, 1.4 mM Deoxy Big Chap, 2mM DTT). This solution was then replaced step-wise by solutions with increasing concentrations of PEG 6000, reaching 20% after five steps (80 mM Tris-Acetate pH 7.0, 286 mM KoAc, 70 mM KSCN, 10 mM $Mg(OAc)_2$, 18% v/v Glycerol, 5% w/v PEG 20,000, 6.5 mM spermidine, 7.5 mM $NH_4OAc$, 20% w/v PEG 6000, 2 mM DTT, without detergent). This solution was then replaced with the same solution supplemented with 2 mM osmium hexamine and the drop was kept in the Petri dish sealed with parafilm for 30 minutes to 1 hour. Investigation by diffraction of crystals taken at different stages of the treatment reveals the gradual improvement of the diffraction limit (Figure 30). Crystals were frozen directly in a stream of gaseous nitrogen at the IGBMC and stored in liquid nitrogen until they were shot on synchrotron.

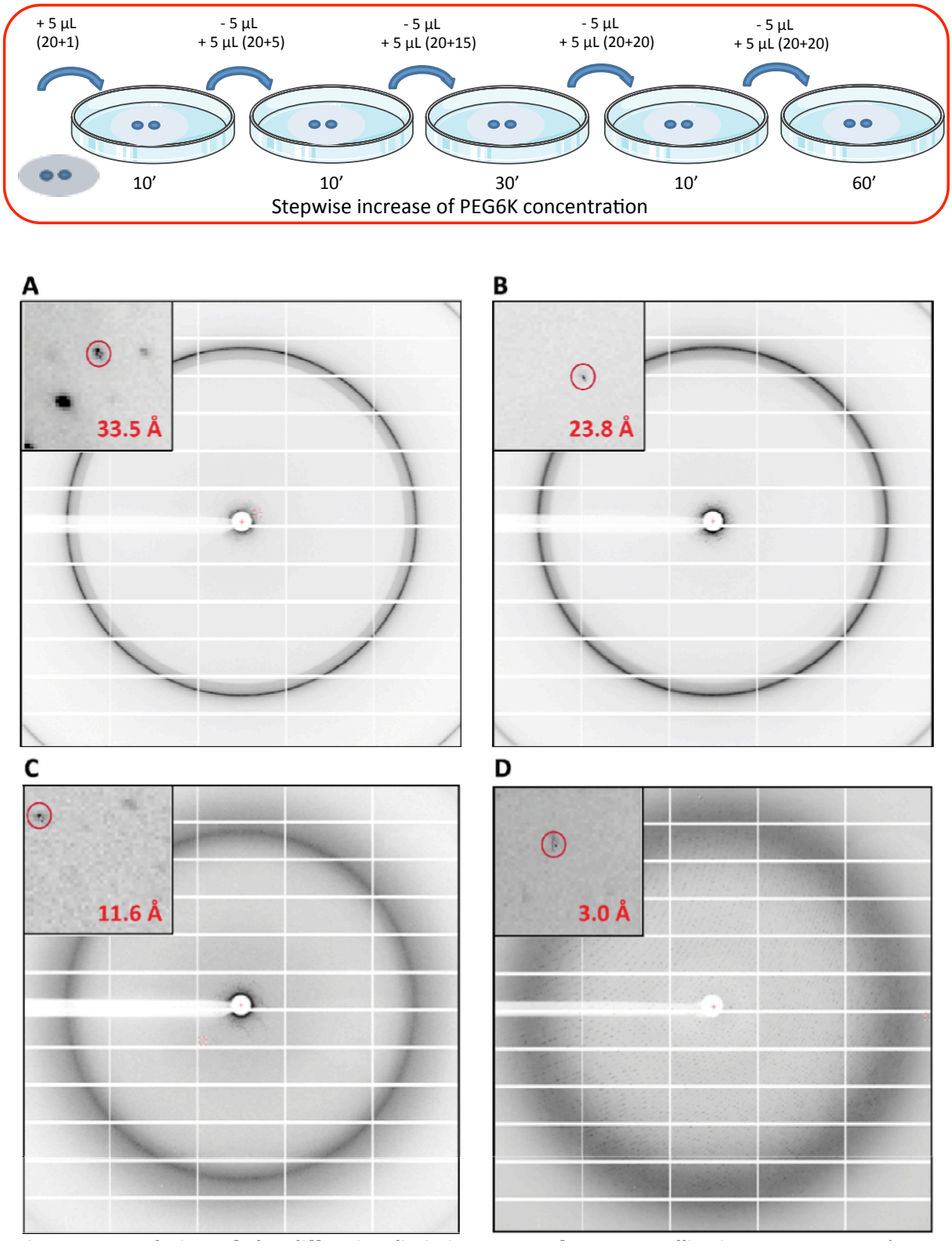


*FIGURE 30: POST-CRYSTALLIZATION TREATMENT SCHEME AND ITS IMPACT ON DIFFRACTION*

*Dehydration of the crystals by stepwise increase of PEG 6K (1% - 5% - 15% - 20%), keeping*

*20% of Glycerol as a cryoprotectant.*

## 5. X-RAY DATA COLLECTION AND INTEGRATION

X-ray data collections were performed at SOLEIL synchrotron (France) using the beamline Proxima 1 headed by Andrew Thompson, and later during this work by Léonard Chavas. Data collections were also performed at Swiss Light Source (SLS) synchrotron (Switzerland), using the beamline PX1-X06SA headed by Meitian Wang and Takashi Tomizaki. Data collection settings were optimized based on a strategy developed at SLS (Mueller *et al.*, 2011) and thanks to the previous publication of the yeast's 80S ribosome structure (Ben-Shem *et al.*, 2011), which exploits the unique features of the new generation pixel single photon counting detector PILATUS 6M (Dectris Ltd), and Eiger4M developed for synchrotron sources.

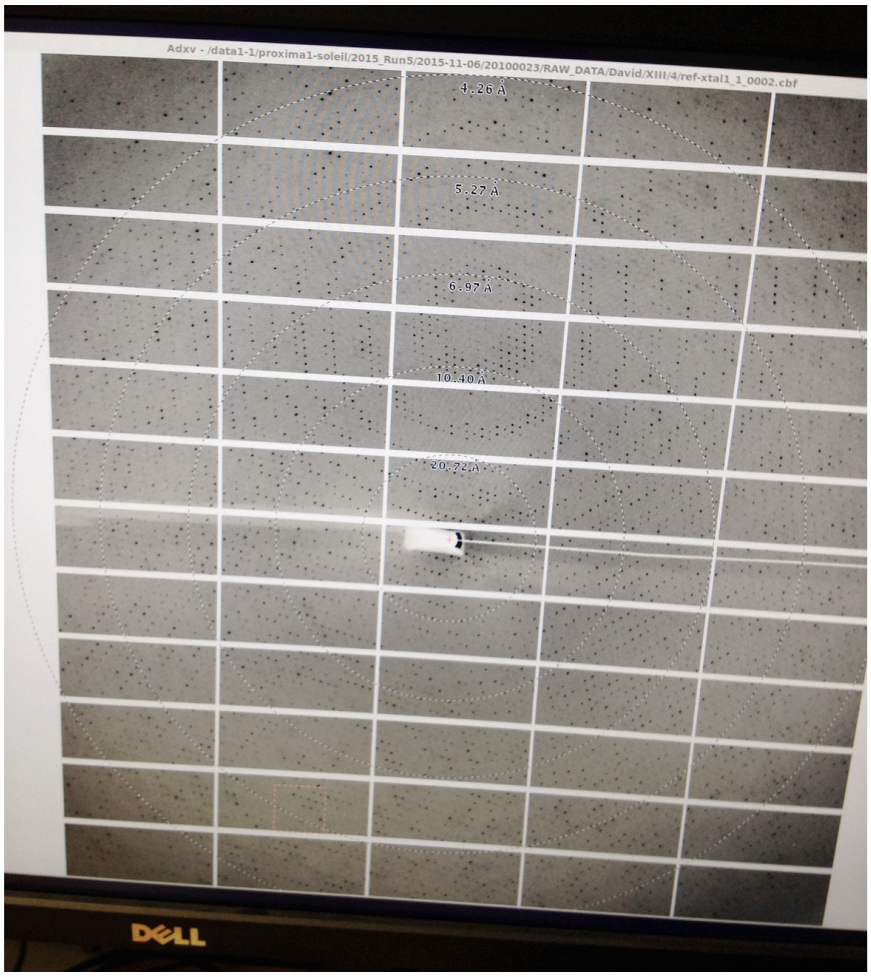


*FIGURE 31: EXAMPLE OF A DIFFRACTION PATTERN OBTAIN ON PROXIMA1 BEAMLINE AT SYNCHROTRON SOLEIL*

*C. albicans* 80S ribosome crystals are small and extremely sensitive to radiation damage, therefore an empirical data collection strategy was developed in both synchrotron sources. Highly redundant data was collected at low exposure in order to accurately measure each reflection a maximum number of times, avoiding excessive damage to the crystal. We collected at several beam size spots when the crystals were big enough: the beam size was set to 50x70 $\mu m^2$ (SOLEIL) or 20x30 $\mu m^2$ (SLS). This allowed us to expose different regions of the crystal to the beam. Last, but not least, the beam is focused on the detector and attenuated to roughly 10-25% of its original flux in order to reduce the amount of photons hitting the crystals. The oscillation range was set to 0.1° and exposure time was decreased step-by-step from 1 to 0.1 second. This allowed us to collect several datasets from many different crystals.

Diffraction data was processed and integrated by XDS software (Kabsch, 2010). Care was taken in excluding images which were contributing to an increase of the mosaicity (a sign of possible radiation damage). Scaling of intensities and merging of the different datasets were performed using XSCALE (Diederichs, 2005) and converted to structure factor amplitudes by XDSCONV. Crystallographic statistics of the final dataset are displayed in Table 5.

| Data collection and refinement statistics | |
|---|---|
| | Crystal 1 name |
| **Data collection** | |
| Space group | $P2_1$ |
| Cell dimensions | |
| *a, b, c* (Å) | 300.85, 291.72, 442.33 |
| *α, β, γ* (°) | 90.00, 100.08, 90.00 |
| Resolution (Å) | 50.00 – 3.70 (3.80 – 3.70) * |
| $R_{mess}$ (%) | 52.0 (266.5) |
| $I/\sigma I$ | 3.84 (0.74) |
| $CC_{1/2}$ (%) | 69.9 (28.7) |
| Completeness (%) | 99.3 (99.0) |
| Redundancy | 9.46 (7.7.48) |
| | |
| **Refinement** | |
| Resolution (Å) | 49.98 – 3.70 |
| No. reflections | 1441978 |
| $R_{work}/R_{free}$ | 0.2710 / 0.3167 |
| No. atoms | |
| Protein | 179119 |
| RNA | 219740 |
| Ions | N/A |
| B-factors | |
| Protein | 155.26 |
| RNA | 144.13 |
| Ions | N/A |
| R.m.s deviations | |
| Bond lengths (Å) | 0.007 |
| Bond angles (°) | 0.82 |
| Number of crystals used: 23 | |
| *Highest resolution shell is shown in parenthesis. | |

*TABLE 5: HIGH-RESOLUTION CANDIDA ALBICANS 80S RIBOSOME DATA COLLECTION, PHASING AND REFINEMENT STATISTICS*

## 6. STRUCTURE DETERMINATION

The 3.0 Å resolution *S. cerevisiae* 80S ribosome (PDB code: 4V88, Ben-Shem *et al.*, 2011) was used as a starting model in order to build the 80S *C. albicans* ribosome structure at a medium-high resolution. Gradual improvement of diffraction quality was observed since this project began and, starting from a first complete data set at 18 Å three years ago, we have today a preliminary structure of the complete ribosome at a 3.70 Å resolution. Indeed, the overall similarity between the ribosomes of these two fungi is higher than 90%. *In silico* modelled ribosomal proteins rRNA were used for creating the first *in silico* model of *C. albicans*' 80S ribosome (chapter IV. 2. 3.). An electron density map (2Fo-Fc) was used as a first validation of the quality of the fold prediction. Several of them had to be remodeled by an advanced tertiary structure prediction program of Phyre2 software in order to fit better in the *C. albicans* electron density map. Unfortunately, the r-protein eS21 has a modelization fully incoherent with its density map, so we replaced the amino acid sequence of the *S. cerevisiae* eS21 r-protein with that of *C. albicans*. By keeping the tertiary structure, it did finally fit in the density map of *C. albicans*. This initial model was improved by several rounds of rigid body refinement in Phenix (Adams *et al.*, 2010). The improved electron density maps guided manual model building in COOT (Emsley and Cowtan, 2004) and showed clear density for most rRNA bases and protein side chains. The table of crystallographic statistics is reported in Table 5.

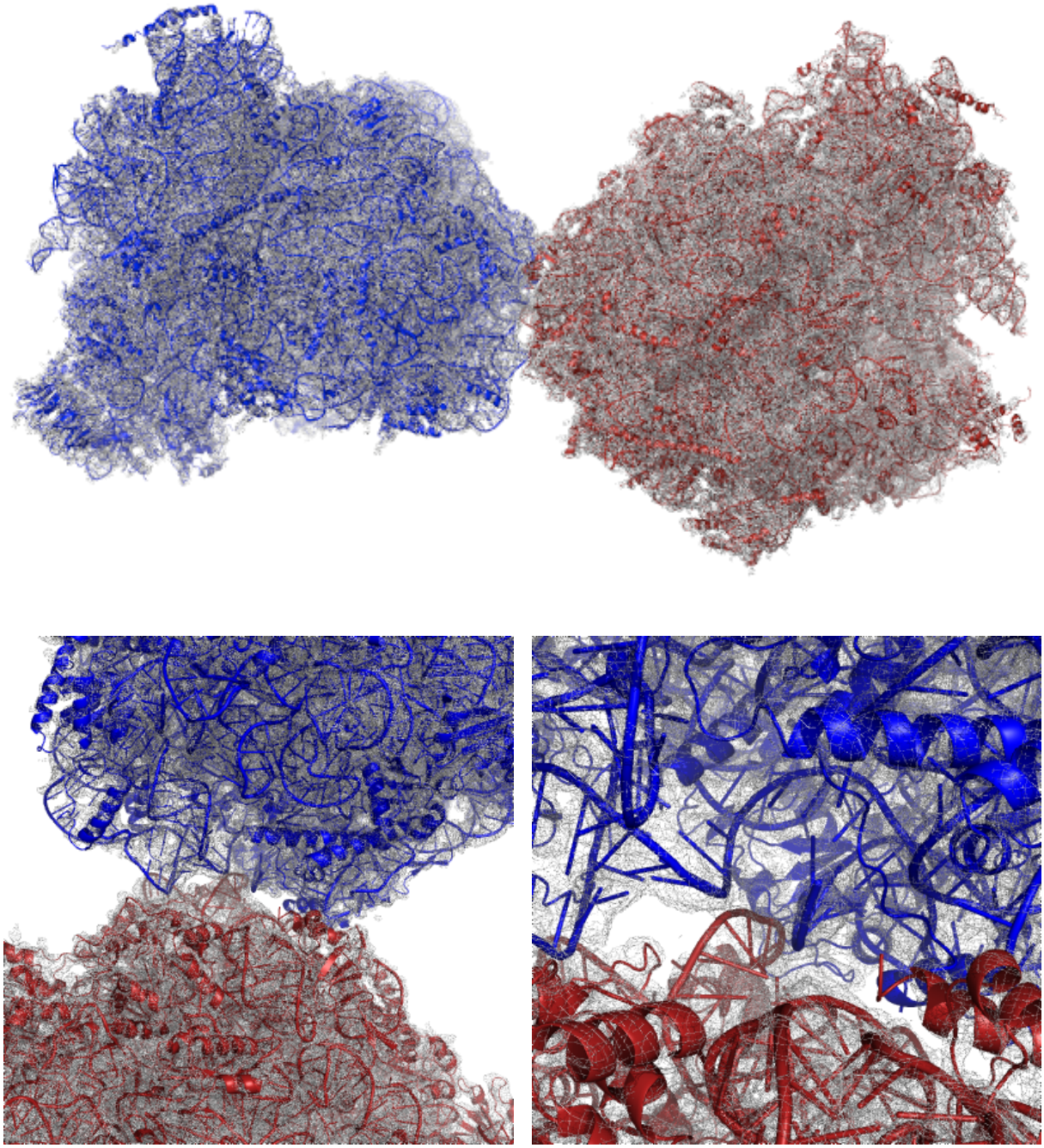

*FIGURE 32: DISPOSITION OF THE TWO CANDIDA ALBICANS 80S RIBOSOMES AND DETAILS OF THEIR INTERACTION IN THE ASYMMETRIC UNIT*

# 3. RESULTS

## 1. FROM YEAST TO RIBOSOME CRYSTAL DIFFRACTIONS

A complete and reproducible purification protocol has been established, from biomass production in IPPTS, to ribosome pure samples in IGBMC. From approximately 5 grams of fresh and just starved *C. albicans* cells, 8 to 11 mg of 80S ribosome are produced, which allowed us to work and realize around 1000 crystallization drops in our established hanging drop crystallization system. After weeks, those drops permitted us to fish around 300 suitable crystals for the dehydration and freezing step. A few of them are lost during this step, depending on the fishing and the temperature conditions. This amount of crystals is shot on beamline; 2 shifts of 8 hours are enough in SLS, but 3 would be necessary in SOLEIL, depending on the general software interface. When the established protocol is followed strictly, 60% of those treated and frozen crystals will diffract on synchrotron to an interesting high resolution below 4 Å.

## 2. X-RAY STRUCTURE OF *C. ALBICANS* 80S RIBOSOME AT 3.70 Å

The preliminary *C. albicans* 80S ribosome structure solved at 3.70 Å, whose statistics are described in table 5, show an X-ray structure which is very close to that of the *S. cerevisiae* 80S ribosome (Figure 33), with which it shares more than 90% similarity overall (Figure 34).

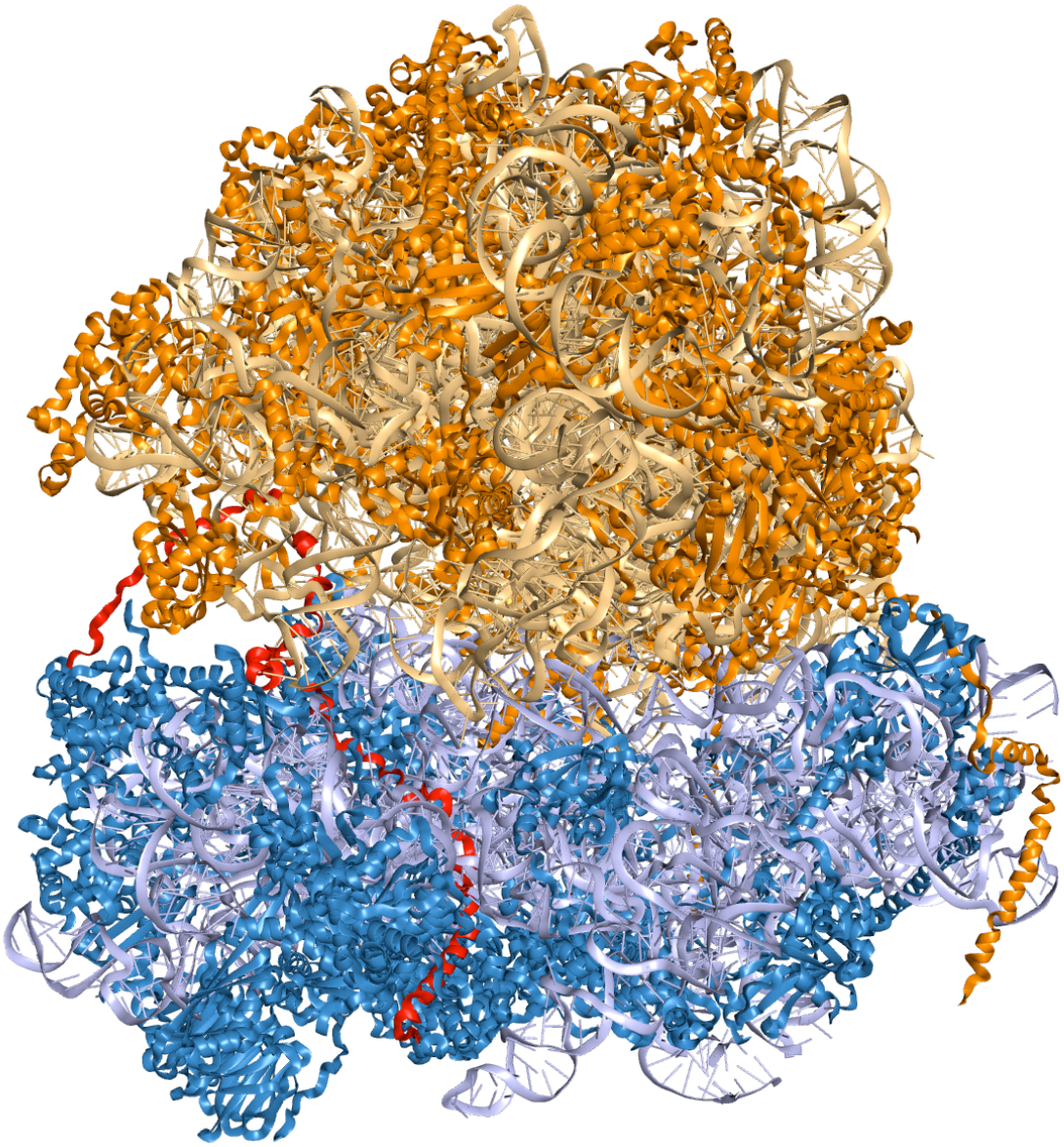

*FIGURE 33: CANDIDA ALBICANS 80S RIBOSOME X-RAY PRELIMINARY STRUCTURE AT 3.70 Å*

*The LSU is colored in orange with r-proteins in dark orange and rRNA in ochre. The SSU is colored in blue with r-proteins in light blue and rRNA in light blue. The stress protein C4YQN5 is colored in red.*

The ribosome structure is considered as a vacant 80S ribosome although the ribosome is not completely empty; indeed, a non-ribosomal protein is found in the structure. C4YQN5, an uncharacterized homologous protein of Stm1p in *S. cerevisiae*, is a stress response protein known to bind the ribosome in the mRNA tunnel. By occupancy of this space, translation is blocked.

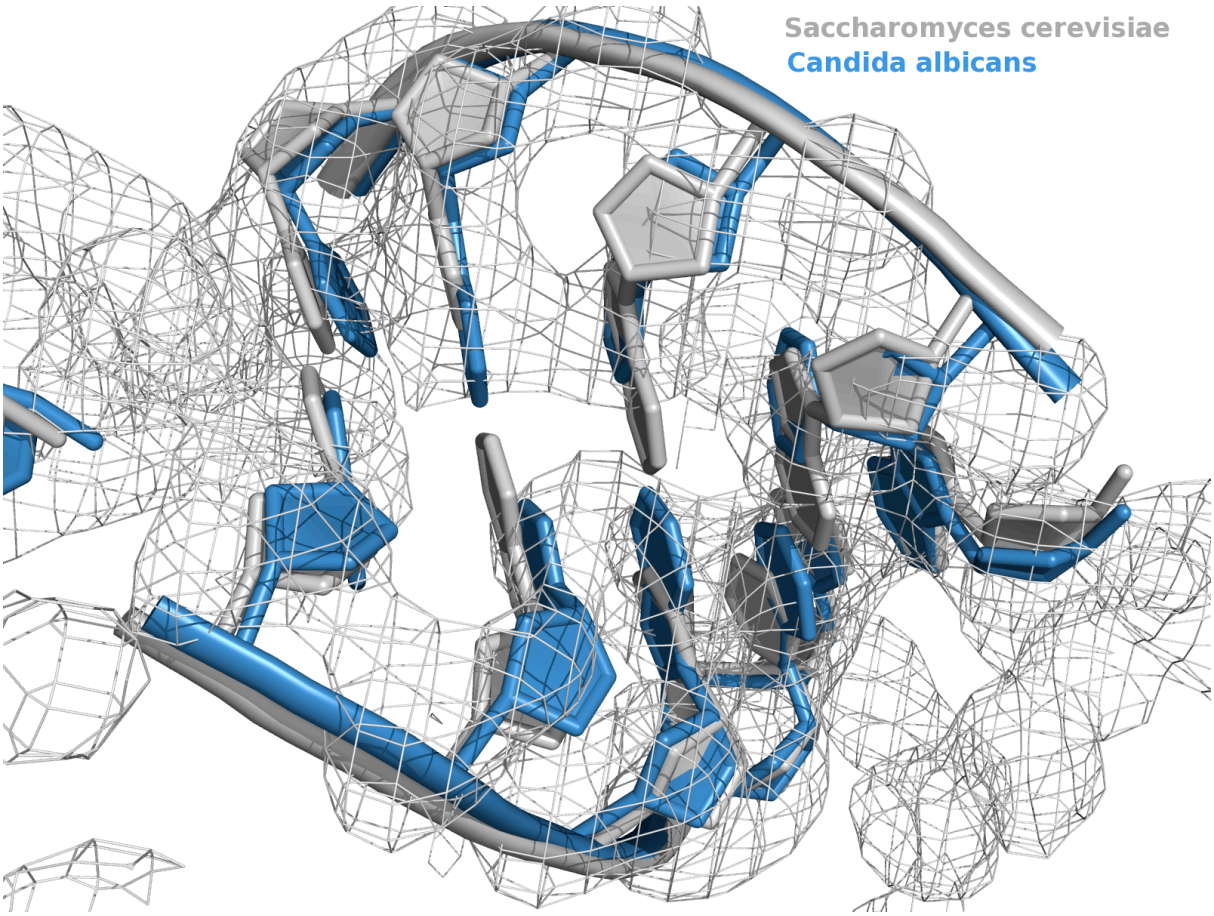


*FIGURE 34: COMPARISON OF THE 5.8S RRNA OF CANDIDA ALBICANS AND SACCHAROMYCES CEREVISIAE*

*Details of 5.8S rRNA strand conformation in both yeasts; S. cerevisiae is colored in grey and C. albicans in blue.*

Structural analyses and comparisons of the 5.8S between *C. albicans* and *S. cerevisiae* have shown that even if the rRNA sequence differs slightly, it folds in a very similar way. Even if the electron density is only at a medium-high resolution, we can clearly track the sequence changes.

## 3. DETAILS OF THE *CANDIDA ALBICANS* DECODING CENTER

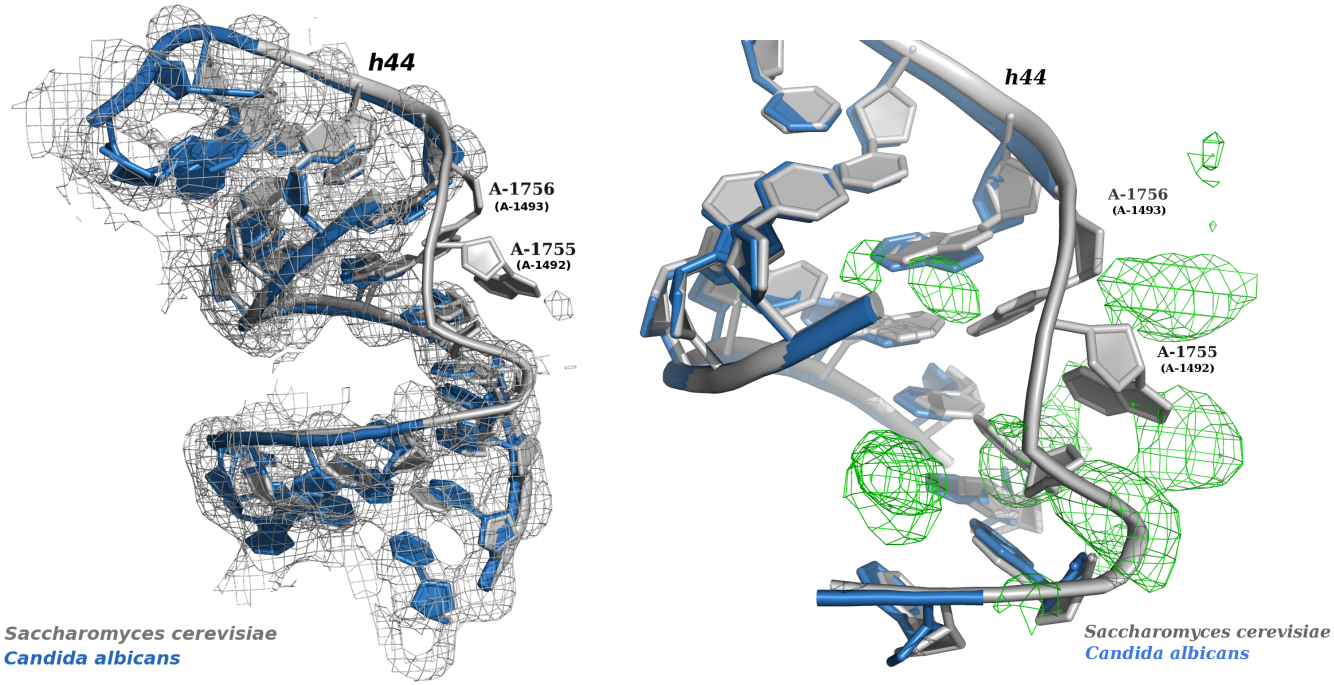


*FIGURE 35: COMPARISON OF THE DECODING CENTERS OF CANDIDA ALBICANS AND SACCHAROMYCES CEREVISIAE*

*Details of the decoding center located on the 25S rRNA strand conformation in both yeasts; S. cerevisiae is colored in grey and C. albicans in blue.*

Even with a medium-high resolution, remarkable differences have been seen at the decoding center, where codon from mRNA and anticodon from tRNA interaction takes place. A difference in density (Fo-Fc) points out that the conformation of the highly conformationally conserved decoding center may be different compared to what is seen in the vacant 80S ribosome of *S. cerevisiae* (Figure 35).

# 4. DISCUSSION

An established and reproducible purification protocol produced in both the IPPTS and the IGBMC allows us today to obtain a satisfactory quantity of *C. albicans* 80s ribosomes. Crystallization conditions were determined in order to obtain, via a sitting-drop system, drops containing crystals of a high-enough quality and size that allows for post-crystallization and freezing treatments. Thanks to an X-ray data collection method in a synchrotron adapted to the extremely fragile crystals of the *C. albicans* ribosome, we have today a preliminary structure of the *C. albicans* 80s ribosome with a resolution of 3.70 Å.

We were able to establish this protocol thanks to others already mastered at the laboratory, concerning the purification of ribosomes of other organisms, such as *Thermus thermophilus* (Yusupova *et al.*, 1991) and most of all *S. cerevisiae* (Ben-Shem *et al.*, 2011). The fundamental knowledge of the biology of the pathogen and its culture conditions also allowed us to produce a quantity of biomass that was as homogenous as possible, the blastospores. Bioinformatics allowed us not only to have access to all of the existing r-protein and rRNA sequences, but also to have important information about the volume and the size of the *C. albicans* ribosome. This information proved crucial in the creation of the crystallization protocol, as well as an in the post-crystallization treatments of crystals, since the dehydration stage differs slightly between *C. albicans* and *S. cerevisiae* due to the volume of solvent contained in the ribosome of the former which is larger than the volume contained in the ribosome of the latter. Finally, all of the interesting sites in the predictive bioinformatics study require a confirmation of their study via a crystallographic resolution.

The resolution of the structure using this approach is still underway in order to obtain a higher resolution, but it so far has produced results that are sufficiently precise in order to attest that there is a high level of structural similarity between the ribosomes of *S. cerevisiae* and *C. albicans*. Indeed, even if the sequence differs slightly, the general structure is conserved (Figure 33). The crystallized ribosome is vacant and does not contain the general factors of translation. It is, however, stabilized by a non-ribosomal protein, a homologue of stm1 (Ben-Shem *et al.*, 2011), that occupies the RNA tunnel in order to inhibit translation during the stress induced by glucose starvation that we induce during our purification. This attests, once again, to the already existing similarity between *S. cerevisiae* and *C. albicans*.

Even if preliminary data does not allow us to observe the fine differences between *C. albicans* and *S. cerevisiae*, certain differences are already evident. This is the case of the decoding center, since the conformational conservation described in eukaryotic organisms with resolved structures (Khatter *et al*., 2015; Hashem *et al,*. 2013; Wong *et al.*, 2014) corresponds in a similar manner, both structurally and sequentially, with that of *S. cerevisiae*. The structural information that we have obtained up until now show a highly important difference in the spatial organization of the decoding center. Indeed, the nitrogen bases implied in the formation of this reactionary site do not have the same orientation (Figure 35), and they differ as well in terms of their composition (Table 3). Even though we do not currently have answers about the translation mechanism of *C. albicans*, many questions have been effectively presented. If such a site is present, it is possible that it is implied in the mechanism that allows *C. albicans* to have a genetic code different from the universal genetic code. It is effectively proven that *C. albicans* and some other *Candida* species can tolerate CUG codon misreading and thus code a serine instead of a leucine. This is observed especially in proteins expressed at low levels at the cell surface, which potentially influence the interaction of the organism with the host (Wong *et al.*, 2014). The understanding of how the translation mechanism takes place in *C. albicans* is therefore of pivotal importance. Moreover, the DC is the target of geneticin G418, and with such a difference in spatial conformation it would be interesting to determine if the nucleotides engaged in the DC formation would be able to flip out as DC nucleotides from *S. cerevisiae*, in order to bind the GEN.

## 5. CONCLUSION AND PERSPECTIVES

In order to verify, specify, and correlate the assumptions made by the bioinformatics study, the X-ray structure of the *C. albicans* 80S ribosome is currently being solved. This will demonstrate our bioinformatic predictions and thus either validate or not the method and the model created *in silico* and will serve for further ribosome bioinformatic structure determination through *in silico* approach. Moreover, it needs to be highlighted that bioinformatics research permits us to have useful supplementary information such as all of the rRNA and r-protein sequences and crucial biophysics parameters in order to set all the experimental protocols, from ribosome purification to crystals diffraction and structure resolution.

As the experimental protocol is actually carried out between two laboratories, we obtained the agreements from hygiene and security facilities so as to have a dedicated P2 lab at the IGBMC, in order to carry out the complete purification at the same lab. This means that the filtration on the 0.45-micron membrane will not be required anymore. Furthermore, all of the steps, such as biomass production, would need to be checked in order to ensure that the ribosome purified entirely at the IGBMC will be of the same quality as the previously purified samples.

Diffraction spots are visible until 3.0-3.2 Å of maximum resolution and we therefore believe that we can improve the overall resolution of the full dataset, in order to gain new detailed insights into the 80S ribosome structure. This will lead us to obtain a more reliable model and to better interpret differences. Similarly, rRNA segments not described nor represented in the *S. cerevisiae* structure due to their instability have been described and represented in *C. albicans*. The improvement of the resolution will allows us to define the structure of not yet represented segments in other ribosomal structures. Slight structural differences highlighted by bioinformatics predictions, such as E-site mutations or mRNA tunnel spatial organization in *C. albicans*, are therefore currently not visible in our preliminary X-ray model. Despite these predicted differences, the evident difference in the DC spatial organization and composition is already visible, and this preliminary X-ray data confirms earlier bioinformatic data. It thus seems extremely interesting to confirm the behavior of this site by identifying the DC inhibitor: geneticin (Garreau de Loubresse *et al*., 2014).

This model will then pave the way for further structural studies of functional complexes involved in the initiation, elongation, and termination phases of the translation, in order to unravel the protein biosynthesis mechanism, and for the future screening and design of new drugs specifically targeting the *C. albicans* ribosome. Indeed, in our laboratory we recently solved the structure of the 80S ribosome of *S. cerevisiae* (Ben-Shem *et al*., 2011) and later a spectrum of 16 different inhibitors bound to it have shed light on the action mechanism active in shutting off protein biosynthesis in these compounds. Furthermore, it has already been shown *in vivo* that not all known inhibitors binding to the 80S ribosome in *S. cerevisiae* (Garreau de Loubresse *et al*., 2014) are effective against *C. albicans*, thus proving that there might be indeed differences between them.

As a polymorphic fungus, *C. albicans* can grow in different forms (described in chapter I). During the purification process we selected all the conditions necessary in order to

obtain a homogenic population of blastospores so as to subsequently obtain a pure ribosome population. In order to do this, only white phase colonies were selected for biomass production. It seems to be extremely interesting to look at what the differences between blastospore ribosomes and hyphae, pseudohyphae, hyperpolarized bud, and mating projection ribosomes would be. Indeed, it already has been reported that some pathogenic organisms have a different ribosome depending on their host or the morphology that they adopt (Wong *et al*., 2014). The same question is addressed at all those microscopic morphologies but in opaque phase. Since opaque-phase cells are more implicated in cutaneous infection than white-phase cells, which are much more aggressive in other kinds of infections such as systemic ones (Kvaal *et al.*, 1999), treatments are different, depending on the localization of the infection. Excluding toxicological aspects, those empiric treatments who work only on topic or deep infections could be related to the type of phase where *C. albicans* is. Related to all of those different possible morphologies, it is also clear that *C. albicans* biofilms are a major cause of nosocomial infections (Kojic & Darouiche, 2004; Douglas, 2003; Lewis, 2007). Since they are described as much more resistant than planktonic cells, but without real reliable information to back this claim up, investigations of ribosome diversity and modification in *C. albicans* biofilms would a good study in order to better understand why these structures are more resistant to antifungal treatments. Even though X-ray crystallography needs crystals in order to produce diffraction patterns and thus solve possible structures, cryo-EM does not need crystals. This technique has allowed scientists to study different ribosome populations from one sample, so this could also be a possible way to study *C. albicans* biofilm ribosomes in order to identify modifications possibly related to *C. albicans*' higher resistance.

# VI. INHIBITION OF THE *CANDIDA ALBICANS* RIBOSOME *IN VITRO*

## 1. AIM OF THE PROJECT

The bioinformatic approach has already highlighted interesting specificities on the *C. albicans* ribosome: the E-site and the decoding center being the most relevant. X-ray structure determination is currently underway in order to confirm this, but our preliminary results already correlate to bioinformatic model and show that the *C. albicans* DC seems different from that of *S. cerevisiae*.

In order to verify these assumptions, *in vivo* inhibitor activity studies are currently being developed. These inhibitors are already positioned on the *S. cerevisiae* ribosome and are effective against this yeast (Garreau de Loubresse *et al*., 2014). They will demonstrate the effect of inhibiting (or not) *C. albicans* active and reactional sites, and thus either provide validation for or disprove our interest, which we need to have *vis-à-vis* these hot spots. This information will be helpful for our interpretations and for our further research.

## 2. MATERIAL & METHODS

All of the following steps, from experiments to results interpretation are performed at the IPPTS and at the Plateau Technique de Microbiologie, 3 Rue Koeberlé, 67000 Strasbourg, in collaboration with Dr. Marcela Sabou. *In vitro* susceptibilities were determined by following the guidelines of the EUCAST definitive document EDef 7.1., found at http://www.eucast.org/ast_of_fungi/.

### 1. ANTIFUNGALS

Pure powders of fluconazole, anisomycin, blasticin S, cycloheximide, geneticin G418, lactimidomycin, and pactamycin were used. For the rest of the substances tested, aliquots of

different concentrations were available from our collaborators and different valorization programs (Table 6).

| Inhibitors | Binding site | Stock | Solvent | Providers | Tested concentrations |
|---|---|---|---|---|---|
| Fluconazole | Enzyme CYP51 | Powder | DMSO | Sigma Aldrich | 64 – 0.125 µg/mL |
| Nagilactone C | Site A | 5.75 mg/mL | DMSO | DTP, NIH | 50 – 0.1 µg/mL |
| Narciclasine | | 33.3 mg/mL | DMSO | Santa Cruz Biotech | 32 – 0.06 µg/mL |
| T-2 toxin | | 0.5 mg/mL | DMSO | DTP, NIH | 5 – 0.01 µg/mL |
| Iso-T-2 toxin | | 0.5 mg/mL | DMSO | DTP, NIH | 5 – 0.01 µg/mL |
| Verrucarin A | | 50 mg/mL | DMSO | Sigma Aldrich | 32 – 0.06 µg/mL |
| Anisomycin | | Powder | DMSO | Sigma Aldrich | 128 – 0.25 µg/mL |
| Deoxinivalenol | | 35.7 mg/mL | DMSO | Sigma Aldrich | 32 – 0.06 µg/mL |
| Homoharringtonine | | 109.9 mg/mL | DMSO | Santa Cruz Biotech | 64 – 0.125 µg/mL |
| Lycorine | | 50 mg/mL | DMSO | Santa Cruz Biotech | 64 – 0.125 µg/mL |
| Blasticidin S | Site P | Powder | Water | Sigma Aldrich | 128 – 0.25 µg/mL |
| Cycloheximide | Site E | Powder | Water | Calbiochem | 32 – 0.06 µg/mL |
| Lactimidomycin | | Powder | DMSO | Calbiochem | 16 – 0.03 µg/mL |
| Phyllantoside | | 46 mg/mL | DMSO | DTP, NIH | 64 – 0.125 µg/mL |
| Geneticin G418 | Decoding center | Powder | Water | Sigma Aldrich | 128 – 0.25 µg/mL |
| Cryptopleurine | mRNA tunnel | 1 mg/mL | DMSO | DTP, NIH | 10 – 0.02 µg/mL |
| Pactamycin | | Powder | DMSO | Sigma Aldrich | 32 – 0.06 µg/mL |

*TABLE 6: ORIGIN, CONCENTRATIONS, AND TARGET OF INHIBITORS TESTED*

The concentrations tested for fluconazole were 64 to 0.125 µg/ml as a template control from EUCAST. For the other substances, concentration choice depended on the available quantity and/or the initial concentration.

## 2. LABWARE

Regular 96-well, flat-bottom, polystyrene plates with low evaporation lids (Falcon®) were used. Once antifungal solutions were prepared, the plates were stored frozen at -80°C.

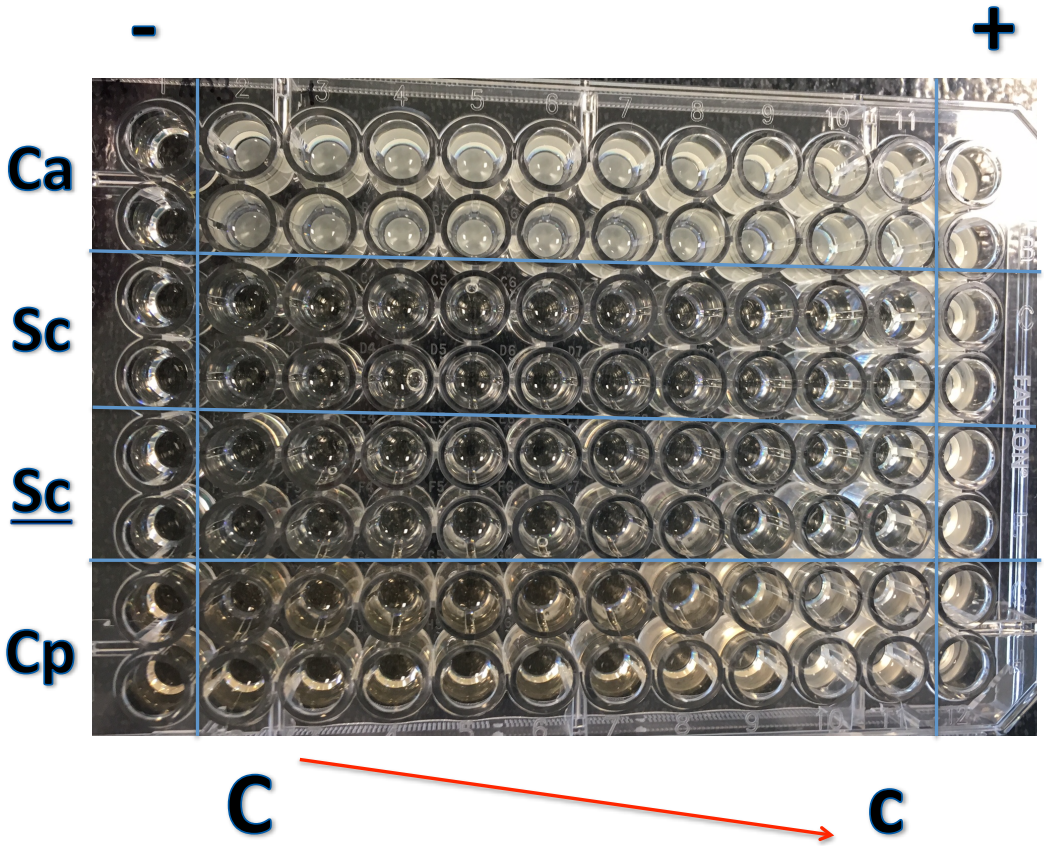


*FIGURE 36: GENERAL SCHEME OF THE TESTS IN 96-WELL PLATES*

*Lignes A-B: C. albicans SC5314 with cycloheximide in AM3*

*Lignes C-D: S. cerevisiae JD1370 with cycloheximide in AM3*

*Lignes E-F : S. cerevisiae HUS with cycloheximide in AM3*

*Lignes G-H : control = C parapsilosis ATCC 22019 with fluconazole in RPMI*

*Each test is at least duplicate. From C to c, inhibitors concentration is reducted by 2 from a well to the other. - & + are respectively proof of non-growing and growing of those strains.*

## 3. ISOLATES

The fungal strains used were a mixture of research-used and patient-isolated ones: *Candida albicans* SC5314 (details on Chap I.), used for bioinformatics and X-ray crystallography studies; *Candida albicans* ATCC 90028; *Candida glabrata* CBS 138; *Candida glabrata* HUS; *Saccharomyces cerevisiae* JD1370, engineered and provided by Jonathan Dinman (University of Maryland, USA), used for X-ray structural studies performed by Marat Yusupov's team and especially the work concerning translation inhibitors of Nicolas Garreau de Loubresse (Garreau de Loubresse et al., 2014); *S. cerevisiae* HUS; and *Aspergillus fumigatus* HUS. The HUS strains are patient isolated strains from the Strasbourg University Hospital collection and are representative of the local epidemiology of the 3 genera. Two reference strains, *Candida krusei* ATCC 6258 and *C. parapsilosis* ATCC 22019, were included in each plate. The final inoculum size was 1-5 x $10^5$ CFU/ml.

## 4. CULTURE MEDIA

An RPMI-1640 medium supplemented with 2% glucose was initially used for all strains. *S. cerevisiae* JD1370 failed to grow in RPMI-1640 medium, so AM3 media supplemented with 2% glucose was then also tested for the yeast strains. (http://www.eucast.org)

## 5. INCUBATION

Once inoculated, the plates were incubated at 35°C for 24 hours. Since *S. cerevisiae* JD1370 failed to grow in 24 hours, supplementary 24 hours incubation was tested for this strain, but no growth was observed. After that, an incubation for 24 hours at 27°C was also tested for this strain. To overcome this problem, we also tried a 2 and a 4 times bigger inoculate.

## 5. MINIMUM INHIBITORY CONCENTRATION ASSESSMENT

Results were reported at 24 hours post inoculation. MICs were determined visually and using a spectrophotometer after 24 hours of incubation at 35°C or 27°C for *S. cerevisiae* JD1370. The MIC was defined as a 50% or more reduction in growth compared to the drug-free well. The MICs for 50% and 90% (80%) growth inhibition of the isolates tested are reported.

MIC breakpoints:

http://www.eucast.org/fileadmin/src/media/PDFs/EUCAST_files/AFST/Clinical_breakpoints/Antifungal_breakpoints_v_8.0_November_2015.pdf

Quality control, MICs *Candida krusei* ATCC 6258 and *C. parapsilosis* ATCC 22019:

http://www.eucast.org/fileadmin/src/media/PDFs/EUCAST_files/AFST/QC/QC_AFST_v_1.0_2015.pdf

Since *S. cerevisiae* JD1370 failed to grow in each condition that we tried with the RPMI medium, we switched to the AM3 medium with incubations at both 27°C and 35°C. In this medium, it finally grew, with no significant differences between the temperatures tested, though 35°C very slightly favored the growth. These results currently need to be checked. Experiments are still ongoing so only the first results of CHX and GEN are available (Table 7). Inhibition results can differ depending on the medium used for those tests as it has already been reported (Bartizal & Odds, 2003).

| **Inhibitors** **RPMI / AM3** | *C. albicans* SC5314 | *C. albicans* ATCC 90028 | *C. glabrata* CBS 138 | *C. glabrata* HUS | *C. krusei* ATCC 6258 | *C. parapsi* ATCC 22019 | *S. cerevisiae* JD1370 | *S. cerevisiae* HUS |
|---|---|---|---|---|---|---|---|---|
| **Fluconazole** **RPMI** - 35°C (64-0,125 µg/ml) | : 0.25 µg/ml $_{90}$ : 125 µg/ml $_{50}$ : 0.5-2 µg/ml | : 0.25 µg/ml $_{90}$ : 125 µg/ml $_{50}$ : 1 µg/ml | >64 µg/ml $_{80}$ : 64 µg/ml $_{50}$ : 8 µg/ml | : 64 µg/ml $_{80}$ : 64 µg/ml $_{50}$ : 8 µg/ml | : 64 µg/ml $_{90}$ : 64 µg/ml $_{50}$ : 32 µg/ml | : 2 µg/ml $_{90}$ : 4 µg/ml $_{50}$ : 1 µg/ml | No growth | Light growth |
| **Fluconazole** **RPMI** - 27°C (64-0,125 µg/ml) | - | - | - | - | - | : 2 µg/ml $_{90}$ : 2 µg/ml $_{50}$ : 1 µg/ml | No growth | Light growth |
| **Fluconazole** **AM3** - 35°C (64-0,125 µg/ml) | >64 µg/ml Inhomogenous growth | >64 µg/ml Inhomogenous growth | : 64 µg/ml $_{80}$ : 64 µg/ml $_{50}$ : 32 µg/ml | : 32 µg/ml $_{80}$ : 16 µg/ml $_{50}$ : 16 µg/ml | : 32 µg/ml $_{90}$ : 32 µg/ml $_{50}$ : 32 µg/ml | : 2 µg/ml $_{90}$ : 4 µg/ml $_{50}$ : 1 µg/ml | : 8 µg/ml $_{80}$ : 8 µg/ml $_{50}$ : 16 µg/ml | : 8 µg/ml $_{80}$ : 8 µg/ml $_{50}$ : 16 µg/ml |
| **Fluconazole** **AM3** - 27°C (64-0,125 µg/ml) | - | - | - | - | - | : 2 µg/ml $_{90}$ : 2 µg/ml $_{50}$ : 1 µg/ml | : 8 µg/ml $_{90/50}$ : 8 µg/ml | : 16 µg/ml $_{90/50}$ : 16 µg/ml |
| | | | | | | | | |
| **Cycloheximide** **AM3** - 35°C (32-0,06 µg/ml) | >32 µg/ml | - | - | - | - | - | <0.006 µg/ml | <0.006 µg/ml |
| **Généticine G418** **AM3** - 35°C (128-0,25 µg/ml) | >128 µg/ml | - | - | - | - | - | : 16 µg/ml $_{90}$ : 16 µg/ml $_{50}$ : 8 µg/ml | : 16 µg/ml $_{90}$ : 16 µg/ml $_{50}$ : 8 µg/ml |
| **Cycloheximide** **AM3** - 27°C **(32-0,06 µg/ml)** | >32 µg/ml | - | - | - | - | - | <0.006 µg/ml | <0.006 µg/ml |
| **Généticine G418** **AM3** - 27°C **(128-0,25 µg/ml)** | >128 µg/ml | - | - | - | - | - | : 32 µg/ml $_{90}$ : 32 µg/ml $_{50}$ : 16 µg/ml | : 16 µg/ml $_{90}$ : 8-16 µg/ml $_{50}$ : 8-16 µg/ml |

*TABLE 7: PRELIMINARY RESULTS MINIMUM INHIBITORY CONCENTRATION ASSESSMENT*

Fluconazole results are those expected and correlated to the EUCAST protocol for our control strains, *C. krusei* ATCC6258 and *C. parapsilosis* ATCC22019. From this information, we can validate and interpret our results.

Currently ongoing tests require a comparative strain of filamentous fungi in order to be able to interpret the results concerning *A. fumigatus*. Moreover, all of our results obtained in an RPMI medium need to be carried out in an AM3 medium in order to have results from *S. cerevisiae* JD1370, our model strain for inhibitor binding.

Since *S. cerevisiae* allows us to establish a link with the structural biology information concerning the ribosome, it is necessary to utilize it in the development of our tests. The molecule activity tests will be carried out in AM3 media at 35°C. Growth in the AM3 medium, which is impossible in the synthetic medium RPMI, is most certainly linked to the presence of growth factors in the yeast and the beef extract. Until now, only the results concerning the activities of CHX and GEN on *C. albicans* SC5314, *S. cerevisiae* JD1370, and *S. cerevisiae* HUS are interpretable.

According to the available crystallographic results, CHX and GEN are, respectively, inhibitors of the E-site and of the decoding center of *S. cerevisiae* (Garreau de Loubresse *et al*., 2014). According to our bioinformatic model, the E-site of the *C. albicans* ribosome (Chapter IV) differs only by one amino acid (P56Q) to that of *S. cerevisiae*. This modification reduces the available space and is thus necessary to the fixation of CHX. We can observe that the two strains of *S. cerevisiae* are extremely sensitive to CHX (complete inhibition at <0.006 µg/mL), which confirms the existing structural information available (Garreau de Loubresse *et al*., 2014). However, as we observe the results for this same inhibitor in the case of *C. albicans* SC5314 we find that they reveal a resistance to CHX (>32 µg/mL). These results corroborate our hypothesis about the resistance of *C. albicans* to CHX of the P56Q mutation.

According to our bioinformatic model and our X-ray structure, the decoding center of the *C. albicans* ribosome (Chapters IV and V) differs its spatial organization in relation to *S. cerevisiae*. This modification affects the available space and led us to the hypothesis that the *C. albicans* nucleotides are perhaps not able to perform the flipping-out observed in *S. cerevisiae* and thus allow for the binding of GEN. We observe that the two *S. cerevisiae* strains are slightly sensitive to GEN (MIC50 8 µg/mL) which thus confirms the existing

structural information (Garreau de Loubresse *et al*., 2014). However, as we observe the results for this same inhibitor in the case of *C. albicans* SC5314, we find that they reveal a resistance to GEN (>128 µg/mL). These results confirm our hypothesis about the possible resistance of *C. albicans* to GEN due to the particular spatial organization of its decoding center.

The subsequent results concerning this study are considered interesting, they will be submitted for publication.

# VII. SCIENTIFIC CONTRIBUTIONS AND GENERAL PERSPECTIVES

Thanks to bioinformatic modeling, many important sites in the ribosome have been described. This sheds light on the fundamental differences between *C. albicans* and *S. cerevisiae*, but also on certain conformational or compositional differences in the ribosomes of these pathogenic yeasts. The modeling also allows for the formulation of hypotheses about the functionality of the ribosome, as well as its possible resistances to already-known inhibitors of eukaryotic ribosomes. The decoding center and the E-site of *C. albicans* especially present particularly interesting differences concerning these aspects.

The structural determination via X-ray approach initially allowed us to establish a complete purification and crystallization protocol for the ribosome of *C. albicans*. This project, though still ongoing, has allowed us to obtain a preliminary structure of the *C. albicans* 80S ribosome at a resolution of 3.70 Å. This structure permits us to confirm our hypotheses concerning the rather different spatial organization of the *C. albicans* decoding center. A higher resolution will allows us to, firstly, confirm the other hypotheses obtained from the bioinformatic model, but most of all to have the precision necessary for the study of the mechanics of translation in this particular organism. Moreover, we could in the future perform studies on the binding of possible inhibitors of the *C. albicans* ribosome directly *in vitro*.

As the E-site of the *C. albicans* ribosome appeared to be extremely interesting for this study, a structural comparison between *H. sapiens*, *S. cerevisiae*, and *C. albicans* was carried out.

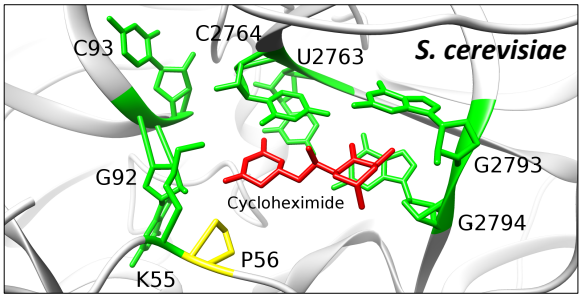


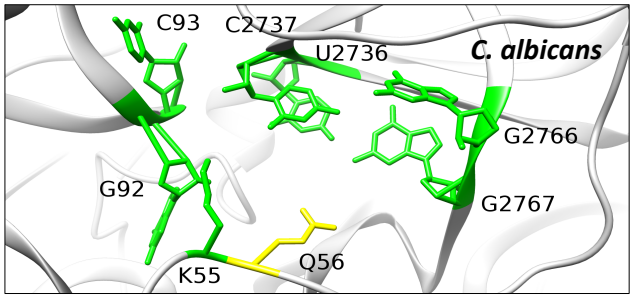


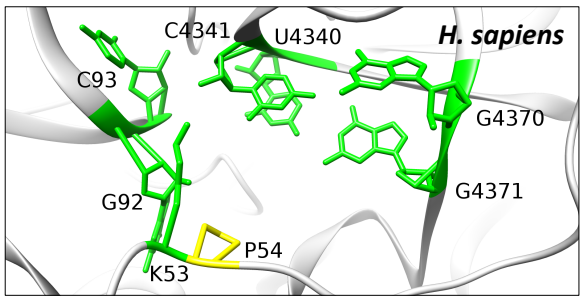


| Site | Residues | *S. cerevisiae* | *H. sapiens* | *C. albicans* |
|---|---|---|---|---|
| E | 25S rRNA | C2764 | C4341 | C2737 |
| | | G2793 | G4370 | G2766 |
| | | G2794 | G4371 | G2767 |
| | Protein eL42 | 43 TYR | 41 TYR | 43 TYR |
| | | 55 LYS | 53 LYS | 53 LYS |
| | | 56 PRO | 54 PRO | 56 GLN |

*FIGURE 37: HOMO SAPIENS, SACCHAROMYCES CEREVISIAE, AND CANDIDA ALBICANS E-SITE COMPARISON*

*Common residues between organisms are colored in green, cycloheximide is colored in red and the residue that varies is highlighted in yellow.*

*S. cerevisiae* and *H. sapiens* are known for being sensitive to CHX. CHX binds the E-site of the ribosome and prevents the ribosome translocation mechanism during translation. We can clearly see that the binding pocket is conserved between these two organisms.

*C. albicans* is known for being resistant to CHX, however, even though this was known empirically in a hospital setting and was finally identified on a protein level, it has not yet been proven in a structural manner. When comparing the E-sites of *S. cerevisiae*, *H. sapiens* (both sensitive), and *C. albicans*, we see that a couple aspects differ: (i) the volume of the binding pocket is smaller, and (ii) the important residues involved in the binding of an inhibitor, in this case CHX, are not all similar. In fact, in *C. albicans*, residue 56 of protein eL42 is not a proline (P) as in *S. cerevisiae* and *H. sapiens*, but a glutamine (Q). This prevents the binding of CHX, due to the obstacle that results. This particularly interesting site due to its high specificity to *C. albicans* is presented here.

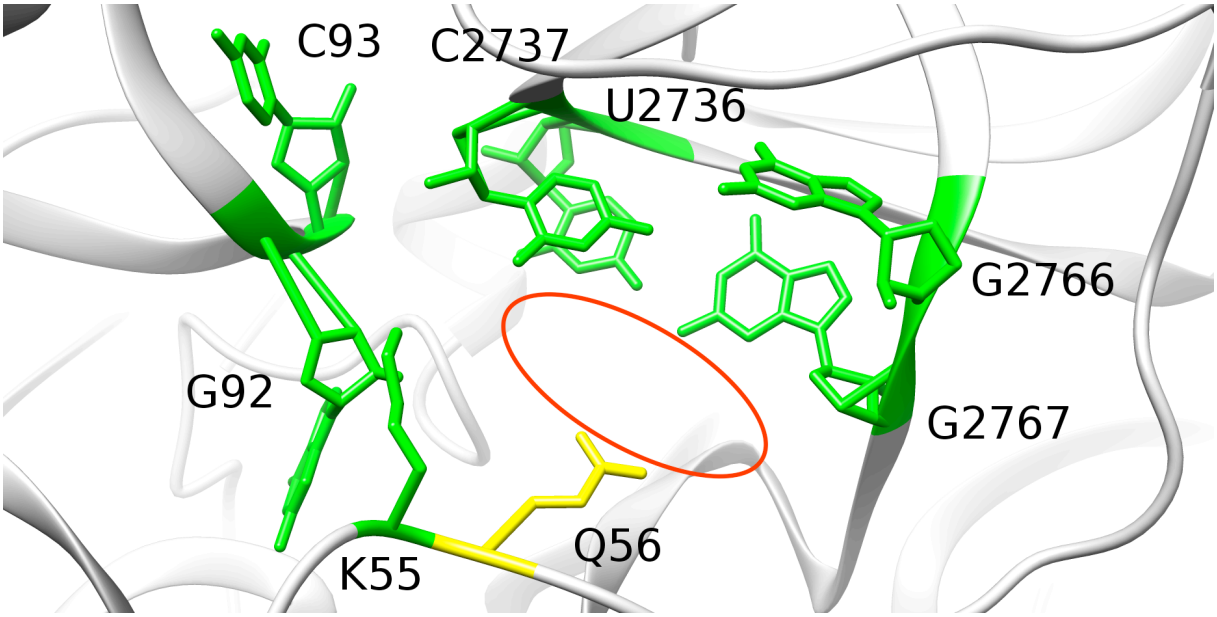


*FIGURE 38: SPECIFIC CANDIDA ALBICANS E-SITE BULK*

Indeed, a pathogen resistance against any available drug often causes a lot of trouble. It is especially true when we are talking about a multi-resistant bacteria such as *Staphylococcus aureus* or fungal infections, since there is not a large therapeutic arsenal with which to combat them. However, a resistance could also be a target. Indeed, the E-site of *C. albicans* is extremely specific due to this Q56. It also means that if we target this particular space between Q56-G2767-G2766-C2736-C2737, we would only and specifically target the *C. albicans* ribosome. Thus, there is an interesting target with which we can carry out drug design work.

Though it provides many answers, this thesis poses many more questions. Indeed, since the universal genetic code is not respected in this organism, we can ask ourselves if the conformation of the *C. albicans* decoding center is not, in fact, partly responsible for this particularity, or at least permits it to happen.

Even in the present day, biofilms remain a mystery in the case of the resistance mechanisms that communities of fixed microorganisms develop. Those belonging to *C. albicans* combine blastospores and filamentous forms, and this could add response elements to the strong resistance of biofilms, but also to their aggressiveness if the ribosomes, as those belonging to other pathogens, were modified or had a translational activity changed. Indeed, a part of this work not elaborated upon in this thesis concerning the multiple alignments of r-proteins shows evidence of conservation between kingdoms, but also more surprisingly shows evidence of particularities exclusive to the pathogens studied.

« The more I learn, the more I learn how little I know »

Socrates

# LIST OF PUBLICATIONS AND COMMUNICATIONS

**List of publication:**

- « E-site of *Candida albicans* ribosome as an interesting druggable target » Bruchlen D., Sabou M., Gass H., Pellegrino S., Candolfi E., Thompson J. & Yusupov M. in preparation

**List of communications: talk –** *poster*

- « *Druggable spots on Candida albicans ribosome* » Bruchlen D, Gass H, Pellegrino S, Candolfi E, Thompson J & Yusupov M
  6th to 10th July 2016, Strasbourg, France: Ribosome structure and function 2016

- « *Druggable spots on Candida albicans ribosome* » Bruchlen D, Gass H, Pellegrino S, Meyer M, Candolfi E, Thompson J & Yusupov M
  2nd et 3rd June 2016, Illkirch, France: Forum BioChem

- « *Mettre en lumière de nouvelles cibles thérapeutiques et si on couplait biologie et physique ?* » Bruchlen D
  17th to 21st May 2016, Liebfrauenberg, France : Les doctoriales d'Alsace 2016

- « ***Candida albicans* ribosome structure determination: a new tool for drug development** » Bruchlen D
  7th to 8th March 2016, Tours, France: Consortium Anti-Parasitaire et anti-Fongique, À la croisée des Mondes

- « **Structure et fonction du ribosome de *Candida albicans*** » Bruchlen D
  3rd March 2016, Illkirch, France : Séminaire de Microbiologie de Strasbourg

- « **Cible thérapeutique intéressante : le ribosome** » Bruchlen D
  26th February 2016, Illkirch, France: Séminaire de vulgarisation scientifique

- « *Candida albicans ribosome structure determination: a new tool for drug development* » Bruchlen D, Sabou M, Pellegrino S, Meyer M, Candolfi E & Yusupov M
  16th to 19th February 2016, Montevideo, Uruguay: Integrative methods in Structural Biology to enhance high impact research in health and disease

- « *Candida albicans ribosome structure determination : new tool for drug devlopment* » Bruchlen D, Sabou M, Candolfi E & Yusupov M

9th to 12th June 2015, Strasbourg, France: 2nd NovAliX Conference – Biophysics in Drug Discovery 2015: Developing the Synergy between Biophysics and Medicinal Chemistry to Deliver Better Drugs

- « ***Candida albicans ribosome structure determination: new tool for drug development*** » Bruchlen D, Sabou M, Candolfi E & Yusupov M
  18th to 22nd May 2015, La Colle-sur-Loup, France: Molecular Mechanisms of Host-Pathogen Internations and Virulence in Human Fungal Pathogens

- « **Screening in hanging drop system** » Bruchlen D, Candolfi E & Yusupov M
  7th July to 1st August 2014, Les Houches, France: Integrated structural and cell biology: from molecules to cells and organisms: thinking out of the box

# BIBLIOGRAPHIE


1. Abramczyk D, Tchorzewski M, Grankowski N. (2003). Non-AUG translation initiation of mRNA encoding acidic ribosomal P2A protein in Candida albicans. Yeast **20**, 1045–1052.
2. Adams, P.D., Afonine, P.V., Bunkoczi, G., Chen, V.B., Davis, I.W., Echols, N., Headd, J.J., Hung, L.W., Kapral, G.J., Grosse-Kunstleve, R.W., et al. (2010). PHENIX: a comprehensive Python-based system for macromolecular structure solution. Acta Crystallogr D Biol Crystallogr **66**, 213-221.
3. Adl, S.M., Simpson, A.G.B., Farmer, M.A., Andersen, R.A., Anderson, O.R., Barta, J.R., Bowser, S.S., Brugerolle, G., Fensome, R.A., Fredericq, S., James, T.Y., Karpov, S., Kugrens, P., Krug, J., Lane, C.E., Lewis, L.A., Lodge, J., Lynn, D.H., Mann, D.G., McCourt, R.M., Mendoza, L., Moestrup, Ø., Mozley-Standridge, S.E., Nerad, T.A., Shearer, C.A., Smirnov, A.V., Spiegel, F.W. & Taylor, M.F.J.R. (2005). The New Higher Level Classification of Eukaryotes with Emphasis on the Taxonomy of Protists. J. Eukaryot. Microbiol. **52**, 399-451.
4. Adl, S.M., Simpson, A.G.B., Lane, C.E., Lukeš, J., Bass, D., Bowser, S.S., Brown, M.W., Burki, F., Dunthorn, M., Hampl, V., Heiss, A., Hoppenrath, M., Lara, E., Le Gall, L., Lynn, D.H., McManus, H., Mitchell, E.A.D., Mozley-Stanridge, S.E., Parfrey, L.W., Pawlowski, J., Rueckert, S., Shadwick, L., Schoch, C.L., Smirnov, A. & Spiegel, F.W. (2012). The Revised Classification of Eukaryotes. J. Eukaryot. Microbiol. **59**, 429–493.
5. Ainsworth G. C. (1986). Introduction to the History of Medical and Veterinary Mycology. Cambridge University Press, London.
6. Anger AM., Armache JP., Berninghausen O., Habeck M., Subklewe M., Wilson D. , Beckmann R. (2013). Structures of the human and Drosophila 80S ribosome. Nature **497**, 80–85.
7. Arnaud, M.B., Costanzo, M.C., Shah, P., Skrzypek, M.S., and Sherlock, G. (2009). Gene Ontology and the annotation of pathogen genomes: the case of Candida albicans. Trends Microbiol **17**, 295–303.
8. Ashe, M.P., De Long, S.K., and Sachs, A.B. (2000). Glucose depletion rapidly inhibits translation initiation in yeast. Mol Biol Cell **11**, 833-848.

9. Auerbach-Nevo Tamar, David Baram, Anat Bashan, Matthew Belousoff, Elinor Breiner, Chen Davidovich, Giuseppe Cimicata, Zohar Eyal, Yehuda Halfon, Miri Krupkin, Donna Matzov, Markus Metz, Mruwat Rufayda, Moshe Peretz, Ophir Pick, Erez Pyetan, Haim Rozenberg, Moran Shalev-Benami, Itai Wekselman, Raz Zarivach, Ella Zimmerman, Nofar Assis, Joel Bloch, Hadar Israeli, Rinat Kalaora, Lisha Lim, Ofir Sade-Falk, Tal Shapira, Leena Taha-Salaime, Hua Tang and Ada Yonath. (2016). Ribosomal Antibiotics: Contemporary Challenges. Antibiotics **5**, 3-24.
10. Bahn, Y. S., and F. A. Mühlschlegel. (2006). CO2 sensing in fungi and beyond. Curr. Opin. Microbiol. **9**, 572-578.
11. Bachewich C, Thomas DY & Whiteway M. (2003). Depletion of a polo-like kinase in Candida albicans activates cyclase-dependent hyphal-like growth. Molecular biology of the cell **14**, 2163-2180.
12. Ban, N., Nissen, P., Hansen, J., Moore, P.B., and Steitz, T.A. (2000). The complete atomic structure of the large ribosomal subunit at 2.4 A resolution. Science **289**, 905‑920.
13. Ban, N., Beckmann, R., Cate, J., Dinman, J., Dragon, F., Ellis, S., Lafontaine, D., Lindahl, L., Liljas, A., Lipton, J., McAlear, M., Moore, P., Noller, H., Ortega, J., Panse, V., Ramakrishnan, V., Spahn, C., Steitz, T., Tchorzewski, M., Tollervey, D., Warren, A., Williamson, J., Wilson, D., Yonath, A., and Yusupov, M. (2014). A new system for naming ribosomal proteins. Curr Opin Struct Biol, 165–169.
14. Bartizal C, Odds FC. (2003). Influences of methodological variables on susceptibility testing of caspofungin against *Candida* species and *Aspergillus fumigatus*. Antimicrob Agents Chemother. **47**, 2100–7.
15. Bassetti M, Merelli M, Ansaldi F. de Florentiis D, Sartor A, Scarparo C, Callegari A, Righi E (2015). Clinical and therapeutic aspects of candidemia: a five year single centre study. PLoS One.10:e0127534.
16. Becker, T., Bhushan, S., Jarasch, A., Armache, J.P., Funes, S., Jossinet, F., Gumbart, J., Mielke, T., Berninghausen, O., Schulten, K. Westhof E, Gilmore R, Mandon EC, Beckmann R (2009). Structure of monomeric yeast and mammalian Sec61 complexes interacting with the translating ribosome. Science **326**, 1369‑1373.
17. Bendel CM, Hess DJ, Garni RM, Henry-Stanley M, Wells CL. (2003). Comparative virulence of Candida albicans yeast and filamentous forms in orally and intravenously inoculated mice. Crit Care Med**. 31**, 501–507.

18. Ben-Shem, A., Garreau de Loubresse, N., Melnikov, S., Jenner, L., Yusupova, G., and Yusupov, M. (2011). The structure of the eukaryotic ribosome at 3.0 A resolution. Science **334**, 1524-1529.
19. Ben-Shem, A., Jenner, L., Yusupova, G., and Yusupov, M. (2010). Crystal structure of the eukaryotic ribosome. Science **330**, 1203-1209.
20. Berkhout CM. (1923). *De schimmelgeslachten Monilia, Oidium, Oospora en Torula*. Utrecht University, Utrecht.
21. Berman J. (2006). Morphogenesis and cell cycle progression in *Candida albicans*. Current opinion in microbiology **9**, 595-601.
22. Berman J & Sudbery PE. (2002). Candida albicans: a molecular revolution built on lessons from budding yeast. Nature reviews **3**, 918-930.
23. Berman J, Forche A. (2016). Correction of the haplotype assignments for chromosome 3 of Assembly 22 in *C. albicans* SC5314, Personal communication to CGD
24. Bezerra A. R., Simoes J., Lee W., Rung J., Weil T., Gut I. G. (2013). Reversion of a fungal genetic code alteration links proteome instability with genomic and phenotypic diversification. Proc. Natl. Acad. Sci. U.S.A. **110**, 11079–11084.
25. Biswas S, Van Dijck P & Datta A. (2007). Environmental sensing and signal transduction pathways regulating morphopathogenic determinants of *Candida albicans*. Microbiol Mol Biol Rev **71**, 348-376.
26. Bloos F, Thomas-Rüddel D, Rüddel H, Engel C, Schwarzkopf D, Marshall JC, Harbarth S, Simon P, Riessen R, Keh D, Dey K, Weiß M, Toussaint S, Schädler D, Weyland A, Ragaller M, Schwarzkopf K, Eiche J, Kuhnle G, Hoyer H, Hartog C, Kaisers U, Reinhart K, (2014). MEDUSA Study Group Impact of compliance with infection management guidelines on outcome in patients with severe sepsis: a prospective observational multi-center study. Crit Care. **18**, R42.
27. Bokov, K., and Steinberg, S.V. (2009). A hierarchical model for evolution of 23S ribosomal RNA. Nature **457**, 977–980.
28. Borg-von Zepelin M, Beggah S, Boggian K, Sanglard D, Monod M. (1998). The expression of the secreted aspartyl proteinases Sap4 to Sap6 from *Candida albicans* in murine macrophages. Mol Microbiol **28**, 543–554.
29. Calderone RA. (2002). Introduction and historical perspectives. In *Candida* and candidiasis, ed. Calderone RA, ASM Press, Washington, D.C. pp. 3-13.
30. Cavalier-Smith T. (2002). The phagotrophic origin of eukaryotes and phylogenetic classification of Protozoa. Int J Syst Evol Microbiol. **52**, 297–354.

31. Cavalier-Smith T., (1998). A revised six-kingdom system of life, Biological Reviews, Cambridge Philosophical Society **73**, 203–266
32. Chabasse D, Bouchara JP, de Gentile L & Chennebault JM. (1988). *Candida albicans* chlamydospores observed in vivo in a patient with AIDS. Annales de biologie clinique **46**, 817-818.
33. Chaffin WL, Lopez-Ribot JL, Casanova M, Gozalbo D & Martinez JP. (1998). Cell wall and secreted proteins of *Candida albicans*: identification, function, and expression. Microbiol Mol Biol Rev **62**, 130-180.
34. Chandra J, Kuhn DM, Mukherjee PK, Hoyer LL, McCormick T & Ghannoum MA. (2001). Biofilm formation by the fungal pathogen *Candida albicans*: development, architecture, and drug resistance. Journal of bacteriology **183**, 5385-5394.
35. Clamp, M., Cuff, J., Searle, S.M., and Barton, G.J. (2004). The Jalview Java alignment editor. Bioinformatics **20**, 426–427.
36. Cleveland A.A., Farley M.M., Harrison L.H., Stein B., Hollick R., Lockhart S.R., Magill S.S., Derado G., Park B.J., Chiller T.M. (2012). Changes in incidence and antifungal drug resistance in candidemia: results from population-based laboratory surveillance in Atlanta and Baltimore, 2008-2011. Clin Infect Dis. **55**,1352–1361
37. Cleveland AA, Harrison LH, Farley MM. (2015). Declining incidence of candidemia and the shifting epidemiology of Candida resistance in two US metropolitan areas, 2008–2013: results from population-based surveillance. PLoS One 10: e0120452.
38. Collaborative‑CCP4 (1994). The CCP4 suite: programs for protein crystallography. Acta Crystallogr D Biol Crystallogr **50**, 760‑763.
39. Costanzo MC, Arnaud MB, Skrzypek MS, Binkley G, Lane C, Miyasato SR & Sherlock G. (2006). The Candida Genome Database: facilitating research on Candida albicans molecular biology. FEMS yeast research **6**, 671-684.
40. Costerton JW, Lewandowski Z, Caldwell DE, Korber DR & Lappin-Scott HM. (1995). Microbial biofilms. Annu Rev Microbiol **49**, 711-745.
41. Delaunay P., Fissore C. (2015). Interactions médicamenteuses des antifongiques systémiques. Journal de Mycologie Médicale / Journal of Medical Mycology, **16** : 152–158.
42. Diederichs K. (2005). Some aspects of quantitative analysis and correction of radiation damage. Biological Crystallography **62**, 96-101.
43. Diekema D., Arbefeville S., Boyken L., Kroeger J. & Pfaller M. (2012). The changing epidemiology of healthcare-associated candidemia over three decades. Diagn. Microbiol. Infect. Dis. **73**, 45–48

44. Donlan RM. (2002). Biofilms: microbial life on surfaces. Emerging infectious diseases **8**, 881-890.
45. Donlan RM & Costerton JW. (2002). Biofilms: survival mechanisms of clinically relevant microorganisms. Clinical microbiology reviews **15**, 167-193.
46. Douglas LJ. (2003). Candida biofilms and their role in infection. Trends in microbiology **11**, 30-36.
47. Druzina, Z., et B.S. Cooperman. (2004). Photolabile anticodon stem-loop analogs of tRNAPhe as probes of ribosomal structure and structural fluctuation at the decoding center. Rna. **10**, 1550-62.
48. Dudzinska-Bajorek, B., Bakowska, K., Twardowski, T.(2006). Conformational changes of L-rRNA during elongation of polypeptide. J Plant Physiol. **163**, 463-74.
49. Dumitru R, Hornby JM & Nickerson KW. (2004). Defined anaerobic growth medium for studying Candida albicans basic biology and resistance to eight antifungal drugs. Antimicrob Agents Chemother **48**, 2350-2354.
50. Dunkle J.A., Xiong L., Mankin A.S., Cate J.H. (2010). Structures of the *Escherichia coli* ribosome with antibiotics bound near the peptidyl transferase center explain spectra of drug action. Proc. Natl. Acad. Sci. USA.**107**, 17152–17157.
51. Emsley, P., and Cowtan, K. (2004). Coot: model-building tools for molecular graphics. Acta Crystallogr D Biol Crystallogr. **60**, 2126-2132.
52. Eriksson, O.E. & Winka, K. (1997). Supraordinal taxa of Ascomycota. Myconet. **1**, 1-16
53. Eyal Z., Matzov D., Krupkin M., Wekselman I., Paukner S., Zimmerman E., Rozenberg H., Bashan A., Yonath A. (2015). Structural insights into species-specific features of the ribosome from the pathogen *Staphylococcus aureus*. Proc. Natl. Acad. Sci. **112**, 5805-5814.
54. Frame GW, Strauss WG & Maibach HI. (1972). Carbon dioxide emission of the human arm and hand. The Journal of investigative dermatology **59**, 155-159.
55. Frank, J., Bretaudiere, J.P., Carazo, J.M., Verschoor, A., and Wagenknecht, T. (1988). Classification of images of biomolecular assemblies: a study of ribosomes and ribosomal subunits of Escherichia coli. J Microsc **150**, 99-115.
56. Fonzi WA., Irwin MY. (1993). Isogenic strain construction and gene mapping in Candida albicans. Genetics. **134**, 717-28.
57. Garreau de Loubresse, N., Prokhorova, I., Holtkamp, W., Rodnina, M.V., Yusupova, G., and Yusupov, M. (2014). Structural basis for the inhibition of the eukaryotic ribosome. Nature **513**, 517–522.

58. Gillum A.M., Tsay E.Y., Kirsch D.R. (1984). Isolation of the Candida albicans gene for orotidine-5′-phosphate decarboxylase by complementation of S. cerevisiae ura3 and E. coli pyrF mutations. Mol. Gen. Genet. **198**, 179–182.
59. Goldman L., Schwarz J., Preston RH., Beyer A, Loutzenhiser J. (1960). Current status of griseofulvin: Report on one hundred seventy-five cases . Journal of the American Medical Association **172**, 532-538
60. Goldway, M., Teff, D., Schmidt, R., Oppenheim, A.B., and Koltin, Y. (1995). Multidrug resistance in Candida albicans: disruption of the BENr gene. Antimicrob Agents Chemother **39**, 422–426.
61. Goudarzi K.M., Lindstrom M.S. (2016). Role of ribosomal protein mutations in tumor development. Int. J. Oncol. **48**, 1313–1324.
62. Granier F. (2000). Les infections fongiques invasives. La presse médicale. **29**, 20-51.
63. Granier F. (2002). Les traitements antifongiques : Synopsis infectiology 42th ICAAC. La Presse médicale. **31**, 1785–1791.
64. Granier F. (2003). Antifongiques : classes thérapeutiques, mécanismes d'action, problèmes de résistance. Antibiotiques. **5**, 39–48.
65. Gubbins PO. (2011). Triazole antifungal agents drug-drug interactions involving hepatic cytochrome P450. Expert opinion on drug metabolism & toxicology, **7**, 1411–1429.
66. Halic, M., Gartmann, M., Schlenker, O., Mielke, T., Pool, M.R., Sinning, I., and Beckmann, R. (2006). Signal recognition particle receptor exposes the ribosomal translocon binding site. Science **312**, 745‑ 747.
67. Hall RA, Cottier F & Muhlschlegel FA. (2009). Molecular networks in the fungal pathogen Candida albicans. Advances in applied microbiology **67**, 191-212.
68. Hall-Stoodley L, Costerton JW & Stoodley P. (2004). Bacterial biofilms: from the natural environment to infectious diseases. Nat Rev Microbiol **2**, 95-108.
69. Harms, J., Schluenzen, F., Zarivach, R., Bashan, A., Gat, S., Agmon, I., Bartels, H., Franceschi, F., and Yonath, A. (2001). High resolution structure of the large ribosomal subunit from a mesophilic eubacterium. Cell **107**, 679‑688.
70. Hashem Y. des Georges A, Fu J, Buss SN, Jossinet F, Jobe A, Zhang Q, Liao HY, Grassucci RA, Bajaj C, Westhof E, Madison-Antenucci S, Frank J. (2013). High-resolution cryo-electron microscopy structure of the *Trypanosoma brucei* ribosome. Nature **494**, 385–389
71. Herbrecht R., Nivoix Y., Fohrer C. (2005). Management of systemic fungal infections: alternatives to itraconazole. Journal of Antimicrobial Chemotherapy. **56**, 39-48.

72. Hibbett, D.S. (2007). "A higher level phylogenetic classification of the Fungi". Mycological Research. **111**, 509–47.
73. Hincky-Vitrat V. (2011). Les antifongiques systémiques. Clinique maladies infectieuses - CHU Grenoble.
74. HOCHART S, BARRIER F, DURAND-JOLY I, HORRENT S, DECAUDIN B, ODOU P. (2008). Les antifongiques systémiques : Partie 1 : éléments pharmaceutiques. Le Pharmacien Hospitalier. **43**, 103–109.
75. Hornby JM, Dumitru R & Nickerson KW. (2004). High phosphate (up to 600 mM) induces pseudohyphal development in five wild type *Candida albicans*. Journal of microbiological methods **56**, 119- 124.
76. Hull CM, Raisner RM & Johnson AD. (2000). Evidence for mating of the "asexual" yeast *Candida albicans* in a mammalian host. Science **289**, 307-310.
77. Ingolia, N.T., Ghaemmaghami, S., Newman, J.R., and Weissman, J.S. (2009). Genome‐wide analysis in vivo of translation with nucleotide resolution using ribosome profiling. Science **324**, 218‐223.
78. Jansons VK & Nickerson WJ. (1970). Induction, morphogenesis, and germination of the chlamydospore of Candida albicans. Journal of bacteriology **104**, 910-921.
79. Jenner, L.B., Demeshkina, N., Yusupova, G., and Yusupov, M. (2010). Structural aspects of messenger RNA reading frame maintenance by the ribosome. Nat Struct Mol Biol **17**, 555‐560.
80. Jones S, White G & Hunter PR. (1994). Increased phenotypic switching in strains of Candida albicans associated with invasive infections. Journal of clinical microbiology **32**, 2869-2870.
81. Jones T, Federspiel NA, Chibana H, Dungan J, Kalman S, Magee BB, Newport G, Thorstenson YR, Agabian N, Magee PT, Davis RW & Scherer S. (2004). The diploid genome sequence of Candida albicans. Proceedings of the National Academy of Sciences of the United States of America **101**, 7329-7334.
82. Kabir MA & Hussain MA. (2009). Human fungal pathogen Candida albicans in the postgenomic era: an overview. Expert review of anti-infective therapy **7**, 121-134.
83. Kabsch, W. (2010). Integration, scaling, space‐group assignment and post‐refinement. Acta Crystallogr D Biol Crystallogr **66**, 133‐144.
84. Karkowska-Kuleta J, Rapala-Kozik M & Kozik A. (2009). Fungi pathogenic to humans: molecular bases of virulence of *Candida albicans, Cryptococcus neoformans* and *Aspergillus fumigatus*. Acta biochimica Polonica **56**, 211-224.

85. Khatter, H., Myasnikov, A.G., Natchiar, S.K., and Klaholz, B.P. (2015). Structure of the human 80S ribosome. Nature **520**, 640–645.
86. Knoke M & Bernhardt H. (2006). The first description of an oesophageal candidosis by Bernhard von Langenbeck in 1839. Mycoses **49**, 283-287.
87. Kojic EM & Darouiche RO. (2004). Candida infections of medical devices. Clinical microbiology reviews **17**, 255-267.
88. Kozak, M. (1978). How do eucaryotic ribosomes select initiation regions in messenger RNA? Cell. **15**,1109-23.
89. Kozak, M. (1980). Evaluation of the "scanning model" for initiation of protein synthesis in eucaryotes. Cell. **22**, 7-8.
90. Kumamoto CA & Vinces MD. (2005). Alternative *Candida albicans* lifestyles: growth on surfaces. Annu Rev Microbiol **59**, 113-133.
91. Kvaal C, Lachke SA, Srikantha T, Daniels K, McCoy J & Soll DR. (1999). Misexpression of the opaque- phase-specific gene PEP1 (SAP1) in the white phase of *Candida albicans* confers increased virulence in a mouse model of cutaneous infection. Infection and immunity **67**, 6652-6662.
92. Laverdiere M. (2006). Progressive loss of echinocandin activity following prolonged use for treatment of *Candida albicans* esophagitis. J. Antimicrob. Chemother. **57**, 705–708.
93. Lewis K. (2007). Persister cells, dormancy and infectious disease. Nat Rev Microbiol **5**, 48-56.
94. Li, X., et Y.H. Chang. (1995). Amino-terminal protein processing in Saccharomyces cerevisiae is an essential function that requires two distinct methionine aminopeptidases. Proc Natl Acad Sci. **92**, 12357-61.
95. Lo HJ, Kohler JR, DiDomenico B, Loebenberg D, Cacciapuoti A & Fink GR. (1997). Nonfilamentous *C. albicans* mutants are avirulent. Cell **90**, 939-949.
96. Locke JB, Hilgers M, Shaw KJ. (2009). Mutations in ribosomal protein L3 are associated with oxazolidinone resistance in staphylococci of clinical origin. Antimicrob Agents Chemother **53**, 5275–5278.
97. Lockhart SR, Iqbal N, Cleveland AA, Farley MM, Harrison LH, Bolden CB. (2012) Species identification and antifungal susceptibility testing of *Candida* bloodstream isolates from population-based surveillance studies in two U.S. cities from 2008 to 2011. J Clin Microbiol. **50**, 3435–42.
98. Lodish, H., A. Berk, P. Matsudaira, C.A. Kaiser, M. Krieger, M.P. Scott, S.L. Zipurky, J. Darnell. (2004). Molecular Cell Biology.

99. Lortholary O., Tod M., Dupont B. (1999). Antifongiques. EMC - Maladies infectieuses, 1-21.

100. Magee BB & Magee PT. (2000). Induction of mating in Candida albicans by construction of MTLa and MTLalpha strains. Science **289**, 310-313.

101. Mailliot, J., Garreau de Loubresse, N., Yusupova, G., Meskauskas, A., Dinman, J.D., and Yusupov, M. (2016). Crystal Structures of the uL3 Mutant Ribosome: Illustration of the Importance of Ribosomal Proteins for Translation Efficiency. Journal of Molecular Biology **428**, 2195–2202.

102. Martins N, Barros L, Henriques M, Silva S, Ferreria I.C.F.R. (2015). In vivo anticandidal activity of phenolic extracts and compounds: future perspectives focusing on effective clinical interventions. Biomed Research International. Article Id: 247382.

103. Mimoz, F Rayeh, B Debaene (2001). Infections liées aux cathéters veineux en réanimation. Physiopathologie, diagnostic, traitement et prévention. Annales Françaises d'Anesthésie et de Réanimation, Volume 20, Issue 6, Pages 520-536

104. Miranda I. et al. (2013). *Candida albicans* CUG mistranslation is a mechanism to create cell surface variation. Mbio 4, e00285-13.

105. Melnikov, S., Ben-Shem, A., Garreau de Loubresse, N., Jenner, L., Yusupova, G., and Yusupov, M. (2012). One core, two shells: bacterial and eukaryotic ribosomes. Nat Struct Mol Biol **19**, 560‑567.

106. Merson-Davies LA & Odds FC. (1989). A morphology index for characterization of cell shape in *Candida albicans*. Journal of general microbiology **135**, 3143-3152.

107. Moore, R.T. (1980). Taxonomic proposals for the classification of marine yeasts and other yeast-like fungi including the smuts.. Bot. Mar. **23**, 361-373.

108. Morgan J, Meltzer MI, Plikaytis BD, et al. (2005). Excess mortality, hospital stay, and cost due to candidemia: a case-control study using data from population-based candidemia surveillance. Infection control and hospital epidemiology. **26**, 540-7

109. Morschhäuser J. (2010). Regulation of white-opaque switching in Candida albicans. Med Microbiol Immunol **199**, 165–172.

110. Mueller, M., Wang, M., and Schulze‑Briese, C. (2011). Optimal fine phi‑slicing for single‑photon‑counting pixel detectors. Acta Crystallogr D Biol Crystallogr **68**, 42‑56.

111. Muzzey D., Schwartz K., Weissman JS., Sherlock G. (2013). Assembly of a phased diploid *Candida albicans* genome facilitates allele-specific measurements and provides a simple model for repeat and indel structure. Genome Biol. **14**, R97.

112. Noble SM & Johnson AD. (2007). Genetics of *Candida albicans*, a diploid human fungal pathogen. Annu Rev Genet **41**, 193-211.

113. Odds FC. (1988). Candida and candidosis. Baillière Tindall, London.

114. Odds FC, Van Nuffel L & Gow NA. (2000). Survival in experimental *Candida albicans* infections depends on inoculum growth conditions as well as animal host. Microbiology **146**, 1881-1889.

115. Odds FC, Brown AJ & Gow NA. (2004). *Candida albicans* genome sequence: a platform for genomics in the absence of genetics. Genome biology **5**, 230.

116. Palade, G.E. (1955). A small particulate component of the cytoplasm. J Biophys Biochem Cytol. **1**, 59-68.

117. Paleiron N., Bizien N., Vinsonneau U. (2011). Insuffisance cardiaque aiguë sous itraconazole : une complication prévisible ? Revue des Maladies Respiratoires **28**, 352–354.

118. Perlroth J, Choi B & Spellberg B. (2007). Nosocomial fungal infections: epidemiology, diagnosis, and treatment. Med Mycol **45**, 321-346.

119. Peske, F., A. Savelsbergh, V.I. Katunin, M.V. Rodnina, et W. Wintermeyer. (2004). Conformational changes of the small ribosomal subunit during elongation factor G-dependent tRNA-mRNA translocation. J Mol Biol. **343**, 1183-94.

120. Pfaller M, Neofytos D, Diekema D, Azie N, Meier-Kriesche HU, Quan SP, Horn D. (2012). Epidemiology and outcomes of candidemia in 3648 patients: data from the Prospective Antifungal Therapy (PATH Alliance(R)) registry, 2004–2008. Diagnostic microbiology and infectious disease. **74**, 323–31.

121. Plewniak F, Bianchetti L, Brelivet Y, Carles A, Chalmel F, Lecompte O, Mochel T, Moulinier L, Muller A, Muller J, Prigent V, Ripp R, Thierry JC, Thompson JD, Wicker N, Poch O. (2003). PipeAlign: A new toolkit for protein family analysis. Nucleic Acids Res. **31**, 3829-32.

122. Radford DR, Challacombe SJ & Walter JD. (1994). A scanning electronmicroscopy investigation of the structure of colonies of different morphologies produced by phenotypic switching of *Candida albicans*. Journal of medical microbiology **40**, 416-423.

123. Ramage G, Mowat E, Jones B, Williams C & Lopez-Ribot J. (2009). Our current understanding of fungal biofilms. Critical reviews in microbiology **35**, 340-355.

124. Renaud JP., Chung CW., Danielson UH., Egner U., Hennig M., Hubbard RE., Nar H. (2016). Biophysics in drug discovery: impact, challenges and opportunities. Nat Rev Drug Discov. **10**, 679-98.

125. Reess M. (1877). Über den Soorpilz. Physikalisch-Medicinische Societät zu Erlangen **9**, 190-193.

126. Robin CP. (1853). Histoire naturelle des végétaux. Parasites qui croissent sur l'homme et sur les animaux vivants. Ballière, Paris.

127. Rodnina, M.V., T. Daviter, K. Gromadski, et W. Wintermeyer. (2002). Structural dynamics of ribosomal RNA during decoding on the ribosome. Biochimie. **84**, 745-54.

128. Ruhnke M & Maschmeyer G. (2002). Management of mycoses in patients with hematologic disease and cancer -- review of the literature. European journal of medical research **7**, 227-235.

129. Rustchenko-Bulgac EP, Sherman F & Hicks JB. (1990). Chromosomal rearrangements associated with morphological mutants provide a means for genetic variation of *Candida albicans*. Journal of bacteriology **172**, 1276-1283.

130. Rustchenko E. (2007). Chromosome instability in *Candida albicans*. FEMS yeast research **7**, 2-11.

131. Santos M.A., Keith G., Tuite M.F. (1993). Non-standard translational events in *Candida albicans* mediated by an unusual seryl-tRNA with a 5′-CAG-3′ (leucine) anticodon. EMBO J. **12**, 607–616.

132. Santos MA, Cheesman C, Costa V, Moradas-Ferreira P, Tuite MF. (1999). Selective advantages created by codon ambiguity allowed for the evolution of an alternative genetic code in Candida spp. Mol Microbiol. **31**, 937–947.

133. Samson J. (1990). [Oral candidiasis: epidemiology, diagnosis and treatment]. Schweizer Monatsschrift fur Zahnmedizin = Revue mensuelle suisse d'odonto-stomatologie = Rivista mensile svizzera di odontologia e stomatologia / SSO 100, 548-559.

134. Sardi, J. C. O. (2016). "Candida species: current epidemiology, pathogenicity, biofilm formation, natural antifungal products and new therapeutic options" (PDF). Journal of Medical Microbiology.

135. Saville SP, Lazzell AL, Monteagudo C & Lopez-Ribot JL. (2003). Engineered control of cell morphology in vivo reveals distinct roles for yeast and filamentous forms of Candida albicans during infection. Eukaryotic cell **2**, 1053-1060.

136. Schmeing, T.M., and Ramakrishnan, V. (2009). What recent ribosome structures have revealed about the mechanism of translation. Nature **461**, 1234-1242.

137. Segal E. (2005). *Candida*, still number one--what do we know and where are we going from there? Mycoses **48**, 3-11.

138. Selmer, M., Dunham, C.M., Murphy, F.V.t., Weixlbaumer, A., Petry, S., Kelley, A.C., Weir, J.R., and Ramakrishnan, V. (2006). Structure of the 70S ribosome complexed with mRNA and tRNA. Science **313**, 1935-1942.

139. Seneviratne CJ, Jin L & Samaranayake LP. (2008). Biofilm lifestyle of Candida: a mini review. Oral diseases **14**, 582-590.

140. Shalev-Benami M., Zhang Y., Matzov D., Halfon Y., Zackay A., Rozenberg H., Zimmerman E., Bashan A., Jaffe CL., Yonath A., Skiniotis G. (2016). 2.8-Å Cryo-EM Structure of the Large Ribosomal Subunit from the Eukaryotic Parasite Leishmania. Cell Rep. **16**, 288-294

141. Shapiro, R.S., Robbins, N., and Cowen, L.E. (2011). Regulatory circuitry governing fungal development, drug resistance, and disease. Microbiol. Mol. Biol. Rev. **75**, 213–267.

142. Shepherd MG. (1990). Biology of *Candida* species. In Oral candidosis, ed. Samaranayake LP & MacFarlane TW, pp. 10-20.

143. Sheppard D. C., Yeaman M. R., Welch W. H., Phan Q. T., Fu Y., Ibrahim A. S., et al. (2004). Functional and structural diversity in the Als protein family of Candida albicans. J. Biol. Chem. **279**, 30480–30489.

144. Singh S, Fatima Z, Hameed S. (2015). Predisposing factors endorsing *Candida* infections. Infez Med. **23**, 211–23.

145. Simões J, Bezerra A, Moura G, Araújo H, Gut I, Bayes M, Santos M. (2016) The Fungus Candida albicans Tolerates Ambiguity at Multiple Codons Front Microbiol. **7**, 401.

146. Soll DR. (2009). Why does *Candida albicans* switch? FEMS yeast research **9**, 973-989.

147. Spahn, C.M., Jan, E., Mulder, A., Grassucci, R.A., Sarnow, P., and Frank, J. (2004). Cryo-EM visualization of a viral internal ribosome entry site bound to human ribosomes: the IRES functions as an RNA-based translation factor. Cell **118**, 465-475.

148. Steitz, T.A. (2008). A structural understanding of the dynamic ribosome machine. Nat Rev Mol Cell Biol **9**, 242-253.

149. Sudbery P, Gow N & Berman J. (2004). The distinct morphogenic states of *Candida albicans*. Trends in microbiology **12**, 317-324.

150. Sullivan DJ, Westerneng TJ, Haynes KA, Bennett DE & Coleman DC. (1995). *Candida dubliniensis* sp. nov.: phenotypic and molecular characterization of a novel

species associated with oral candidosis in HIV-infected individuals. Microbiology **141**, 1507- 1521.

151. Sydnor, Emily (2011). "Hospital Epidemiology and Infection Control in Acute-Care Settings". Clinical Microbiology Reviews. **24**, 141–173

152. Tan B.H., A. Chakrabarti, R.Y. Li, A.K. Patel, S.P. Watcharananan, Z. Liu, A. Chindamporn, A.L. Tan, P.-L. Sun, U.-I. Wu Y.-C. Chen (2015). Incidence and species distribution of candidaemia in Asia: a laboratory-based surveillance study. Clinical Microbiology and Infection **21**, 946-953

153. Taylor JW. (1995). Making the Deuteromycota redundant: a practical intergration of mitosporic fungi. Canadian journal of botany **73**, 754-759.

154. ten Cate JM, Klis FM, Pereira-Cenci T, Crielaard W & de Groot PW. (2009). Molecular and cellular mechanisms that lead to Candida biofilm formation. Journal of dental research **88**, 105-115.

155. Thompson, J.D., Muller, A., Waterhouse, A., Procter, J., Barton, G.J., Plewniak, F., and Poch, O. (2006). MACSIMS: multiple alignment of complete sequences information management system. BMC Bioinformatics **7**, 318.

156. Christian Touriol, Stéphanie Bornes, Sophie Bonnal, Sylvie Audigier, Hervé Prats, Anne-Catherine Prats and Stéphan Vagner (2003). « Generation of protein isoform diversity by alternative initiation of translation at non-AUG codons », Biology of the Cell, **95**, 169-178

157. Trakhanov, S., Yusupov, M., Shirokov, V., Garber, M., Mitschler, A., Ruff, M., Thierry, J.C., and Moras, D. (1989). Preliminary X-ray investigation of 70 S ribosome crystals from Thermus thermophilus. J Mol Biol **209**, 327-328.

158. het Hoog M, Rast TJ, Martchenko M, Grindle S, Dignard D, Hogues H, Cuomo C, Berriman M, Scherer S, Magee BB, Whiteway M, Chibana H, Nantel A & Magee PT. (2007). Assembly of the *Candida albicans* genome into sixteen supercontigs aligned on the eight chromosomes. Genome biology **8**, R52.

159. Vandeputte P. (2008). Mécanismes moléculaires de la résistance aux antifongiques chez *Candida glabrata*. Th : Biologie des organismes : Angers, 930.

160. Vanhoutreve, R., Legrand, B., Gass, H., Kress, A., Poch, O., and Thompson, JD. LEON-BIS: Multiple alignment evaluation of sequence neighbours using a Bayesian inference system. 2016 (submitted).

161. Vargas K, Srikantha R, Holke A, Sifri T, Morris R & Joly S. (2004). Candida albicans switch phenotypes display differential levels of fitness. Med Sci Monit **10**, 198-206.

162. Verschoor A, Frank J. (1990). Three-dimensional structure of the mammalian cytoplasmic ribosome. J Mol Biol. **5**, 737–749

163. Voss, N.R., and Gerstein, M. (2010). 3V: cavity, channel and cleft volume calculator and extractor. Nucleic Acids Res. **38**, 555-562.

164. Washburn, M.P., Wolters, D., and Yates, J.R., 3rd (2001). Large-scale analysis of the yeast proteome by multidimensional protein identification technology. Nat Biotechnol **19**, 242-247.

165. Weinberger, M (2016). Characteristics of candidaemia with Candida-albicans compared with non-albicans *Candida* species and predictors of mortality. J Hosp Infect. X

166. Whiteway M & Bachewich C. (2007). Morphogenesis in *Candida albicans*. Annual Review of Microbiology **61**, 529-553.

167. R.H. Whittaker, (1968). New Concepts of Kingdoms of Organisms. Science 1**63**, 150-160

168. R.H. Whittaker et L. Margulis. (1978). Protist classification and the kingdoms of organisms, Biosystems **10**, 3-18

169. Wimberly, B.T., Brodersen, D.E., Clemons, W.M., Jr., Morgan-Warren, R.J., Carter, A.P., Vonrhein, C., Hartsch, T., and Ramakrishnan, V. (2000). Structure of the 30S ribosomal subunit. Nature **407**, 327-339.

170. Wisplinghoff H, Ebbers J, Geurtz L, Stefanik D, Major Y, Edmond MB, et al. (2014) Nosocomial bloodstream infections due to Candida spp. in the USA: species distribution, clinical features and antifungal susceptibilities. Int J Antimicrob Agents. **43**, 78–81.

171. Wong W, Bai X-c, Brown A, Fernandez IS, Hanssen E, Condron M, et al. (2014) Cryo-EM structure of the *Plasmodium falciparum* 80S ribosome bound to the anti-protozoan drug emetine. eLife.;3:e3080

172. Woolford, J.L., and Baserga, S.J. (2013). Ribosome Biogenesis in the Yeast Saccharomyces cerevisiae. Genetics **195**, 643–681.

173. Yonath, A., Tesche, B., Lorenz, S., Mussig, J., Erdmann, V.A., and Wittmann, H.G. (1983). Several crystal forms of the *Bacillus stearothermophilus* 50 S ribosomal particles. FEBS Lett **154**, 15-20.

174. Yusupov, M.M., G.Z. Yusupova, A. Baucom, K. Lieberman, T.N. Earnest, J.H. Cate, et H.F. Noller. (2001). Crystal structure of the ribosome at 5.5 A resolution. Science. **292**, 883-96.

175. Yusupova, G., Yusupov, M., Spirin, A., Ebel, J.P., Moras, D., Ehresmann, C., and Ehresmann, B. (1991). Formation and crystallization of Thermus thermophilus 70S ribosome/tRNA complexes. FEBS Lett **290**, 69–72.

176. Yusupova, G.Z., Yusupov, M.M., Cate, J.H., and Noller, H.F. (2001). The path of messenger RNA through the ribosome. Cell **106**, 233-241.

177. Zopf W. (1890). Die Pilze. Verlang von E. Trewendt, Breslau.

# RESUME DE LA THESE EN FRANÇAIS

## 1. PREFACE

Si dans l'imaginaire commun, les champignons ne sont présentés que par leurs sporophores ou appareils fructifères macroscopiques, ils représentent un groupe extrêmement large et varié d'organismes vivants. Les fossiles attestent de leur présence sur Terre depuis l'époque du Silurien et via les mycorhyses ils auraient vraisemblablement aidé les premières plantes à coloniser les terres émergées de la planète. Ils sont retrouvés dans un très grand nombre de niche écologique où ils jouent un rôle très important dans les cycles biogéochimiques. Très présents en symbolique, en héraldique, dans la mythologie, même dans un grand nombre d'expression populaire, les champignons ont longtemps été considérés comme étant mystiques et surnaturels.

L'Histoire laisse très peu de traces écrites concernant les champignons et leurs usages, ainsi on retrouve quels vestiges, au début de notre ère, d'utilisation thérapeutique dans *De materia medica* de Discoride pour une vingtaine d'espèces et quelques appellations qui sont toujours conservés : *Amanita* ou encore *Boletus*.

Sénèque les appelait *voluptuarium venenum* pour poison voluptueux et Pline *anceps cibus* pour mets suspect. Les différentes façons de nommer les champignons sont en lien avec leur funeste implication. Appelés mycètes ou *Fungi*, l'étymologie les rapproche de leur néfaste implication. Si mycètes vient du grec *mykes*, pour mucus puisque proche de la moisissure et pourriture, le mot *Fungi* vient d'une contraction populaire latine entre *funus* pour funérailles et d'*ago* pour produire, dénotant ainsi les nombreux décès provoqués par les champignons.

Considérés comme des plantes primitives voire dégénérées, même classés au plus bas de la *Scala naturæ* au Moyen Age puisqu'associés exclusivement à la mort et la putréfaction. Ils sont considérés comme des « excréments de la terre », les champignons sont alors utilisés par les adeptes de la magie noire lors de la préparation de leurs élixirs voire utilisés pour leur propriété hallucinogène depuis plus longtemps encore par des chamanes, oracles et autre guérisseurs dans différentes civilisation de la planète.

Le début des études les concernant remonte supposément au XVIème siècle avec des descriptions d'espèces particulières (Junius, Reiner Solenander, Fabi Columna) et quelques essais de classification (Hermolaus, Charles de L'Ecluse, Matthiole). La fin de ce siècle voit Giambattista della Porta qui s'intéresse à décortiquer le divin et la magie des mécanismes naturelles de la vie être le premier affirmer que les champignons se reproduisent pas semence.

Ce n'est qu'au XVIIème siècle, que l'invention du microscope permet d'observer les parties invisibles jusque là des champignons : spores, thalles et autres mycélium sont décrits sans que leurs fonctions soient connues.

Si Carl Von Linné pose les bases de la systématique avec son ouvrage *Systema Naturae* en 1735 *via* l'introduction de la nomenclature à dénomination binomiale et de la hiérarchisation de la classification, celle-ci décrivait à ce moment précis le monde du vivant en trois règnes : bactérien, animal et végétal. A l'époque, champignon, moisissure, algue et autre fougère étaient considérés comme une des 24 classes de végétaux et étaient classés parmi l'embranchement des cryptogames c'est-à-dire des organismes végétaux dont les organes reproducteurs sont peu apparents voire cachés.

En 1795, est baptisée mycologie, la science qui s'attèle à étudier les champignons, le terme est proposé par Jean-Jacques Paulet, le terme étant préféré à fungologie.

Au vue de leur développement, de leur culture capricieuse et éphémère, pas toujours très bien maitrisée, la mycologie se trouve privée d'un grand nombre de moyens qui ont permis l'avancée plus rapide d'autres branches de l'Histoire naturelle. De plus les observations *in vitro* ne donne qu'une vague idée de la physiologie globale des champignons puisque bon nombre de caractères disparaissent en laboratoire.

En 1827, les champignons sont encore considérés par la plupart comme des produits de la génération spontanée. Elias Magnus Fries, pose les bases de la mycologie moderne en donnant la première classification systématique des champignons dans « *Systema mycologicum* » en 1832. Entre 1836 et 1840, Stephan Ladislaus Endlicher propose dans son ouvrage *Genera plantarum secundum ordines naturales disposita* une séparation du règne des *Plantae* en cormophytes, végétal dont l'appareil végétatif est composé d'une tige et de feuilles, et en thallophytes, plantes inférieures ou non vascularisées, possédant un corps indifférencié : un thalle, ceci regroupe à ce moment là : champignons, mousses, lichens, hépatiques, algues et même cyanobactérie. Ce n'est qu'après la publication de *The origin of species* en 1859, que Charles Darwin fait voler en éclat cette théorie, ainsi les botanistes

cessent de croire à la génération spontanée des champignons et commencent à les détacher des plantes vascularisées.

Or jusqu'au milieu du XXème siècle, les naturalistes classent les champignons parmi les plantes, ce n'est qu'en 1969, qu'ils sont individualisés dans un règne particulier : les *Fungi*, en effet le botaniste Robert Harding Whittaker propose une division du vivant en cinq règnes : Procaryotae, Protozoan, Plantae, Animalia et Fungi (Science, 1969).

Grâce aux travaux de Carl Woese et Georges E. Fox, en 1977, cette classification est à nouveau secouée avec la découverte confirmée des archéobactéries et la création de leur propre domaine mais aussi de leur propre règne.

Ce n'est qu'avec l'avènement et les améliorations technologiques du séquençage génomique que l'individualisation du règne fongique balbutie à nouveau. En effet la comparaison des séquences de gènes permet de retracer l'histoire évolutive des êtres vivants en suivant la modification de leur génome. Ces améliorations technologiques ne remettent pas seulement en question le règne fongique mais également la division en 6 règnes, la limite entre procaryote et eucaryote n'est plus si forte, la division entre règne animal et végétal n'est plus si sûre et enfin l'unité du règne fongique n'est plus qu'un pseudo-concept.

En 2005, une nouvelle classification est proposée et révisée en 2012 par Adl et al, 2012, qui fait toujours l'objet de discussions et débats. Ainsi le groupe des opisthocontes est apparu via proposition du rapprochement d'organismes très divers en apparence dont les champignons et les métazoaires. Ce rapprochement de leur taxon est fondé sur l'étude de plusieurs gènes analysés individuellement, d'où la fiabilité de cette théorie. A partir de ces mises en évidence moléculaire, d'autres synapomorphies sont apparues et confirment l'holophylie de ce groupe.

Les champignons sont actuellement considérés comme un taxon artificiel et polyphylétique, en effet deux grandes lignées composent ce groupe les eumycètes ou champignons vrais, proches parents des animaux et les pseudomycètes, plus proche des plantes. Ce dernier groupe est le fruit de nombreuses convergences évolutives et cela amène donc à penser qu'il sera remanié très prochainement.

En somme les champignons n'ont surement pas finis de nous faire revoir, remanier et perfectionner leur classification.

## 2. CONTEXTE

Candida albicans est une levure commensale saprophyte du tube digestif ayant la capacité à devenir un pathogène opportuniste dans certaines circonstances favorisantes. Elle est responsable de diverses infections de la peau, des phanères et des muqueuses chez les sujets immunocompétents lors d'antibiothérapie prolongée. Elle peut ainsi provoquer des infections systémiques mortelles chez les patients hospitalisés dans des services de réanimation ou ayant subi des interventions chirurgicales digestives. Elle est la quatrième pathologie nosocomiale au monde engendrant des coûts estimés à 1 milliard de dollars par an (Shapiro et al., 2011).

C. albicans utilise diverses stratégies pour infecter son hôte. Elle sécrète des enzymes hydrolytiques induisant des dommages aux cellules hôtes, elle s'adapte au stress métabolique et elle est capable de produire des biofilms contribuant à la résistance aux antifongiques (Shapiro et al., 2011). L'augmentation de l'utilisation de traitements antifongiques est responsable de l'augmentation du nombre de résistance et est à l'origine d'échecs thérapeutiques. De nouvelles voies thérapeutiques doivent être explorées. L'inhibition de la synthèse des protéines par l'inactivation du mécanisme de traduction effectuée par le ribosome semble être une stratégie radicale car l'agent pathogène aura plus de mal à s'adapter et à devenir résistant aux médicaments (Champney and Miller, 2014).

Toutefois l'inhibition de la traduction représente un défi majeur pour les chercheurs et nécessite une compréhension accrue de la structure des ribosomes. En février 2009, des biophysiciens de l'Université de Montréal publient dans la revue Nature (Bokov and Steinberg, 2009) une première explication des mécanismes de formation du ribosome qui peut contenir jusqu'à 300 000 atomes. Il s'agit du complexe macromoléculaire asymétrique biologique le plus grand dont la structure a été résolue par cristallographie. Il est composé de deux sous-unités comprenant différents éléments. Chez les eucaryotes, la grande sous-unité 60S est composée de 46 protéines et de 3 ARNr (25S, 3396 nucléotides ; 5.8S, 158 nucléotides ; 5S, 121 nucléotides), représentant 2.8 MDa et la petite sous-unité 40S est composée de 33 protéines et d'un ARNr (18S, 1800 nucléotides), représentant 1.4MDa

(Woolford and Baserga, 2013). Dans cette structure, les ARNr ont un rôle de liaisons et d'interactions qui permettent le maintien entre les protéines d'une sous-unité mais aussi avec les protéines de l'autre sous-unité.

## 3. ETAT DE LA QUESTION

De nombreuses structures ont déjà été cristallisées, 118280 structures dans la Protein Data Bank, dont 105619 par cristallographie et plus spécifiquement 1181 ribosomes ou partie de ribosome. Le ribosome en lui-même, étant donné sa taille et sa complexité, est l'une des dernières structures complètes à avoir été résolue. Sa structure 3D est compliquée à obtenir vu la difficulté de la production d'un complexe pur et cristallisable contenant tous les éléments, raison pour laquelle les premiers ribosomes étudiés via cristallographie furent procaryotes (Yusupov et al., 2001). Ce n'est qu'en 2010 qu'Adam Ben-Shem dans l'équipe de Marat Yusupov décrypte, à 3,5A, la première structure complète d'un ribosome eucaryote, celle de Saccharomyces cerevisiae (Ben-Shem et al., 2010). L'année suivante une résolution de 3A est obtenue (Ben-Shem et al., 2011). Elle a permis d'observer des mouvements dans le ribosome, plus particulièrement entre les sous-unités et d'en définir la mécanique de la traduction. Quant à celle d'Homo sapiens, elle a été obtenue en 2015 par cryo-microscopie électronique (Khatter et al., 2015), avec une résolution moyenne de 3,6A.

## 4. PROBLEMATIQUE

Bien que sa fonctionnalité soit universellement conservée dans la monde du vivant, le ribosome présente des différences majeures entre les règnes (eucaryote, procaryote, archéé) mais aussi à l'intérieur de ces règnes (métazoaire, protozoaire, mycète).

L'étude proposée au cours de cette thèse s'intéresse en particulier à la structure du ribosome de C. albicans, qui n'a encore jamais été résolue. Le décryptage de cette structure par cristallographie servira de base solide à la poursuite d'études quant au mécanisme de traduction dans cet organisme.

En parallèle, nous avons effectué des études bioinformatiques comparatives entre la structure de C. albicans et celles de S. cerevisiae et d'H. sapiens afin de mettre en évidence des sites spécifiques à C. albicans. L'étude permettra de mettre en évidence de voies thérapeutiques contribuant au développement de nouveaux antifongiques spécialement et très spécifiquement dirigés contre C. albicans.

## 5. APPROCHES EXPERIMENTALES

La détermination de la structure du ribosome de C. albicans a été réalisée via deux approches :

- Par modélisation bio-informatique grâce à la réalisation d'alignements et la modélisation des séquences de protéines et ARN ribosomiques
- Par radiocristallographie au rayon X

L'identification de sites cibles potentiellement intéressants a été réalisée par une approche bio-informatique dans un premier temps puis confirmée par cristallographie.

L'intérêt de ces sites cibles potentiels a été confirmé par la réalisation de test d'inhibition in vivo et détermination de CMI, en utilisant des inhibiteurs connus du ribosome eucaryote.

# 6. RESULTATS

Les résultats des alignements ont démontré un niveau élevé de similarité entre le ribosome, connu de S. cerevisiae et dont la structure avait été précédemment résolue au sein de l'équipe, et celle de C. albicans. Un certain nombre de séquences de protéines ribosomiques de C. albicans étaient encore non identifiées comme des protéines ribosomiques mais simplement de possibles ORF, d'autres mal prédites ont même dû être reconstruites. Malgré cela une des protéines ribosomiques (eL42) resta absente, introuvable dans les banques de données et impossible à reconstruire, est-elle simplement absente du ribosome ? Cela sera à confirmer avec les résultats de cristallographie et de biochimie.

La modélisation des r-protéines et des ARNr a permis d'assembler un modèle bioinformatique du ribosome de C. albicans. Ce modèle a permis de :

- Localiser, identifier et annoter les sites fonctionnels du ribosome chez C. albicans
- Localiser des sites spécifiques de C. albicans par comparaison entre H. sapiens et S. cerevisiae.
- Identifier des sites représentant des cibles potentielles de molécules inhibitrices

L'approche de détermination structurale par radiocristallographie au rayon X a nécessité :

- L'établissement d'un protocole de culture et production de biomasse
- L'établissement d'un protocole de purification du ribosome
- La détermination des paramètres de cristallisation du ribosome
- La détermination des conditions de déshydratation et de congélation de cristaux
- L'établissement de paramètres de collecte de données de diffraction

La résolution de la structure via cette approche est toujours en cours mais a permis d'avoir des résultats suffisamment précis pour attester qu'il existe un haut niveau de similarité structurelle entre les ribosomes de S. cerevisiae et C. albicans. Ainsi des segments d'ARNr non décrits et non représentés dans la structure de S.cerevisiae parce que trop instables ont pu être décrits et représentés chez C. albicans.

L'identification de sites cibles chez C. albicans a permis de mettre en évidence les différences existantes sur les sites fonctionnels du ribosome avec ceux de S. cerevisae. En effet les résidus impliqués ne sont pas à certains endroits similaires et il en résulte dans des cas précis des résistances à certains antifongiques connus, type cycloheximide/actidione.

Les tests in vivo, en cours de réalisation, permettront de vérifier l'intérêt des sites cibles prédits par bioinformatique. De plus, ils apporteront une information quantitative vis à vis de l'inhibition qu'ils entrainent ou non sur la souche de C. albicans.

## 7. DISCUSSIONS ET PERSPECTIVES

La résolution de la structure du ribosome de C. albicans apportera des informations cruciales quant aux développements de nouveaux antifongiques. En effet des cibles moléculaires ont été mises en évidence et des sites de liaisons ont été identifiés. Les prédictions bioinformatiques ont apporté des informations précieuses quant à la structure du ribosome tant d'un point de vue fondamental qu'au niveau des applications de drug discovery possibles.

Cette étude faisant le lien entre recherche fondamentale en biologie structurale, l'identification de cibles moléculaires potentiellement d'intérêt thérapeutique et l'essai d'inhibiteurs du ribosome de C. albicans, servira de base solide quant à l'élaboration d'inhibiteurs spécifiques du ribosome de C. albicans. Et dans un aspect plus fondamentale, de décortiquer les mécanismes de la traduction au sein de cette levure.

Un protocole efficace et reproductible de production, purification et de cristallisation du ribosome de C. albicans a été mis en place. L'apport de la résolution via rayon X a permis d'apporter une meilleure précision aux données et de corréler ou non les données obtenues via une modélisation bio-informatique. Ce modèle permettra en plus des nombreuses applications possibles, d'étudier la mécanique de la traduction au sein de ce microorganisme.

Enfin les études in vivo de l'action d'inhibiteurs du ribosome sur C. albicans permettront

d’apporter des réponses quant à une partie des hypothèses amenées via les différentes approches de résolutions structurales.

# ANNEXES

## 1. MOLECULAR MASS OF *CANDIDA ALBICANS* 80S RIBOSOME

| Large Sub Unit | | Small Sub Unit | | rRNA | |
|---|---|---|---|---|---|
| Name | Size | Name | Size | Name | Size |
| uL1_RPL1 | 218 | eS1_RPS1 | 257 | 5S | 121 |
| uL2_RPL2 | 255 | eS4_RPS4 | 263 | 5,8S | 157 |
| uL3_RPL3 | 242 | eS6_RPS6 | 237 | 18S | 1800 |
| uL4_RPL4 | 364 | eS7_RPS7 | 187 | 25S | 3361 |
| uL5_RPL11 | 175 | eS8_RPS8 | 207 | | |
| uL6_RPL9 | 192 | eS10_RPS10 | 119 | | |
| uL10_RPP0 | 313 | eS12_RPS12 | 144 | | |
| uL11_RPL12 | 166 | eS17_RPS17 | 138 | | |
| uL13_RPL16 | 201 | eS19_RPS19 | 146 | | |
| eL6_RPL6 | 177 | eS21_RPS21 | 88 | | |
| eL8_RPL8 | 263 | eS24_RPS24 | 136 | | |
| eL13_RPL13 | 203 | eS25_RPS25 | 106 | | |
| eL14_RPL14 | 132 | eS26_RPS26 | 120 | | |
| eL15_RPL15 | 205 | eS27_RPS27 | 83 | | |
| eL18_RPL18 | 187 | eS28_RPS28 | 68 | | |
| eL19_RPL19 | 191 | eS30_RPS30 | 64 | | |
| eL20_RPL20 | 173 | eS31_RPS31 | 194 | | |
| eL21_RPL21 | 161 | P1 | 107 | | |
| eL22_RPL22 | 125 | P2 | 112 | | |
| eL24_RPL24 | 156 | RACK1 | 318 | | |
| eL27_RPL27 | 137 | uS2_RPS0 | 262 | | |
| eL29_RPL29 | 64 | uS3_RPS3 | 252 | | |
| eL30_RPL30 | 107 | uS4_RPS9 | 190 | | |
| eL31_RPL31 | 113 | uS5_RPS2 | 250 | | |
| eL32_RPL32 | 132 | uS7_RPS5 | 226 | | |
| eL33_RPL33 | 108 | uS8_RPS22 | 131 | | |
| eL34_RPL24 | 123 | uS9_RPS16 | 143 | | |
| eL36_RPL36 | 100 | uS10_RPS20 | 120 | | |
| eL37_RPL37 | 91 | uS11_RPS14 | 133 | | |
| eL38_RPL38 | 79 | uS12_RPS23 | 146 | | |

| | | | | | |
|---|---|---|---|---|---|
| eL39_RPL39 | 52 | uS13_RPS18 | 146 | | |
| eL40_RPL40 | 230 | uS14_RPS29 | 57 | | |
| eL41_RPL41 | 0 | uS15_RPS13 | 152 | | |
| eL42_RPL42 | 107 | uS17_RPS11 | 156 | | |
| eL43_RPL43 | 93 | uS19_RPS15 | 143 | | |
| uL14_RPL23 | 138 | | | | |
| uL15_RPL28 | 150 | | | | |
| uL16_RPL10 | 221 | | | | |
| uL18_RPL5 | 299 | | | | |
| uL22_RPL17 | 186 | | | | |
| uL23_RPL25 | 143 | | | | |
| uL24_RPL26 | 128 | | | | |
| uL29_RPL35 | 121 | | | | |
| uL30_RPL7 | 242 | | | | |

| | | | | | | |
|---|---|---|---|---|---|---|
| **Total** | **7263** | | **5601** | | **5439** | |
| | 12864x110 | aa | | 5439 | nucleotides 1794870 | Da |
| **Total weight** | 3209910 | Da | **3.2 MDa** | | | |
| **Ratio (%)** | r-protein | 44,08347898 | rRNA | 55,916521 02 | | |
| RNA/protein | 1,26842350 7 | | | | | |

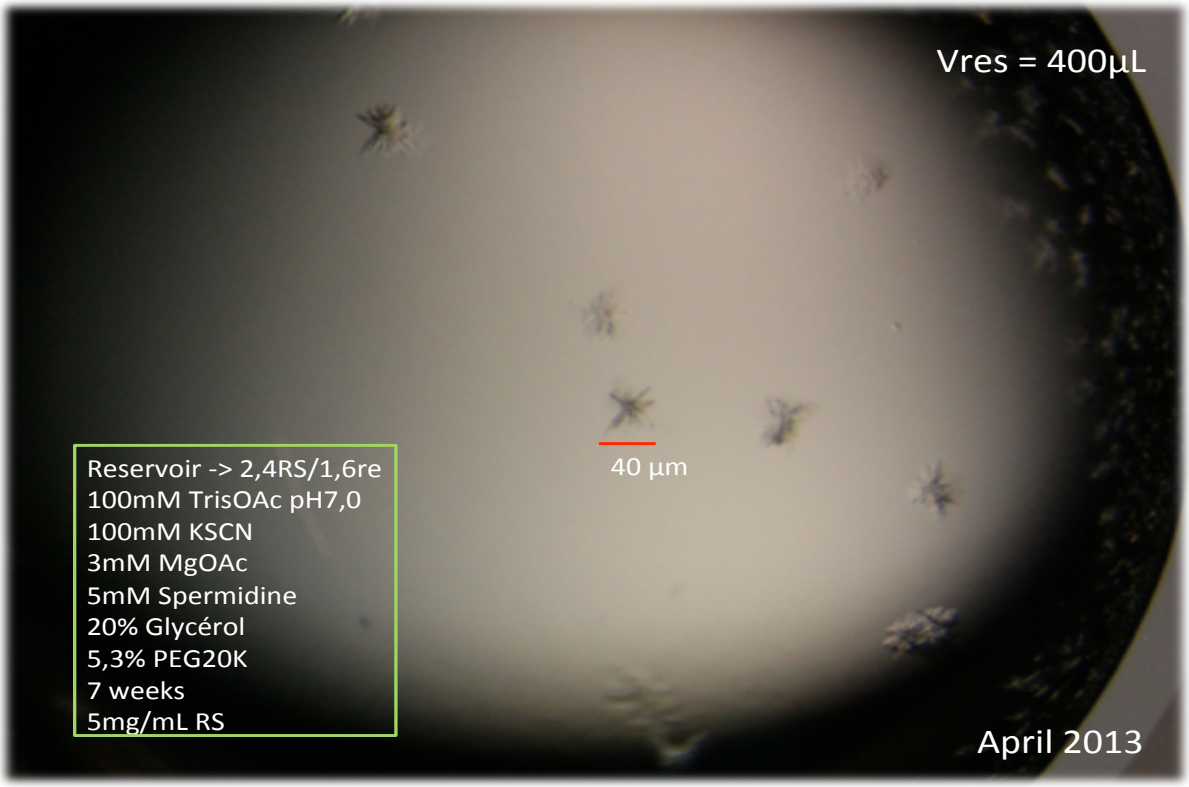
Vres = 400µL
40 µm
Reservoir -> 2,4RS/1,6re
100mM TrisOAc pH7,0
100mM KSCN
3mM MgOAc
5mM Spermidine
20% Glycérol
5,3% PEG20K
7 weeks
5mg/mL RS
April 2013

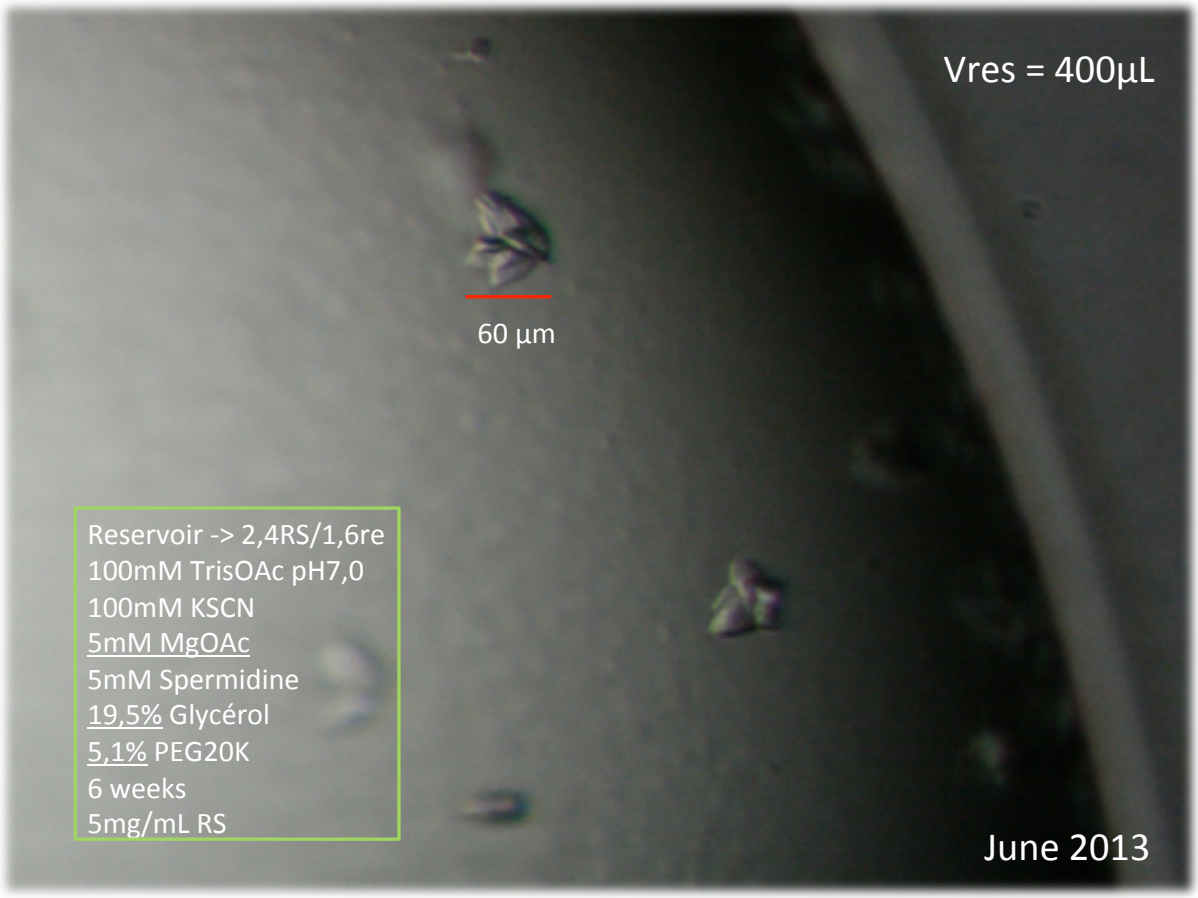
Vres = 400µL
60 µm
Reservoir -> 2,4RS/1,6re
100mM TrisOAc pH7,0
100mM KSCN
5mM MgOAc
5mM Spermidine
19,5% Glycérol
5,1% PEG20K
6 weeks
5mg/mL RS
June 2013

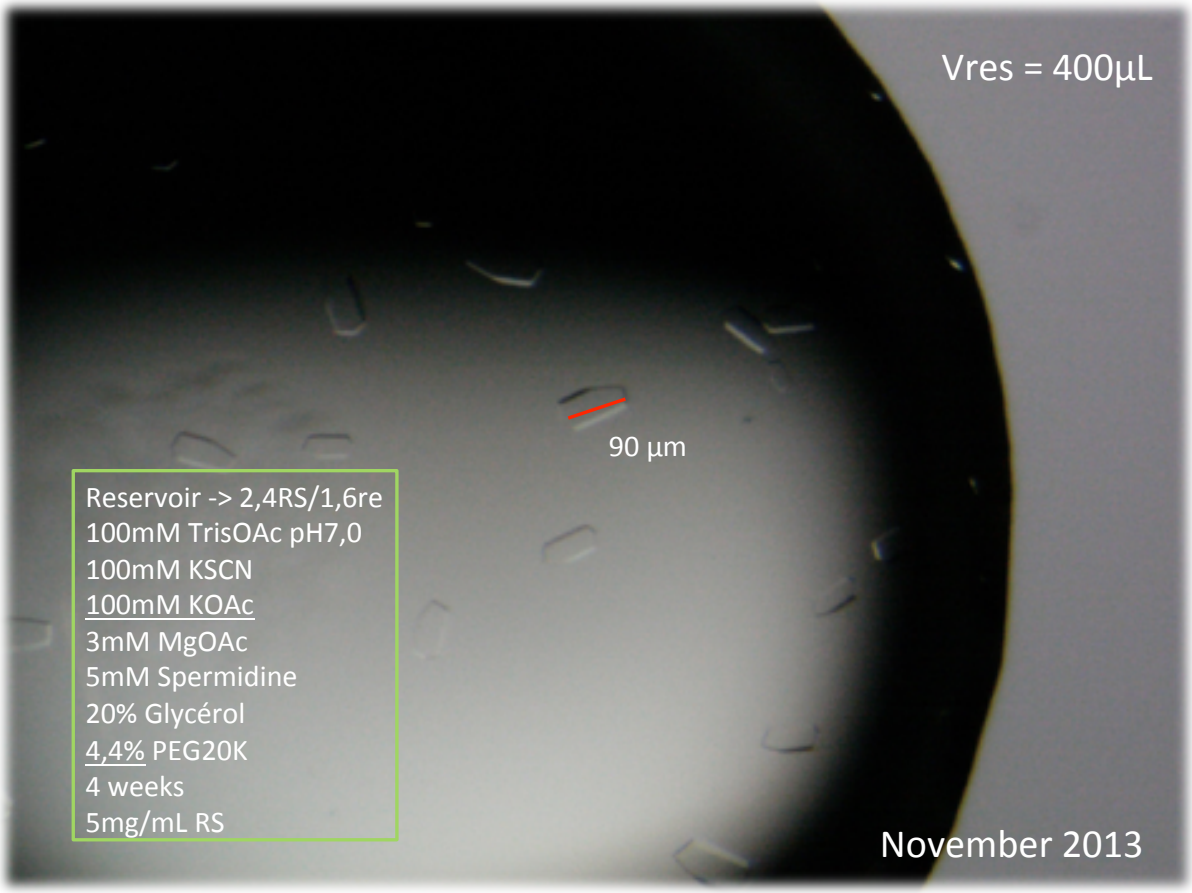
Vres = 400µL
90 µm
Reservoir -> 2,4RS/1,6re
100mM TrisOAc pH7,0
100mM KSCN
100mM KOAc
3mM MgOAc
5mM Spermidine
20% Glycérol
4,4% PEG20K
4 weeks
5mg/mL RS
November 2013

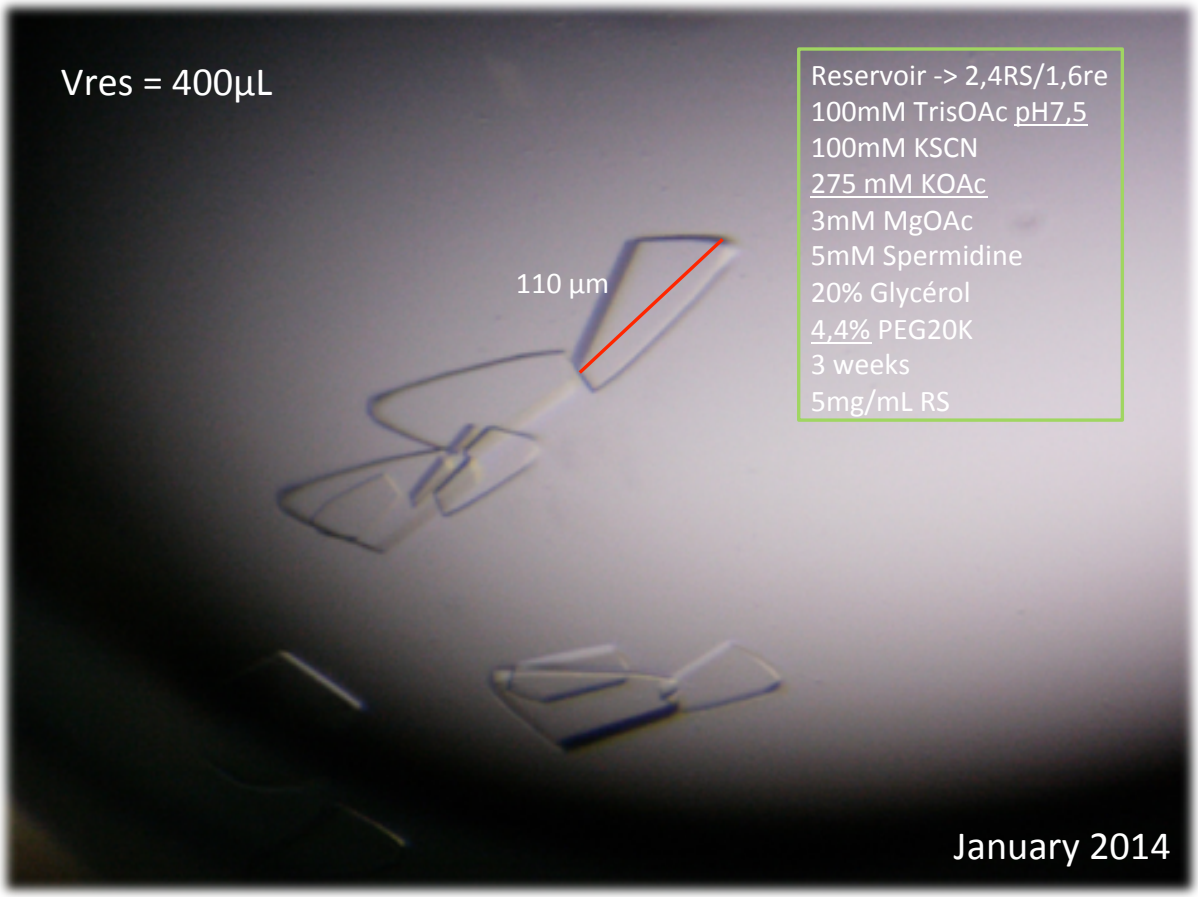
Vres = 400µL
110 µm
Reservoir -> 2,4RS/1,6re
100mM TrisOAc pH7,5
100mM KSCN
275 mM KOAc
3mM MgOAc
5mM Spermidine
20% Glycérol
4,4% PEG20K
3 weeks
5mg/mL RS
January 2014

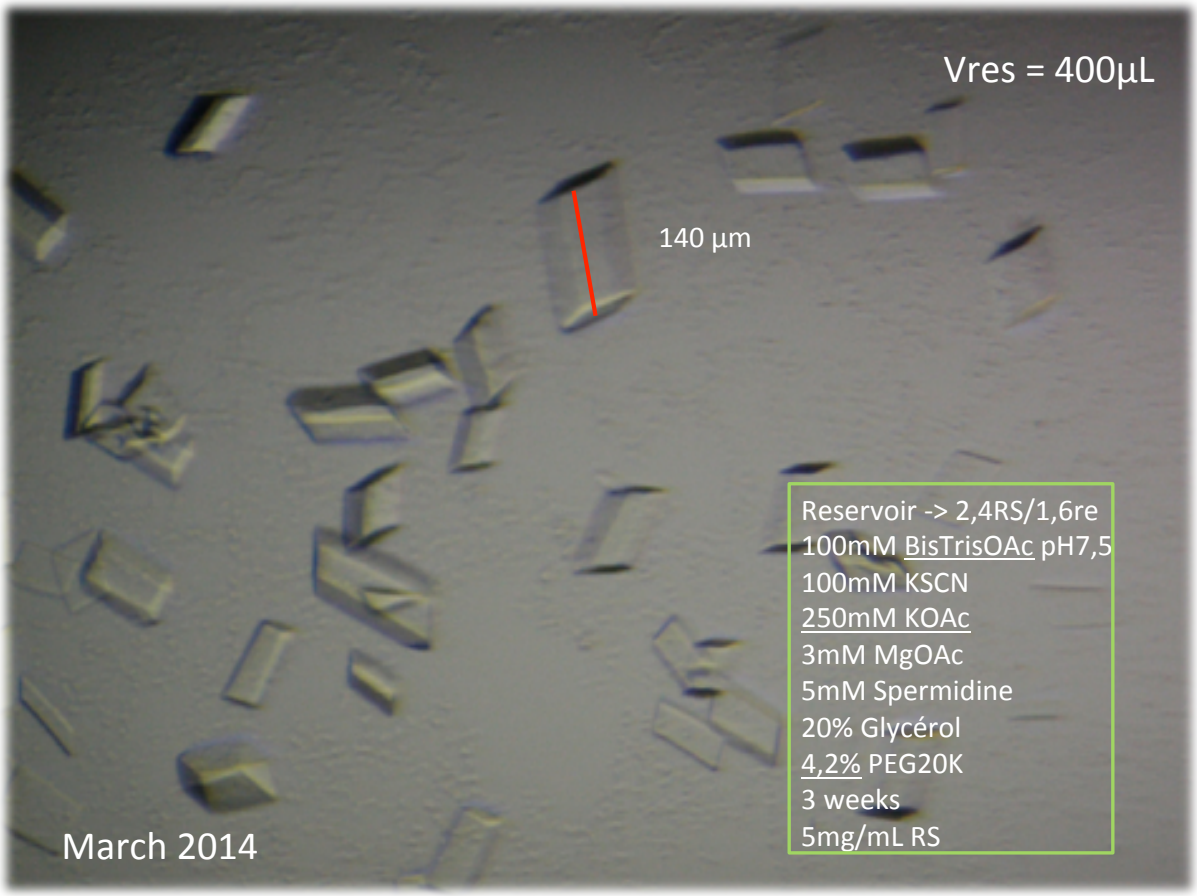
Vres = 400µL
140 µm
Reservoir -> 2,4RS/1,6re
100mM BisTrisOAc pH7,5
100mM KSCN
250mM KOAc
3mM MgOAc
5mM Spermidine
20% Glycérol
4,2% PEG20K
3 weeks
5mg/mL RS
March 2014

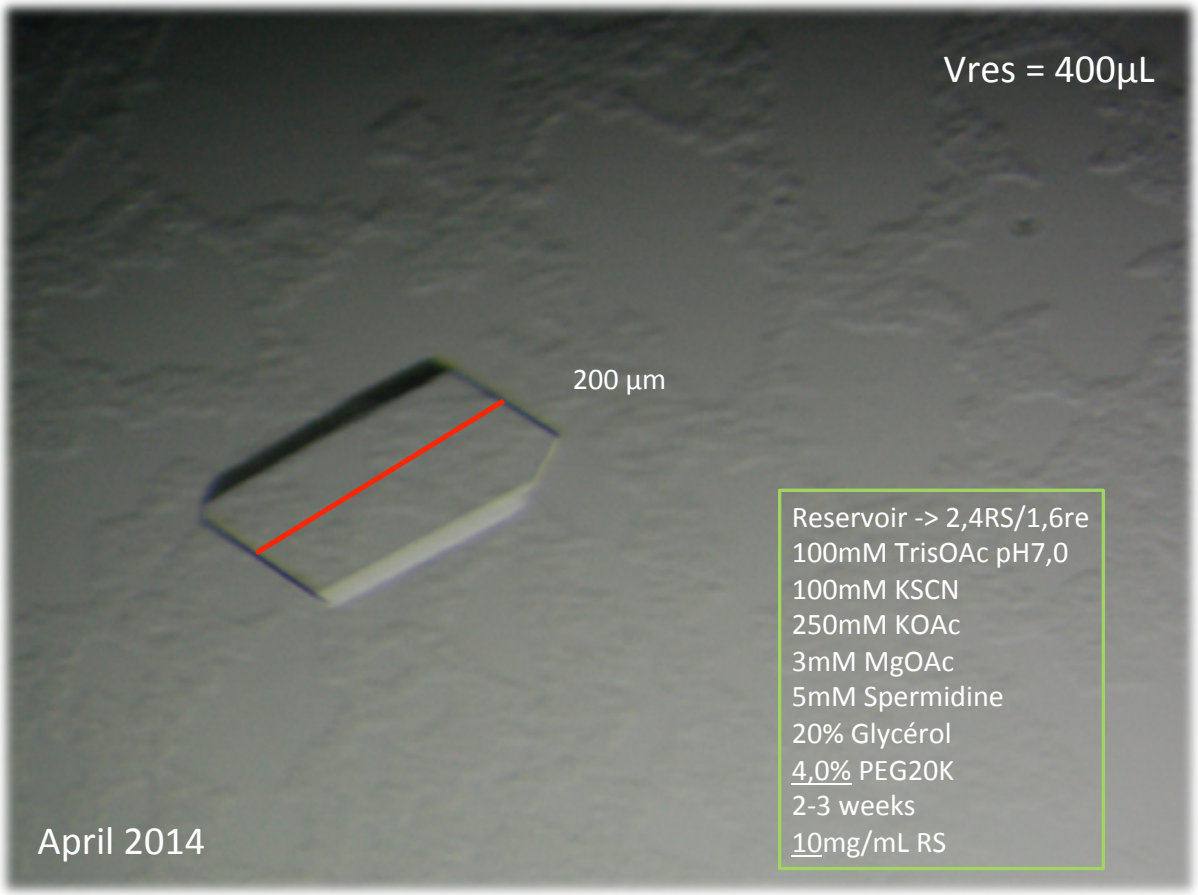
Vres = 400µL
200 µm
Reservoir -> 2,4RS/1,6re
100mM TrisOAc pH7,0
100mM KSCN
250mM KOAc
3mM MgOAc
5mM Spermidine
20% Glycérol
4,0% PEG20K
2-3 weeks
10mg/mL RS
April 2014


Sept 2014
Vres = 425µL
170 µm
Reservoir -> 2,4RS/1,6re
100mM BisTrisOAc pH7,0
100mM KSCN
250mM KOAc
3mM MgOAc
5mM Spermidine
20% Glycérol
4,3% PEG20K
3 weeks
5mg/mL RS

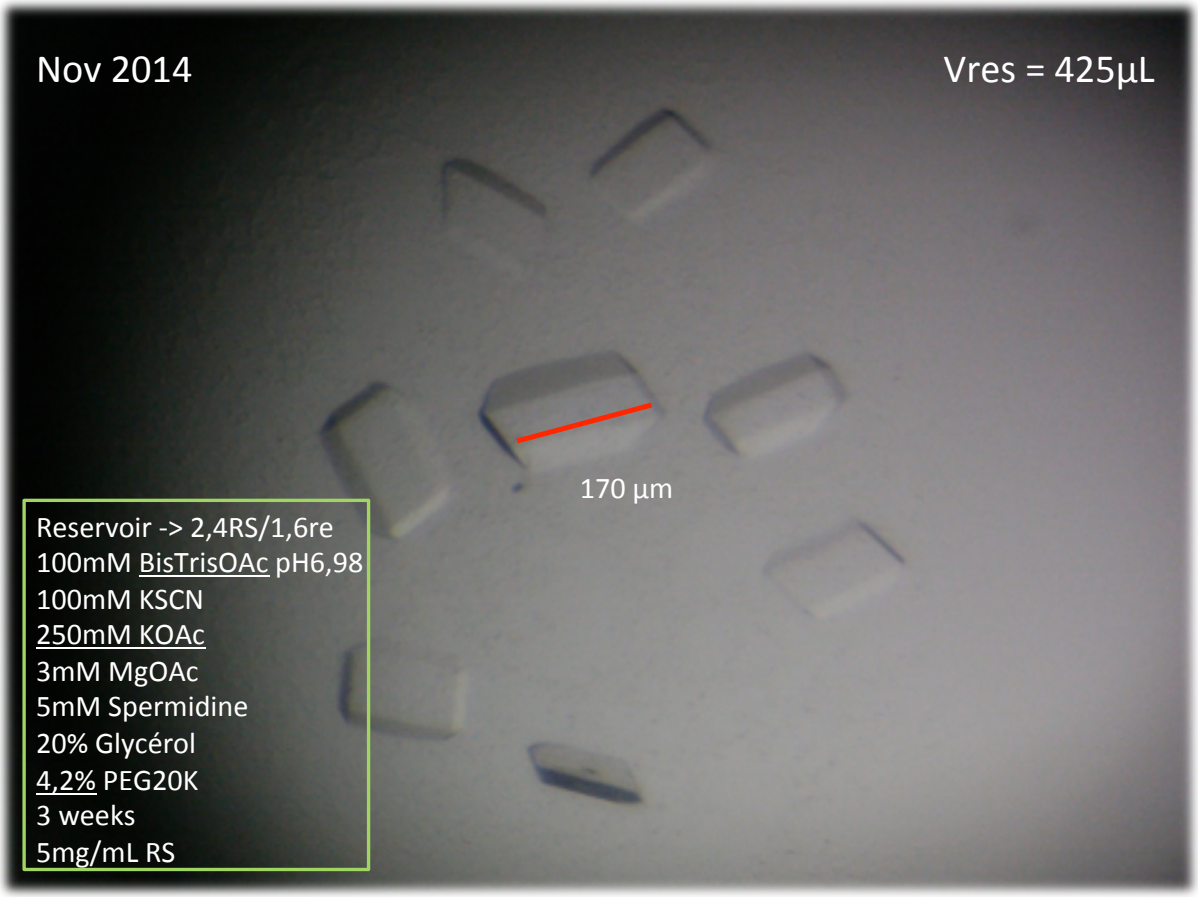
Nov 2014
Vres = 425µL
170 µm
Reservoir -> 2,4RS/1,6re
100mM BisTrisOAc pH6,98
100mM KSCN
250mM KOAc
3mM MgOAc
5mM Spermidine
20% Glycérol
4,2% PEG20K
3 weeks
5mg/mL RS

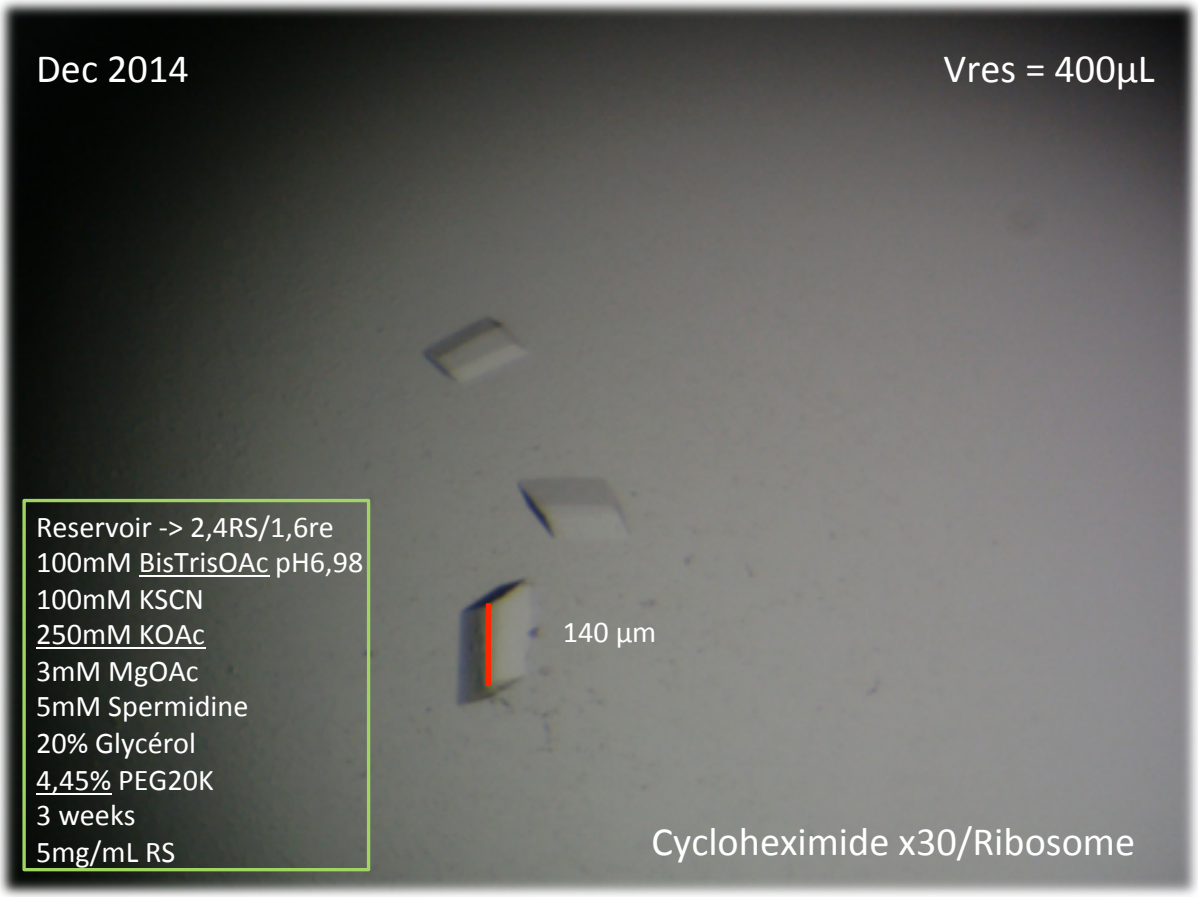
Dec 2014
Vres = 400µL
Reservoir -> 2,4RS/1,6re
100mM BisTrisOAc pH6,98
100mM KSCN
250mM KOAc
3mM MgOAc
5mM Spermidine
20% Glycérol
4,45% PEG20K
3 weeks
5mg/mL RS
140 µm
Cycloheximide x30/Ribosome

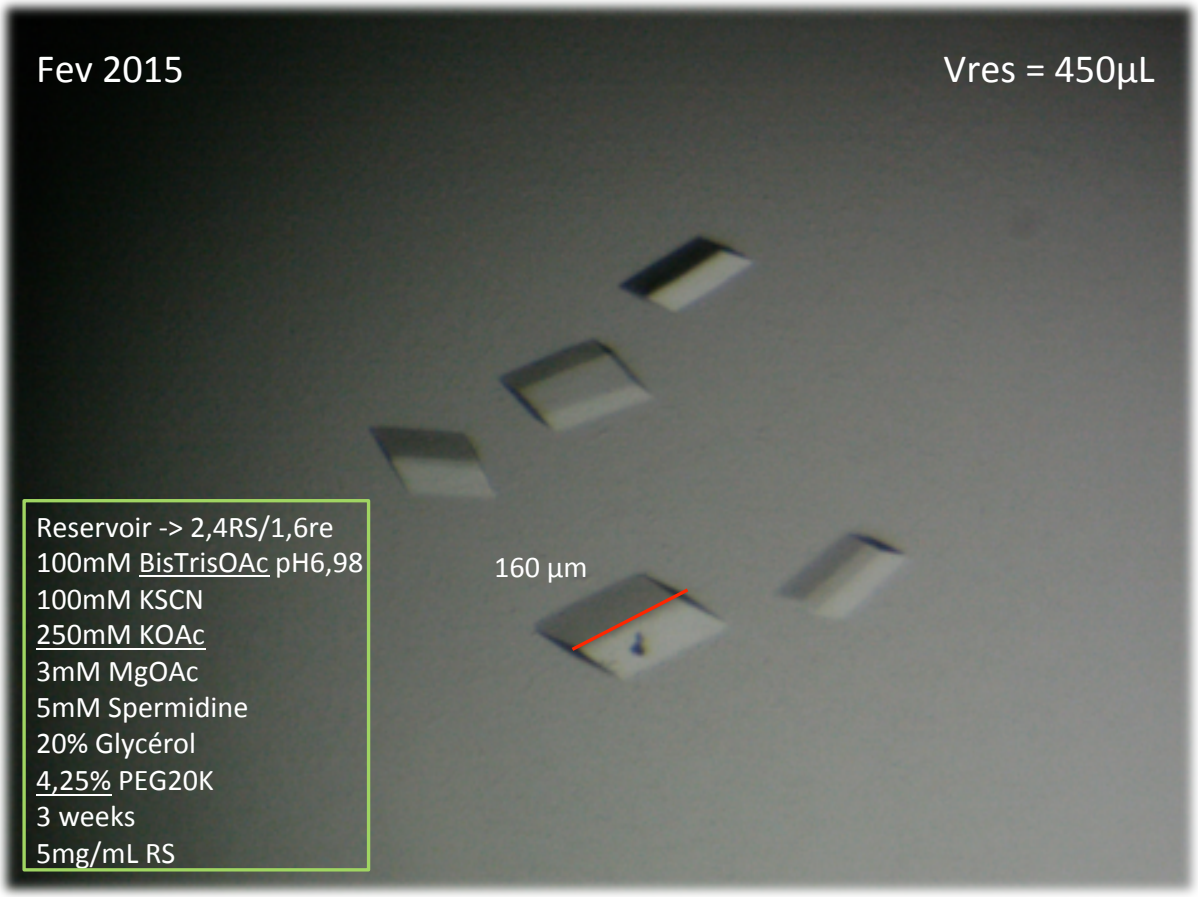
Fev 2015
Vres = 450µL
Reservoir -> 2,4RS/1,6re
100mM BisTrisOAc pH6,98
100mM KSCN
250mM KOAc
3mM MgOAc
5mM Spermidine
20% Glycérol
4,25% PEG20K
3 weeks
5mg/mL RS
160 µm

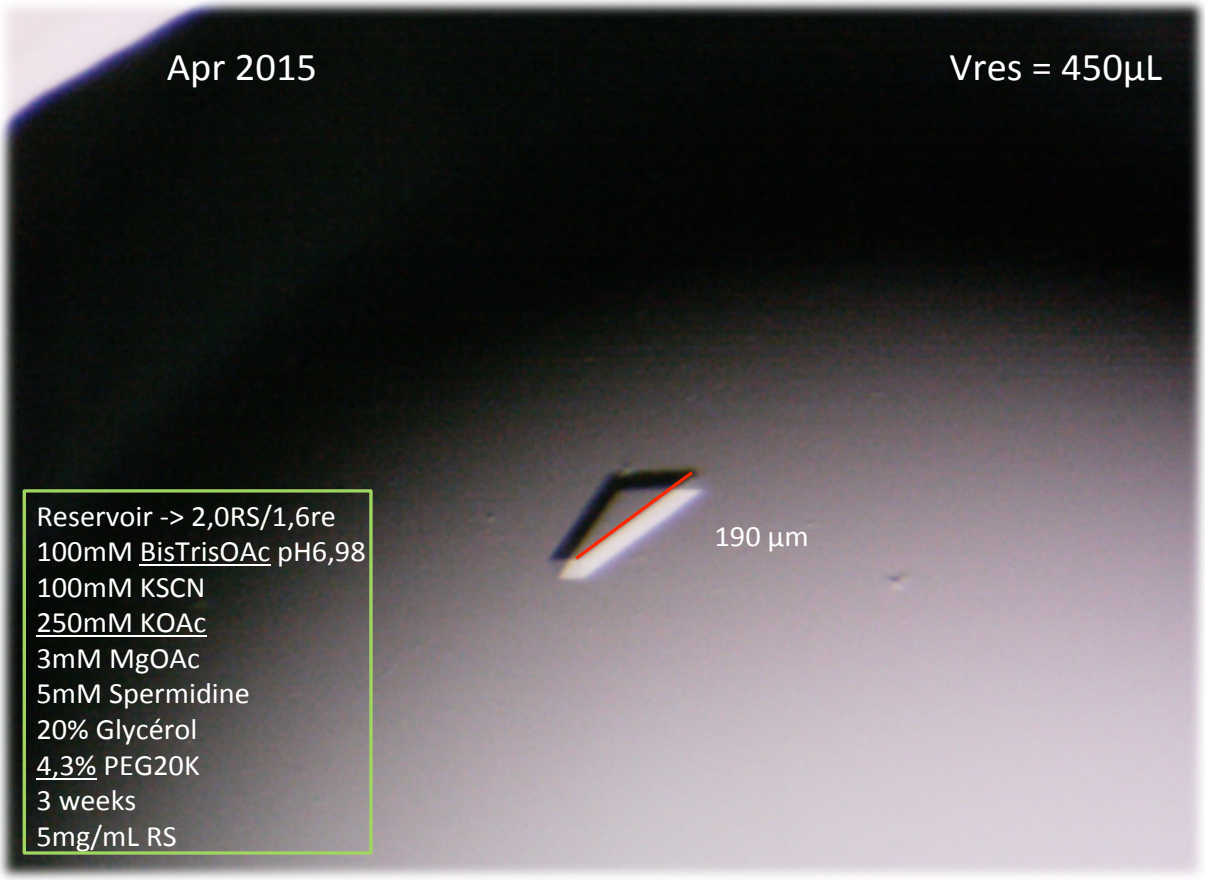
Apr 2015
Vres = 450µL
Reservoir -> 2,0RS/1,6re
100mM BisTrisOAc pH6,98
100mM KSCN
250mM KOAc
3mM MgOAc
5mM Spermidine
20% Glycérol
4,3% PEG20K
3 weeks
5mg/mL RS
190 µm

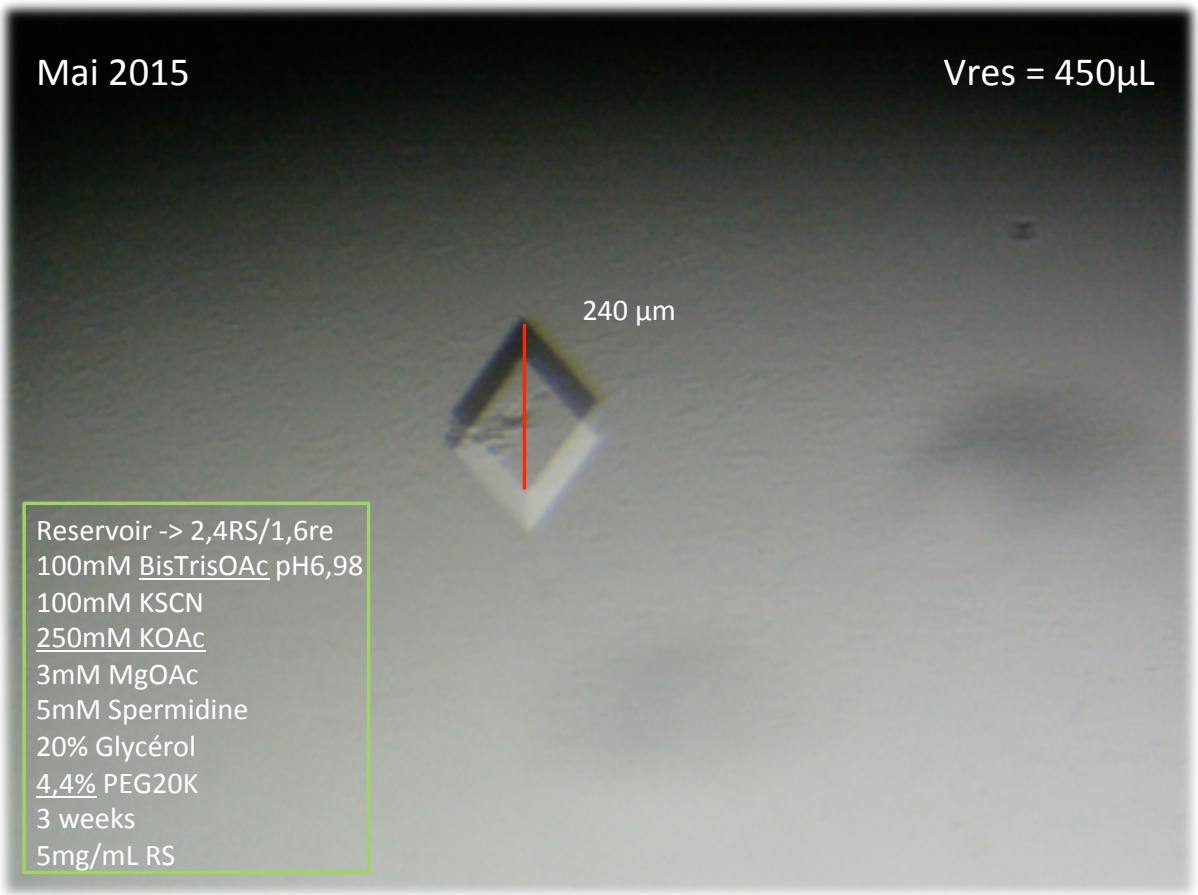
Mai 2015
Vres = 450µL
240 µm
Reservoir -> 2,4RS/1,6re
100mM BisTrisOAc pH6,98
100mM KSCN
250mM KOAc
3mM MgOAc
5mM Spermidine
20% Glycérol
4,4% PEG20K
3 weeks
5mg/mL RS

**David BRUCHLEN**

Structure, fonction et inhibition du ribosome de *Candida albicans*


## Résumé en français

*Candida albicans* est un champignon polymorphe, membre de la flore normale humaine, où il réside comme un organisme commensal tout au long de la vie. Cependant, dans certaines circonstances il peut causer des mycoses qui vont des infections superficielles de la peau à des infections systémiques mortelles. Très peu de choses sont connues sur les différences au sein des mécanismes fondamentaux de la croissance cellulaire, comme la synthèse des protéines par exemple, chez *C. albicans* par rapport aux organismes modèles tel *Saccharomyces cerevisiae*. À titre d'exemple, il a été démontré que son code génétique ne répond pas au code génétique universel. En effet, le codon CUG, codant normalement une leucine, code une sérine dans ces espèces, en particulier dans les protéines peu exprimées à la surface de la cellule, influençant potentiellement l'interaction de l'organisme avec l'être humain. La compréhension de la façon dont le mécanisme de traduction a lieu dans *C. albicans* est donc d'une importance cruciale. Le ribosome est la machinerie cellulaire responsable de la biosynthèse des protéines. Trouvé dans chaque organisme vivant, sa fonction est conservée, bien que sa structure puisse varier. Ces variations sont les particularités que nous cherchons à mettre en évidences, en effet elles sont les premières pistes de réponses aux questions concernant le mécanisme de traduction, potentiellement différentes de ce que l'on connait, de plus ces différences constitueront une base solide dans le développement de nouvelles molécules antifongiques. Le premier aspect de cette thèse tente de révéler l'intimité de la structure du ribosome 80S de *C. albicans* à haute résolution par modélisation *in silico* et confirmée par une approche de cristallographie aux rayons X. Ce modèle ouvrira la voie à d'autres études structurales de complexes fonctionnels, afin de déterminer la mécanique de la traduction des protéines dans cet organisme. Le deuxième aspect concerne l'inhibition du ribosome de *C. albicans*. Afin d'identifier des cibles intéressantes, des tests de concentration minimale inhibitrice ont été établies afin de confronter nos hypothèses structurales et de permettre d'évaluer l'efficacité de molécules inhibitrices et de guider le développement de nouveaux médicaments ciblant spécifiquement le ribosome de *C. albicans*.


**Mots clefs** : *Candida albicans*, ribosome, structure, cristallographie, inhibiteurs


## Résumé en anglais

*Candida albicans* is a polymorphic fungus, member of the normal human microbiome, where it resides as a lifelong, harmless commensal organism. Under certain circumstances, however, it can cause infections that range from superficial infections of the skin to life-threatening systemic infections. Very little is known about differences in fundamental mechanisms of cell growth, like protein synthesis for instance, in *C. albicans* compared to model systems, like *Saccharomyces cerevisiae*. As an example, it has been shown that its genetic code is not exactly the same as the universal genetic code. Indeed, the CUG codon, which normally specifies leucine, specifies serine in these species, especially in proteins expressed at a low level at the cell surface, potentially influencing the interaction of the organism with the human host. The understanding of how the translation mechanism takes place in *C. albicans* is therefore of pivotal importance. The ribosome is the cellular machinery responsible for protein biosynthesis. Found in every living organism, its function is conserved, although its structure can vary. These variations are especially what we would like to highlight, since they are indeed the first elements to respond to questions concerning the translation mechanism, potentially different from what is known, and these differences will be a solid foundation in the development of new antifungal molecules. The first aspect of this thesis attempts to reveal the intimacy of the *C. albicans* 80S ribosome structure at medium high resolution by *in silico* modelization and confirmed by an X-ray approach. This model will then pave the way for further structural studies of functional complexes, in order to unravel the protein translation mechanism in this organism. The second aspect concerns the inhibition of the *C. albicans* ribosome. In order to identify interesting druggable spots, MIC assessments have been set so as to justify our hypothesis and to allow for future screening tests and the design of new drugs specifically targeting the *C. albicans* ribosome.


**Keywords**: *Candida albicans*, ribosome, structure, crystallography, inhibitors